Available online at www.sciencedirect.com
ScienceDirect
Physics Reports 444 (2007) 51–99
PHYSICS REPORTS
www.elsevier.com/locate/physrep

Elementary excitations of biomembranes: Differential geometry of undulations in elastic surfaces

J. Leo van Hemmen*, Christian Leibold[1]

Physik Department, Technical University of Munich, 85747 Garching bei München, Germany

Accepted 31 December 2006
Available online 23 March 2007
editor: E. Sackmann

Abstract

Biomembrane undulations are elementary excitations in the elastic surfaces of cells and vesicles. As such they can provide surprising insights into the mechanical processes that shape and stabilize biomembranes. We explain how naturally these undulations can be described by classical differential geometry. In particular, we apply the analytical formalism of differential-geometric calculus to the surfaces generated by a cell membrane and underlying cytoskeleton. After a short derivation of the energy due to a membrane's elasticity, we show how undulations arise as elementary excitations originating from the second derivative of an energy functional. Furthermore, we expound the efficiency of classical differential-geometric formalism to understand the effect of differential operators that characterize processes involved in membrane physics. As an introduction to concepts the paper is self-contained and rarely exceeds calculus level.

PACS: 87.16.Dg; 68.35.Gy

Keywords: Biomembrane undulations; Excitations in soft matter

Contents

* Corresponding author. Fax: +49 89 28914656.
E-mail address: lvh@tum.de (J.L. van Hemmen).
[1] Present address. Department of Biology II, LMU—University of Munich, 82152 Planegg-Martinsried, Germany.

0370-1573/$ - see front matter © 2007 Elsevier B.V. All rights reserved.
doi:10.1016/j.physrep.2006.12.007

1. Introduction

Soft matter physics is a highly active, and fascinating, part of condensed matter physics. As a consequence of being soft, this kind of matter can change form easily and, as we will show, classical differential geometry is a natural and efficient tool to describe many of the physically intriguing phenomena that evolve at the surface of soft matter. The theory of the mechanics of soft surfaces has a long tradition starting as early as 1805 with the work of Laplace and Young (Isenberg, 1992) on surface tension. In addition to surface tension, the energy of a surface is determined by the bending rigidity of the membrane itself and also by forces that arise externally, e.g. from the cytoskeleton. Considering all these contributions, a geometric theory of elastic surfaces has to provide general answers to the questions of what the equilibrium configuration of a cell is and how elementary excitations from an equilibrium configuration look.

Fig. 1 shows a few moments out of the "flickering" life of a red blood cell and the inherent undulations of its membrane surface. Since the surface tension of its cell membrane is low and the membrane is highly flexible (so that the cell can penetrate easily through narrow veins) the fluctuation amplitudes are high. Hence flickering is even clearly visible under an ordinary microscope. It was discovered more than a century ago (Brouricz, 1890). As we see, *waves* sweep over the cell membrane (Marx et al., 2002) despite its having a (typically) ovoid equilibrium form at rest. Why is this so? How can we describe it? And how successful is this description?

Biomembrane undulations. As has been shown convincingly by Brochard and Lennon (1975), the aqueous solution enveloping the cell acts as a heat bath generating undulations (Fig. 1). To describe the cell's equilibrium form physically, it is natural to assume it is a minimum of an energy function or, in the present case, an energy functional. Minima are obtained by differentiation and follow from a vanishing of the first derivative. This, then, would assign to a cell its equilibrium form, being defined through the minimal elastic energy of both cell and cell membrane. But an equilibrium form does not tell us anything about the steady flickering a cell is subject to.

The idea to explain flickering and many other phenomena of 'lower excited states' such as phonons in a crystal is that of *elementary excitations*, dating back to Landau (Landau, 1941); for a more recent and comprehensive vision, see Anderson (1963). Key to this construct is the concept of energy function. Setting its first derivative equal to zero we find extrema that are to be associated with equilibria. Computing the second derivative we may find elementary excitations from a state corresponding to an extremum. If their energies are positive, the extremum is a minimum, maybe a local one, and stable. If some of the energies are negative, the extremum is a saddle point and unstable. Second derivatives give rise to *quadratic* forms that can be diagonalized and, hence, to exact solutions making elementary excitations as a notion so popular. So the next question is: How to get a suitable energy functional describing a biomembrane?

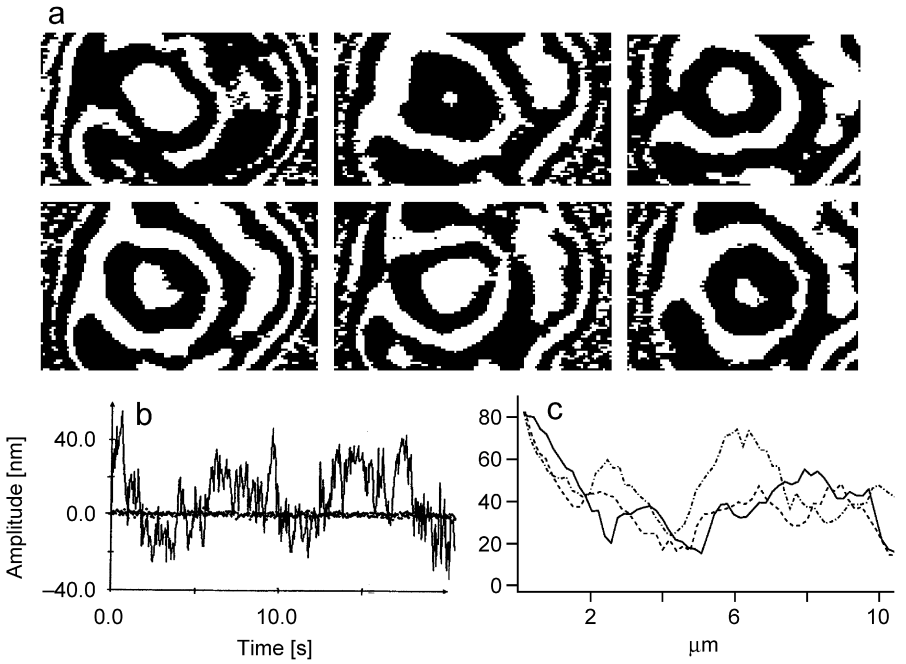

Fig. 1. Membrane fluctuations, so-called undulations, of a red blood cell of size $\approx 10\,\mu$m. (a). Temporal sequence of contrast-enhanced pictures of thermally excited surface undulations of a red blood cell provided by dynamic reflection interference contrast microscopy (RICM) (Zilker et al., 1987). One sees the time-dependent lateral deformation of Newtonian rings generated by the cell-membrane fluctuations. The temporal separation between the pictures (left-right, top-bottom) is 0.2 s. (b). Resolution [nm] of amplitude fluctuations at a specific site as a function of time and (c) along a 10 μm strip of a giant DEPC (50 mol cholesterol) vesicle at three different times: 0 s (dot–dashed), 4.8 s (solid) and 5.3 s (dashed). Picture courtesy of Andreas Zilker (a, b), Stefanie Marx (c).

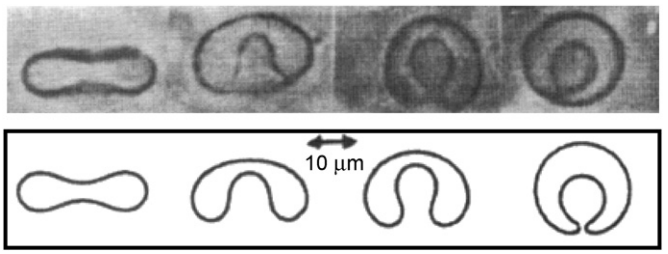

Fig. 2. Discocyte–stomatocyte transition of a free vesicle with a 'fluid' membrane. Top: experimental pictures (Berndl et al., 1990) for increasing temperatures: 43.8, 43.9, 44.0, and 44.1 °C. The shapes are axisymmetric with respect to the vertical. Bottom: corresponding equilibrium shapes as provided by the theory of Seifert et al. (1991), which explains the complicated phase diagram as well.

Biomembrane undulations and continuum mechanics. An energy functional describing a biomembrane depends on its *shape*. Depending on shape it is a functional and not a function anymore. But why can we for instance reduce a biomembrane, a lipid bilayer of finite thickness $h > 0$, to a "shape"? Let us describe a cell membrane as a curved surface equipped with a finite thickness h and curvature R^{-1} where R is a "typical" radius of curvature; we just want to estimate orders of magnitude. A glance at Figs. 1c and 2 suffices to convince us that, say, $R \geqslant 1\,\mu$m. The central idea is that $h \ll R$. This is indeed correct since $h \approx 10\,$nm is two orders of magnitude smaller. We now replace the membrane by a smooth surface, also called manifold, and apply *continuum* mechanics to this sheet of finite thickness, leaving us in Section 3 with an energy functional neatly depending on geometric quantities only and containing h as a *pre*factor. Even inhomogeneous "sandwich" membranes can be described this way. Though this sounds physically quite appealing, we may and, in fact, should ask: How good is it?

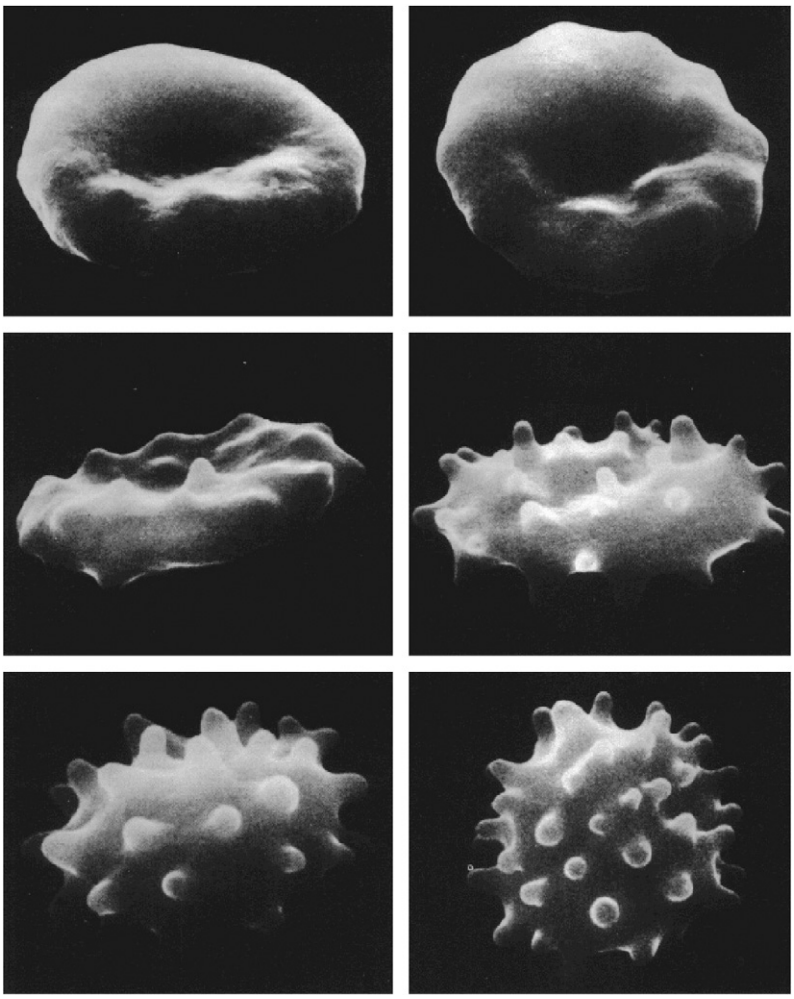

Fig. 3. Red blood cell undergoing the so-called stomatocyte–discocyte–echinocyte transition (Ponder, 1948), left → right & top → bottom. It passes through a 'main sequence' of shapes as one increases a specific parameter such as the pH or salt of the aqueous solution it is in. The main sequence does not depend on the specific parameter that is varied, i.e., it is universal. It starts as a concavely shaped stomatocyte, becomes a round discocyte, and finally ends up as an echinocyte with convex rounded protrusions or spicules. Analogously to Fig. 2, the universal 'main sequence' can be described fully (Lim et al., 2002; Mukhopadhyay et al., 2002) by the geometric theory of elasticity explained in Section 3. Picture courtesy of Erich Sackmann.

As a first example we turn to shape transformations of a vesicle induced by a change in temperature. The vesicle is freely floating in an aqueous solution, keeping area and volume constant. Its energy is that given by (19), which will be derived below, and the ensuing analysis stems from Seifert et al. (1991). A more general and, in fact, simpler derivation is presented in Section 11.1; see also Section 11.3. As Fig. 2 shows, experiment and theory agree nicely.

The shape transformations of mammalian red blood cells are even more spectacular. Their natural shape is a biconcave disk of diameter $\approx 8\,\mu m$ (Fig. 3, top-left corner). Unlike most human cells, red blood cells have no internal formed elements; in particular, no three-dimensional protein meshwork. Instead, a two-dimensional protein skeleton is apposed to the cytoplasmic side of the membrane (cf. the sandwich plate of Section 3). Both the lipid bilayer and the skeleton are highly flexible and elastic, allowing the red cell to squeeze through narrow capillaries. A variety of membrane intercalators can modify this shape dramatically and reversibly at constant area and volume as illustrated in Fig. 3.

One class of agents such as high salt or high pH induces a series of crenated shapes, called echinocytes, with their characteristic convex rounded protrusions or spicules. On the other hand, for low salt or low pH concave shapes called stomatocytes appear, as in the top left corner of Fig 3. The total, *main sequence* is universal in the sense that the

shapes seen and the order of appearance do not depend on the specific agent. It is therefore natural to look for intrinsic membrane properties as an explanation of the main sequence of red-blood-cell shapes.

Sheetz and Singer (1974) were the first to come up with such a universal explanation in that they hypothesized induction of a small change ΔA in the relaxed area difference between the two leaflets of the cell membrane, a lipid bilayer, to be the driving mechanism. An expansion of the outer leaflet with respect to the inner one ($\Delta A > 0$) produces a tendency to form convex structures on the cell surface such as spicules so as to accommodate the extra area. On the other hand, a decrease ($\Delta A < 0$) would favor concavities such as stomatocytic structures.

It is a major achievement of Wortis and coworkers (Lim et al., 2002; Mukhopadhyay et al., 2002) to have devised a mathematical model (see Section 9) based on merely geometric structures such as mean and Gaussian curvature (see Section 4) to explain the complete main sequence as described above and part of which is shown in Fig. 3. That is, here too we have a striking confirmation of the usefulness of continuum mechanics in conjunction with classical differential geometry to fully explain the behavior of cell membranes on the basis of a free-energy functional expressed in terms of geometric quantities only.

Biomembrane undulations and differential geometry. All this is quickly said but not that quickly done. The novel, and fascinating, aspect of the membrane problem in general and the biomembrane problem in particular (Nelson et al., 1989; Lipowsky, 1991; Seifert et al., 1991; Sackmann, 1994; Safran, 1994; Peliti, 1996; Seifert, 1997; Boal, 2002) is that its energy is a functional depending on the shape of the membrane surface instead of being a function depending on the particles' coordinates. Furthermore, membrane undulations show a dazzling richness of behavior (Engelhardt et al., 1985; Zilker et al., 1987; Duwe and Sackmann, 1990; Marx et al., 2002; Peterson et al., 1992; Strey et al., 1995; Zilker et al., 1992) and often provide surprising insight into underlying processes, e.g., as a consequence of the elasticity depending critically on constituents and additives. In fact, at many occasions (Hyde et al., 1997) shape is a dominating aspect of science. Or, as Hildebrandt and Tromba (1996) aptly put it, why does nature produce certain forms, and why does it prefer them to other conceivable forms?

Differentiation with respect to shapes, though in principle well-known from the calculus of variations, is nontrivial in practice and therefore needs efficient tools. It is the goal of the present paper to offer these tools through classical differential geometry. As we will see, this kind of geometry provides us with explicit and simple but nevertheless efficient techniques to fully solve the elementary excitation problem of biomembranes. A novel and promising application is *adhesion* of membranes and vesicles on a substrate. See, for instance, Komura and Andelman (2000), Bruinsma and Sackmann (2001), Guttenberg et al. (2001), Marx et al. (2002), and Zidovska and Sackmann (2006); theoretical foundations date back to Seifert and Lipowsky (1990). For various other types of undulation phenomenon we refer to the literature (Boal, 2002; de Jeu et al., 2003; Kleman and Lavrentovich, 2002).

We first analyze the elementary excitation idea proper in the much simpler phonon context, then provide a concise derivation of the energy functional describing the most general case of an elastic membrane equipped with locally specified spontaneous curvature, present the classical differential-geometric formalism that is needed for the solution of this continuum problem in two parts separated by the nearly flat membrane, which functions as a motivation for what follows, and finish with a general derivation of the first and second functional derivatives, independent of the specific shape or symmetry of the membrane, once a notoriously difficult problem. The paper is self-contained and rarely exceeds calculus level. As such, it is presented with the intent of stimulating independent work by novice investigators.

2. Specimen of elementary excitations: phonons

A crystal is described by a Hamilton function, in short energy, of the form

$$\mathcal{H} = \sum_{i=1}^{N} \frac{1}{2m} \boldsymbol{p}(i)^2 + V(\boldsymbol{q}(i); 1 \leqslant i \leqslant N), \tag{1}$$

where $V = V(\boldsymbol{q}(1), \ldots, \boldsymbol{q}(N))$ is the potential energy of N classical particles with momenta $\boldsymbol{p}(i)$ and coordinates $\boldsymbol{q}(i)$ and i running from 1 to N. The equations of motion directly follow from $\mathcal{H}$ through Hamilton's equations of motion $\dot{q}_\alpha(i) = \partial\mathcal{H}/\partial p_\alpha(i)$ and $\dot{p}_\alpha(i) = -\partial\mathcal{H}/\partial q_\alpha(i)$ so as to read

$$m\ddot{q}_\alpha(i) = -\partial_{q_\alpha(i)} V, \quad 1 \leqslant \alpha \leqslant 3, \quad 1 \leqslant i \leqslant N, \tag{2}$$

a rewording of Newton's law for N particles interacting through a potential V in three-dimensional space.

At zero temperature we require the crystal to be in equilibrium at a stationary configuration where $\partial_{q_\alpha(i)} V := \partial V/\partial q_\alpha(i) = 0$, whatever i and α. We choose coordinates so that $\boldsymbol{q}(i) \equiv 0$, $1 \leqslant i \leqslant N$, characterizes the stationary point $\partial V = 0$ and study *small deviations* $\boldsymbol{q}(i) \neq 0$, corresponding to low-temperature behavior. A Taylor expansion then gives

$$V(\boldsymbol{q}(i); 1 \leqslant i \leqslant N) = V(0) + \sum_{\alpha,i} \underbrace{\partial_{q_\alpha(i)} V(0)}_{0} q_\alpha(i) + \frac{1}{2} \sum_{\alpha,i;\beta,j} \underbrace{\partial_{q_\alpha(i)} \partial_{q_\beta(j)} V(0)}_{\Phi^{i,j}_{\alpha,\beta}} q_\alpha(i) q_\beta(j) + \mathcal{O}(q^3)$$

$$=: V(0) + \frac{1}{2} \boldsymbol{q} \Phi \boldsymbol{q} \tag{3}$$

with $\boldsymbol{q} = (\boldsymbol{q}(i); 1 \leqslant i \leqslant N) \in \mathbb{R}^{3N}$. The configuration $\boldsymbol{q} = 0$ is stable, if and only if $\boldsymbol{q}\Phi\boldsymbol{q} > 0$ for all $\boldsymbol{q} \neq 0$.

The second derivative of V is a *quadratic* form corresponding the real *symmetric* matrix Φ. The symmetry $\Phi^{i,j}_{\alpha,\beta} = \Phi^{j,i}_{\beta,\alpha}$ follows from V being smooth enough so that

$$\partial_{q_\alpha(i)} \partial_{q_\beta(j)} V = \partial_{q_\beta(j)} \partial_{q_\alpha(i)} V, \tag{4}$$

a property that we will often invoke in a more general context. Φ's eigenvalues λ are real and positive once $\boldsymbol{q}\Phi\boldsymbol{q} \geqslant 0$ for all $\boldsymbol{q}$. Its eigenvectors $\boldsymbol{e}_\lambda$ can be taken to be orthonormal. The equations of motion for the approximate potential (3) follow from (2) so as to read $\ddot{\boldsymbol{q}} = -m^{-1}\Phi\boldsymbol{q}$. Being linear, this system is exactly soluble. Making the ansatz $\boldsymbol{q} = x(t)\boldsymbol{e}_\lambda$ we directly find $\ddot{x} + (\lambda/m)x = 0$. The solution is oscillating for $\lambda > 0$, signaling stability, and explodes for $\lambda < 0$, indicating instability of the stationary configuration we started with.

Finally, the eigenvectors $\boldsymbol{e}_\lambda$ being orthonormal, we can build an orthogonal matrix $O = \{\boldsymbol{e}_1, \ldots, \boldsymbol{e}_{3N}\}$ out of them. This matrix diagonalizes Φ in that

$$\Phi = O \operatorname{diag}(\lambda_1, \ldots, \lambda_{3N}) O^\dagger \Leftrightarrow O^\dagger \Phi O = \Lambda \tag{5}$$

with $\Lambda = \operatorname{diag}(\lambda_1, \ldots, \lambda_{3n})$ being diagonal. Since the dynamics is linear we get $\ddot{\boldsymbol{Q}} = -\Lambda\boldsymbol{Q}$ corresponding to a canonical transformation $\boldsymbol{q} = O\boldsymbol{Q}$ that gives the Hamilton function $\mathcal{H} = \boldsymbol{P}\mathbb{1}\boldsymbol{P}/2m + \boldsymbol{Q}\Lambda\boldsymbol{Q}/2$ for $3N$ independent harmonic oscillators. In a heat bath at temperature T the mean potential energy (Huang, 1987) of each of them is $k_\mathrm{B}T/2$.

3. Elastic energy of biomembranes

To gain motivation for studying classical differential geometry, we are going to derive the elastic energy of a biomembrane by studying it as if it were a thin plate. The advantage of the present argument is its generality in that it needs no additional assumptions on top of the standard ones. Furthermore, the result has been shown experimentally to be generally applicable (Lipowsky, 1991; Seifert et al., 1991; Sackmann, 1994; Lim et al., 2002). The underlying physical assumptions are the following.

First, the thin plate we are considering has a *neutral surface* on which, to first order, there is no extension or compression, and on opposite sides of which the deformation has opposite signs. For a truly elastic medium this is not an *ad hoc* assumption but a decent approximation (Landau and Lifshitz, 1986).

Second, the plate is so thin that tension along any normal is negligible.

Third, our theory is *linear*. We consider the plate locally and, if it is already curved, assume that the small piece we are focusing on has its x and y axes parallel to the principal directions; cf. Section 4.5. Linearity implies that the relative change $\Delta l/l$ for given tension σ_{xx} parallel to the x-axis satisfies Hooke's law $(\Delta l/l)_x = \sigma_{xx}/E$ with E as Young's modulus. There is an additional contraction $\sigma(\Delta l/l)_x$ along the y-axis, where σ is Poisson's ratio, which can never lead to ambiguity since it never has a suffix; for some materials $\sigma < 0$ (Boal et al., 1993; Bowick et al., 2001; Lakes, 2001). Because of linearity, the amount of work done by the tension σ_{yy} can be *added* to that originating from σ_{xx}. In passing we note that $\sigma_{\alpha\beta}$ is defined (Landau and Lifshitz, 1986) to be the α-component of a force on unit area perpendicular to the β-axis.

Fourth, we initially assume the plate is homogeneous but we will see this is not necessary. That is to say, the same arguments apply to "sandwich" plates such as biomembranes, of which bottom and top are harder than the interior; cf. (17) and (18). We will also see that for a thin plate or membrane *with spontaneous curvature* the same arguments are valid so that e.g. the energy in (15) contains a fit parameter $\kappa_0 \neq 0$ to start with.

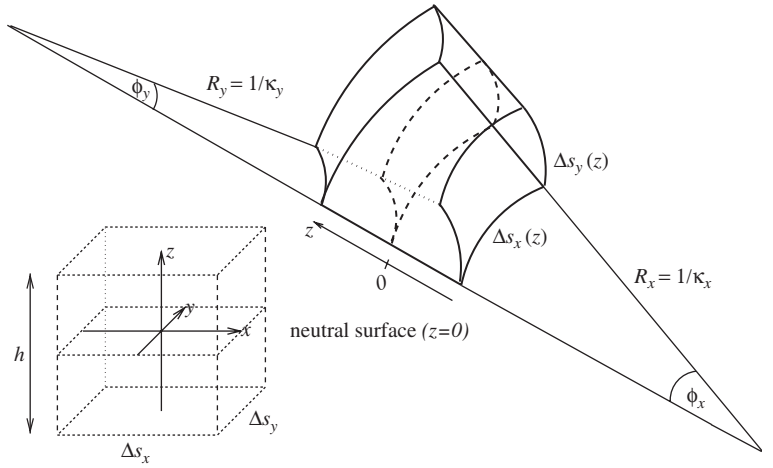

Fig. 4. An element of a thin plate idealizing a membrane with thickness h (Rayleigh, 1894) and surface area $\Delta s_x \Delta s_y$ is bent first in the x-, then in the y-direction. Lengths are thereby changed in dependence upon the height z and the angles $\phi = \Delta s/R$. The neutral surface is at $z = 0$.

In summary, the first assumption is natural, the second is relatively harmless as biomembranes are remarkably rigid in normal direction, the third is essential but justified by experiment, and the fourth can be dispensed with.

Let

$$\Delta s_{x/y}(z) = (R_{x/y} + z)\phi_{x/y}, \tag{6}$$

be the length of either side of a surface element in x- and y-direction in dependence upon the height z; see Fig. 4. The neutral surface is at $z = 0$ and we take it as the manifold $\mathcal{M}$ that represents the form of the membrane; see Section 4.1. The angles $\phi_{x/y}$ can be assumed to be small since the surface element is small itself. As shown by Fig. 4, the radii of curvature $R_{1/2} = |\kappa_{1/2}|^{-1}$ describe our piece of surface. According to Meusnier (Section 4.6), we can take $\kappa_{1/2}$ to be the usual curvatures (Thomas, 1972) of the intersection of our surface and a plane through the normal vector and the x- and y-axis, respectively. The $\kappa_{1/2}$ are principal curvatures (Section 4.6), if the x- and y-axis are principal directions; by construction these directions are in the tangent plane.

For relative length changes in the direction of x- and y-axis, viz.,

$$u_{xx} := \frac{\Delta s_x(z) - \Delta s_x(0)}{\Delta s_x(0)} = \frac{z}{R_1} = \kappa_1 z, \tag{7}$$

$$u_{yy} := \frac{\Delta s_y(z) - \Delta s_y(0)}{\Delta s_y(0)} = \frac{z}{R_2} = \kappa_2 z, \tag{8}$$

Hooke's law holds,

$$u_{xx} = \frac{1}{E}(\sigma_{xx} - \sigma\sigma_{yy}), \tag{9}$$

$$u_{yy} = \frac{1}{E}(\sigma_{yy} - \sigma\sigma_{xx}), \tag{10}$$

with E as Young's modulus and σ as Poisson's ratio. One can solve Eqs. (9) and (10) for the tensions σ_{xx} and σ_{yy},

$$\sigma_{xx} = \frac{E}{1-\sigma^2}(u_{xx} + \sigma u_{yy}), \tag{11}$$

$$\sigma_{yy} = \frac{E}{1-\sigma^2}(u_{yy} + \sigma u_{xx}). \tag{12}$$

For the moments of force in x- and y-direction (force = tension times area so that $f_{x/y} = \sigma_{xx/yy}\Delta s_{y/x}\,\mathrm{d}z$) we obtain from (11) and (12) in conjunction with (7) and (8)

$$\begin{aligned} M_x &= \int_{-h/2}^{h/2} \mathrm{d}z \Delta s_y z \sigma_{xx} = \frac{E}{1-\sigma^2}\Delta s_y \int_{-h/2}^{h/2} \mathrm{d}z(\kappa_1 + \sigma\kappa_2)z^2 \\ &= \frac{E}{1-\sigma^2}\Delta s_y \frac{h^3}{12}(\kappa_1 + \sigma\kappa_2), \end{aligned} \tag{13}$$

$$M_y = \frac{E}{1-\sigma^2}\Delta s_x \frac{h^3}{12}(\kappa_2 + \sigma\kappa_1). \tag{14}$$

A torque $\mathbf{M} = \mathbf{r} \times \mathbf{F}$ is generated by a force $\mathbf{F}$ acting at position $\mathbf{r}$ and rotated by a small angle $\mathrm{d}\phi$ about an axis $\hat{\mathbf{e}}$, a unit vector. It gives rise to an infinitesimal amount of work $\mathbf{F}\,\mathrm{d}\mathbf{s}$ where, due to the rotation, $\mathrm{d}\mathbf{s} = \mathrm{d}\phi\hat{\mathbf{e}} \times \mathbf{r}$. Hence $\mathbf{F}\mathrm{d}\mathbf{s} = \mathbf{M}(\mathrm{d}\phi\hat{\mathbf{e}})$. The infinitesimal amount of work needed to bend a surface area $\Delta f := \Delta s_x \Delta s_y$ and generate a potential energy $d(\Delta E_{\mathrm{pot}})$ is therefore

$$\begin{aligned} d(\Delta E_{\mathrm{pot}}) &= M_x\,\mathrm{d}\phi_x + M_y\,\mathrm{d}\phi_y \\ &= M_x \Delta s_x\,\mathrm{d}\kappa_1 + M_y \Delta s_y\,\mathrm{d}\kappa_2 \\ &= \frac{Eh^3}{12(1-\sigma^2)}\Delta s_x \Delta s_y[(\kappa_1 + \sigma\kappa_2)\,\mathrm{d}\kappa_1 + (\kappa_2 + \sigma\kappa_1)\,\mathrm{d}\kappa_2] \\ &= \frac{Eh^3}{12(1-\sigma^2)}\Delta f\left[\frac{1}{2}d(\kappa_1^2 + \kappa_2^2) + \sigma d(\kappa_1\kappa_2)\right] \\ &= \frac{Eh^3}{12(1-\sigma^2)}\Delta f\left[\frac{1}{2}\,\mathrm{d}\mathbb{H}^2 + (\sigma-1)\,\mathrm{d}\mathbb{K}\right], \end{aligned} \tag{15}$$

where $\kappa_i = 1/R_i$ for $i = 1, 2$, $\mathrm{d}\phi_{x/y} = \Delta s_{x/y}(0)\,\mathrm{d}\kappa_{1/2}$ since the neutral surface is at $z = 0$, and $\mathbb{H} = \kappa_1 + \kappa_2$ is the mean while $\mathbb{K} = \kappa_1\kappa_2$ is the Gaussian curvature; cf. Fig. 4 and Section 4.6 below. Both $\mathbb{H}$ and $\mathbb{K}$ are quantities independent of the parametrization because they can be written as trace and determinant of a linear operator that depends on the local shape only; cf. Section 4.6. Hence $\mathrm{d}\mathbb{H}^2$ and $\mathrm{d}\mathbb{K}$ are *total* differentials.

We can now simply integrate (15) from initial to final configuration and obtain for a surface element $\Delta f = \Delta s_x \Delta s_y$

$$\Delta E_{\mathrm{pot}} = \Delta s_x \Delta s_y \left(\frac{k_c}{2}\mathbb{H}^2 + \frac{k_g}{2}\mathbb{K}\right). \tag{16}$$

In so doing we have defined *bending rigidities* $k_c > 0$ and $k_g < 0$ (as a fit parameter k_g turns out to have either sign) through

$$k_c = \frac{E}{1-\sigma^2}\frac{h^3}{12}, \quad k_g = -\frac{E}{1+\sigma}\frac{h^3}{6}. \tag{17}$$

With different names for E and σ expressions (16) and (17) have already been given by Rayleigh (1894, Section 214), who credits Thomson and Tait (1878, Sections 639, 642, 720).

Biological membranes are in general not as homogeneous as we had assumed in the above derivation. Nevertheless we can easily improve on (16) & (17) by substituting $E \to E(z)$ and $\sigma \to \sigma(z)$, and assuming $E(z)$ and $\sigma(z)$ to be functions of the height z so as to get a "sandwich" plate, a self-explanatory notion dating back to at least the forties of the last century (Reissner, 1947; Schäfer, 1952). We then find completely analogously to the homogeneous case

$$k_c = \int_{-h/2}^{h/2} \mathrm{d}z \frac{z^2 E(z)}{1-\sigma(z)^2}, \quad k_g = -\int_{-h/2}^{h/2} \mathrm{d}z \frac{2z^2 E(z)}{1+\sigma(z)}. \tag{18}$$

Completing the Riemann sum in (16) over all the Δf's, i.e., integrating (16) with respect to $\mathrm{d}f$ over the whole manifold, for instance a vesicle, and incorporating spontaneous curvature for the moment as a fit parameter κ_0, we arrive at the energy functional

$$\mathcal{F} = \frac{1}{2}k_c \int \mathrm{d}f\,(\kappa_1 + \kappa_2 - \kappa_0)^2 + \frac{1}{2}k_g \int \mathrm{d}f\,\kappa_1\kappa_2. \tag{19}$$

To take care of lateral tension we can add ΣA where A is the total area and the surface tension Σ plays the role of a Lagrange multiplier (Segel, 1977) for the total area of $\mathcal{M}$. In a similar vein one can handle volume effects by adding $-PV$ to (19) with V as volume and P as pressure.

Let us suppose for a moment the side conditions of constant area A and volume V were not there. According to Theorem (61) of Gauss–Bonnet the term $\int \mathrm{d}f\,(\mathbb{K} = \kappa_1\kappa_2)$ is a topological invariant that plays no role as long we punch no holes into and eliminate no handles from $\mathcal{M}$. Then the solution to (19) is simply a surface of constant mean curvature $\mathbb{H} := \kappa_1 + \kappa_2 = \kappa_0$; a *minimal* surface has $\mathbb{H} = 0$ (Oprea, 2000; Kenmotsu, 2003). The trouble, however, is that a surface such as a 'minimal' one characterized by $\mathbb{H} = 0$ provides a minimum to (19) but is in general *not* closed. Hence it cannot represent the biological physics of, say, a cell membrane.

The functional (19) is also called a "free" energy, though neither its derivation nor its mathematical appearance show any temperature dependence or entropy yet. It was introduced by Canham (1970), Helfrich (1973), and Evans (1974) while Boruvka and Neumann (1977) studied its first but not its second derivative in the more general context of capillarity as conceived originally by J.W. Gibbs. It has been reviewed and further developed ever since (Deuling and Helfrich, 1976; Nelson et al., 1989; Lipowsky, 1991; Seifert et al., 1991; Sackmann, 1994; Safran, 1994; Peliti, 1996; Seifert, 1997; Boal, 2002); see in particular Seifert (1997) for an enlightening overview of the older literature.

It was also Seifert (1991) who stressed the relevance of $\int \mathrm{d}f\,\mathbb{H}^2$ being invariant under conformal transformations, i.e., angle-preserving mappings (Willmore, 1982). It is a nontrivial result dating back to Liouville (1850) that in $\mathbb{R}^3$ only translations, rotations, and inversions, viz., reflections, in spheres are conformal. We will see how conformal invariance comes about in Section 9. It was already known to Thomsen (1924) and rediscovered for physics by Duplantier (1990, Section 7); see Duplantier et al. (1990) for a first application.

Evans (1974) introduced the 'bilayer coupling model' (BCM), refraining from the spontaneous curvature κ_0 as such but requiring instead that the integrated mean curvature $M := \int \mathrm{d}f\,\mathbb{H}$ be fixed. One then introduces curvature through the lipid-*bi*layer character of a biomembrane in that the total area ΔA of the inner leaf of the lipid bilayer be slightly different from that of the outer one. In practice this means that one puts $\kappa_0 = 0$ in (19) and adds a term QM with Q as Lagrange multiplier. The proof of this assertion is a simple computation provided by (128) below.

By writing out (19) we can easily verify that BCM and (19) are formally equivalent if we put $\Sigma_{\mathrm{BCM}} := \Sigma + 1/2k_c\kappa_0^2$ and $Q_{\mathrm{BCM}} := -k_c\kappa_0$. Their stationary points with vanishing first derivative are identical. We then have to apply the side constraints of fixed surface area A, volume V, and mean curvature M so that the formal equivalence is not a real one by lack of freedom in the parameters. Accordingly, the second derivatives and, thus, stability are different (Peterson, 1988; Seifert, 1995); for additional information one may also consult Svetina and Žekš (1989) and Miao et al. (1994).

The latter did not fix a vesicle's area and volume but described the complete phase diagram for budding and vesiculation in the context of an area-difference elasticity (ADE) model that takes into account elastic stretching associated with ΔA as well; see also Döbereiner et al. (1997) and Zeman et al. (1990). In a sense (Miao et al., 1994), the ADE model interpolates between BCM and (19). We now turn to the question of where spontaneous curvature comes from and present a direct solution, which is even more general than simply justifying κ_0.

Energy and spontaneous curvature. Let us start with an a priori *given*, so to speak pre-curved, membrane form. For cell membranes this starting point is quite natural since an actin network in the cell often stabilizes the membrane's shape (Boulbitch et al., 2000; Sackmann et al., 2002). Let $\mathcal{M}^0$ be the original cell form specified as a manifold and let $\{(\kappa_1^{(0)}(\boldsymbol{x}), \kappa_2^{(0)}(\boldsymbol{x})); \boldsymbol{x} \in \mathcal{M}^0\}$ be its "spontaneous" curvatures. In other words, as in a pre-bent plate, each surface element already exhibits two principal curvatures $\kappa_1^{(0)} = 1/R_1^{(0)}$ and $\kappa_2^{(0)} = 1/R_2^{(0)}$ along two orthogonal principal directions; cf. Fig. 4 and Section 4.5. Here a, maybe local, energy minimum is realized. Accordingly we return to Eqs. (7)–(10) and modify Hooke's law so that a relative change $u_{xx/yy}^{(0)}(z) = \kappa_{1/2}^{(0)} z$ induces no tension, for example, through the natural ansatz

$$\sigma_{xx/yy} = \frac{E}{1-\sigma^2}\left[(u_{xx/yy} - u_{xx/yy}^{(0)}) + \sigma(u_{yy/xx} - u_{yy/xx}^{(0)})\right],$$

where x- and y-axis agree with the principal directions in $\boldsymbol{x} \in \mathcal{M}^{(0)}$. Proceeding as before, with $\mathbb{H} = \kappa_1 + \kappa_2$ and $\mathbb{K} = \kappa_1\kappa_2$, we arrive at

$$\begin{aligned} d(\Delta E_{\rm pot}) &= M_x\,\mathrm{d}\phi_x + M_y\,\mathrm{d}\phi_y = M_x\Delta s_x\,\mathrm{d}\kappa_1 + M_y\Delta s_y\,\mathrm{d}\kappa_2 \\ &= \frac{Eh^3}{12(1-\sigma^2)}\Delta s_x\Delta s_y\{[(\kappa_1-\kappa_1^{(0)})+\sigma(\kappa_2-\kappa_2^{(0)})]d(\kappa_1-\kappa_1^{(0)}) \\ &\quad + [(\kappa_2-\kappa_2^{(0)})+\sigma(\kappa_1-\kappa_1^{(0)})]d(\kappa_2-\kappa_2^{(0)})]\} \\ &= \frac{Eh^3}{12(1-\sigma^2)}\Delta f\left[\frac{1}{2}d(\mathbb{H}-\mathbb{H}^{(0)})^2+(\sigma-1)d(\kappa_1-\kappa_1^{(0)})(\kappa_2-\kappa_2^{(0)})\right] \\ &= \Delta f\left[\frac{k_c}{2}d(\mathbb{H}-\mathbb{H}^{(0)})^2+\frac{k_g}{2}d(\kappa_1-\kappa_1^{(0)})(\kappa_2-\kappa_2^{(0)})\right]. \end{aligned}$$

In case of an isotropic spontaneous curvature we end up with $\kappa_1^{(0)} = \kappa_2^{(0)} = \kappa_0/2$, e.g., because the actin network is isotropic, or absent as in a vesicle (Boal, 2002). Hence

$$d(\kappa_1-\kappa_1^{(0)})(\kappa_2-\kappa_2^{(0)}) = \mathrm{d}\mathbb{K} - (\kappa_0/2)\,\mathrm{d}\mathbb{H}$$

is a total differential so that after integration we get

$$\Delta E_{\rm pot} = \Delta f\left[\frac{k_c}{2}(\mathbb{H}-\mathbb{H}^{(0)})^2+\frac{k_g}{2}(\mathbb{K}-\mathbb{H}\kappa_0/2)\right] \tag{20}$$

plus a trivial additive constant $k_g\kappa_0^2/8$. The paraboloid $E_{\rm pot}(\kappa_1,\kappa_2)$ has a minimum $E_{\rm pot} = 0$ in the force-free state $\kappa_1 = \kappa_2 = \kappa_0/2$, provided $k_c > |k_g|/4$.

As a continuum approach incorporating cytoskeleton effects, the present arguments can be called fine-grained; see also Kuzman et al. (2004). The cytoskeleton as a network of filamentous proteins, then, is 'coarse'-grained and a much harder analysis such as that of Head et al. (2003) and Wilhelm and Frey (2003) leads to a deeper and more detailed understanding of viscoelastic cell response.

Heading for an analysis of membrane fluctuations in Section 11 we could also accept a 'medium'-sized approach in between as advocated by Gov et al. (2003) and Gov and Safran (2005), who incorporated confining effects of the cytoskeleton, e.g., for red blood cells a spectrin network, by taking the latter to be a *fixed* open mesh separated from the membrane through a 'confining' harmonic potential keeping it at a distance $\approx \ell$ but attached to it by at discrete points that are relatively far apart; for instance, 100 nm with $\ell = 25$ nm. In this way the attachment of the membrane to the cytoskeleton causes stretching and gives rise to a relatively high surface tension Σ. The *confining shell model* of Gov et al. is an intriguing new idea that we will touch upon at the end of Section 5.

The functional (19) or (20) integrated over the membrane surface is defined on smooth *membrane shapes*. As an energy it should be minimized. That is, it should be "differentiated". Its first derivative should vanish and its second derivative should be positive-definite so as to guarantee stability. To handle differentiation efficiently we need classical differential geometry, the more so since in the above derivation of the membrane energy we have already met several of its standard notions, such as differentiable manifold, curvature, principal, mean, and Gaussian curvature, principal direction, and Meusnier's theorem. So this is what we now embark on.

4. Classical differential geometry

Elastic response of biological membranes is practically synonymous with the physics of curved surfaces, and differential geometry is the mathematics that is most natural to describing them. Membranes are concrete physical objects and one of the purposes of the present paper is to show that abstract mathematics is undue. Even better, we will show that classical differential geometry has an intrinsic elegance allowing direct insight into what is going on and also providing, as we will see, an ideal access to describing a membrane's elementary excitations, viz., its undulations. In addition, it is widely applicable in soft-matter physics; see, for example, de Jeu et al. (2003).

Though there is a plethora of specific references, particularly on general relativity (Misner et al., 1973; Stephani, 1990), there are not too many focusing on differential geometry and physics of curved surfaces in general. An accessible

one Frankel (1997). Handling differential geometry from an abstract, hence coordinate-free, point of view, it is at a high level and, all in all, far too advanced for most of the problems in biological and condensed-matter physics. The introductory text of Boal (2002) treats the mechanics of the cell in a clear and succinct way but, as a consequence, has to effectively skip curvature. As we would say later on, here the metric tensor is taken to be the unit matrix $\mathbb{1}$.

The paper by Kamien (2002) and the present one both expound classical differential geometry (Gerretsen, 1962; Millman and Parker, 1977; Struik, 1961) as fascinating mathematics, apt to solve many problems in soft-matter physics. The two papers complement each other. Kamien's elegant composition is mainly devoted to curves on surfaces and related theorems, such as Gauss-Bonnet, and is thus directly applicable to clarifying mechanisms inherent to line-shaped structures, e.g., bacterial flagellar motion (Goldstein et al., 1998, 2000; Coombs et al., 2002). The present work focuses on intrinsic properties of a surface such as metric tensor, mean curvature, and derived quantities, notably energy densities and associated operators à la Laplace–Beltrami. Together they present a natural language for describing membrane undulations. We are now going to introduce the underlying formalism and start with the central object of our study, a manifold.

4.1. Hypersurfaces and manifolds

The main object of membrane physics is a hypersurface, an n-dimensional differentiable manifold in $(n+1)$-dimensional space $\mathbb{R}^{n+1}$, throughout what follows simply called a *manifold* $\mathcal{M}$. In our case $n=2$ but it is good to keep in mind that practically all results that are derived below hold for any finite n. Sloppily formulated, positions $\boldsymbol{x}$ on our surface depend smoothly on n parameters q^κ with $1\leqslant\kappa\leqslant n$ so that for a point $\boldsymbol{x}\in\mathcal{M}$ we have an at least three times continuously differentiable map

$$\mathbb{R}^n \ni (q^\kappa) \mapsto \boldsymbol{x}(q^\kappa) \in \mathcal{M} \subset \mathbb{R}^{n+1}. \tag{21}$$

This map is called a coordinate map or chart, is locally one-to-one, and as smooth as needed. A specific chart is nothing but a specific parametrization. Different charts are then packed into an atlas (Milnor, 1997); see below for the sphere as an example. In practice we can often dispense with the atlas. Evidently, geometric properties do not depend on the specific parametrization we are working with.

Let us take as a parametrization example the surface $\mathcal{M}$ of a two-dimensional sphere or two-sphere $x^2+y^2+z^2=R^2$ in $\mathbb{R}^3$, i.e., $n=2$. Here the coordinate map

$$(x,y)\mapsto\left(x,y,\sqrt{R^2-x^2-y^2}\right) \tag{22}$$

with $x^2+y^2<R^2$ parametrizes the region $z>0$. It is one-to-one and smooth. By interchanging x, y, and z, and changing signs of variables we obtain six charts that cover all of the two-sphere. So to fully describe $\mathcal{M}$ we need several charts, which are to be compatible (here they are) before they can be packed into an atlas. The latter need not be unique either. For instance, for the two-sphere one could also take spherical coordinates with $r=R$ fixed. There is even an atlas of the two-sphere that gets along with only two charts, viz., two stereographic projections (Blair, 2000, Section 2.2).

4.2. Tangent space

For a point $\boldsymbol{x}$ on the surface of the manifold $\mathcal{M}$ the *tangent space* is spanned by n tangent vectors

$$\partial_\kappa\boldsymbol{x} := \partial\boldsymbol{x}/\partial q^\kappa, \quad 1\leqslant\kappa\leqslant n, \tag{23}$$

resulting from differentiating curves $\boldsymbol{x}(\ldots,q^\lambda,\ldots)$ where $\ldots$ is fixed and $1\leqslant\lambda\leqslant n$; cf. Fig. 5 for the case $n=2$. The point $\boldsymbol{x}$ is *regular*, if the n tangent vectors $\partial_\kappa\boldsymbol{x}$ are linearly independent and, thus, span an n-dimensional plane in $\mathbb{R}^{n+1}$, the tangent plane $\mathcal{T}_{\boldsymbol{x}}$. Hence one dimension is left and it is here where the normal vector $\boldsymbol{n}$ lives, which is normal to the tangent plane. That is to say, $\boldsymbol{n}\partial_\kappa\boldsymbol{x}=0$ for $1\leqslant\kappa\leqslant n$. If the tangent vectors at $\boldsymbol{x}$ are linearly dependent, the point is called an irregular one. One meets irregular points of a membrane surface at tips and cusps.

A normal vector $\boldsymbol{n}$ is not unique since $-\boldsymbol{n}$ is another one. To get uniqueness we need two requirements. A glance suffices to convince us that manifolds such as those in Figs. 2, 3, and 11 are *orientable*. That is, they have an inside and an outside. More precisely, the normal vector $\boldsymbol{n}(\boldsymbol{x})$ depends *continuously* on $\boldsymbol{x}\in\mathcal{M}$ as $\boldsymbol{x}$ varies through the manifold

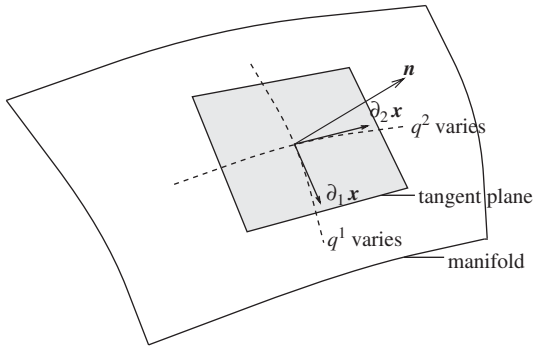

Fig. 5. Two-dimensional hypersurface $\mathcal{M}$ and its tangent space, the tangent plane, at $\boldsymbol{x} \in \mathcal{M} \subset \mathbb{R}^3$. The tangent space at the regular point $\boldsymbol{x}$ is spanned by the two tangent vectors $\partial_1 \boldsymbol{x}$ and $\partial_2 \boldsymbol{x}$. The normal vector $\boldsymbol{n}$ is orthogonal to the tangent plane at $\boldsymbol{x}$ and has unit length; the same holds for $-\boldsymbol{n}$. It is a differential-geometric convention to let the normal vector $\boldsymbol{n}$ point *outwards* for a sphere; as Fig. 7 shows, by good reason. The vectors $\partial_1 \boldsymbol{x}$, $\partial_2 \boldsymbol{x}$, and $\boldsymbol{n}$ span all of $\mathbb{R}^3$.

$\mathcal{M}$. For instance, the Möbius band (take a strip of paper, twist it once, and glue it together) is not orientable since $\boldsymbol{n}(\boldsymbol{x}_\circ)$ is transformed into $-\boldsymbol{n}(\boldsymbol{x}_\circ)$ as, starting in $\boldsymbol{x}_\circ$, we travel with $\boldsymbol{x}$ along the band $\mathcal{M}$ back to $\boldsymbol{x}_\circ$. We now require that our membranes constitute orientable surfaces with the normal pointing outward. The former requirement is natural and for the latter we make a choice; cf. Fig. 7.

Furthermore, $\boldsymbol{n}$ has always length one, i.e., $\boldsymbol{nn} := \boldsymbol{n} \cdot \boldsymbol{n} = 1$. Throughout what follows we will drop the dot indicating a scalar product, unless ambiguity arises. Differentiating $\boldsymbol{nn} = 1$ we directly find $\boldsymbol{n}\partial_\lambda \boldsymbol{n} = 0$ so that the $\partial_\lambda \boldsymbol{n}(q^\kappa)$ are back in the tangent plane of $\boldsymbol{x}(q^\kappa)$. As a consequence of being a unit vector normalized to one, $\boldsymbol{n}$ is dimensionless, as is $\mathrm{d}_s \boldsymbol{x}$.

4.3. Metric: arc length and how to measure it on a curved surface

A curve in $\mathbb{R}^{n+1}$ can be parametrized by a *single* variable t so that $\{\boldsymbol{x}(t), t \in I \subset \mathbb{R}\}$ is a suitable representation with $\mathrm{d}_t \boldsymbol{x} \neq 0$; here and elsewhere d_t is a shorthand for $\mathrm{d}/\mathrm{d}t$. The arc length as we go from t_0 to t_1 is given by $\int_{t_0}^{t_1} \mathrm{d}t \|\mathrm{d}_t \boldsymbol{x}\|$ where $\|\boldsymbol{x}\| = (\boldsymbol{xx})^{1/2}$ is the norm, i.e., the Euclidean length, inherited from $\mathbb{R}^{n+1}$ we started with. We nearly always take the arc length s to parametrize a curve. Then $\|\mathrm{d}_s \boldsymbol{x}\| = 1$ since in the limit $\Delta s \to 0$ we have $\|\Delta \boldsymbol{x}/\Delta s\| = \|\Delta \boldsymbol{x}\|/\Delta s = \Delta s/\Delta s = 1$. In other words, $\mathrm{d}_s \boldsymbol{x}$ is a unit vector—a valuable property.

We now turn to a curve $\{\boldsymbol{x}(t) := \boldsymbol{x}(q^\kappa(t))\}$ on a surface $\mathcal{M} \subset \mathbb{R}^{n+1}$. Since the surface is parametrized by means of n q^κs, our curve is effectively one in q-space. Hence we first differentiate with respect to q^κ and put

$$\boldsymbol{x}_\kappa := \partial_\kappa \boldsymbol{x} = \partial \boldsymbol{x}/\partial q^\kappa. \tag{24}$$

At a regular point the $\boldsymbol{x}_\kappa$ with $1 \leqslant \kappa \leqslant n$ are a basis spanning tangent space. Furthermore, using summation convention where we sum over equal indices, we obtain

$$\mathrm{d}\boldsymbol{x}(s) = \mathrm{d}_s \boldsymbol{x}\, \mathrm{d}s = \boldsymbol{x}_\kappa\, \mathrm{d}_s q^\kappa\, \mathrm{d}s = \boldsymbol{x}_\kappa\, \mathrm{d}q^\kappa. \tag{25}$$

Three remarks are in order here. First, though $\mathrm{d}\boldsymbol{x}(s)$ is a differential, it won't hurt to imagine it as a finite difference $\Delta \boldsymbol{x}$ with the expressions on the right in (25) being a decent approximation as Δs or Δq^κ gets small. Throughout what follows this is implicitly understood as it corresponds to physical reality. Second, dividing (25) interpreted as just indicated by Δs so as to get $\Delta \boldsymbol{x}/\Delta s$ and taking the limit $\Delta s \to 0$ we find the tangent vector

$$\mathrm{d}_s \boldsymbol{x} = \mathrm{d}\boldsymbol{x}/\mathrm{d}s = \boldsymbol{x}_\kappa\, \mathrm{d}_s q^\kappa = \boldsymbol{x}_\kappa u^\kappa, \tag{26}$$

where $u^\kappa := \mathrm{d}q^\kappa/\mathrm{d}s = \mathrm{d}_s q^\kappa$. That is, an arbitrary tangent vector $\mathrm{d}\boldsymbol{x}(s)/\mathrm{d}s$ is a linear combination of the $\boldsymbol{x}_\kappa$, $1 \leqslant \kappa \leqslant n$—as expected. We will soon meet the u^κ quite often. Furthermore, by the very geometry of its construction, $\mathrm{d}_s \boldsymbol{x} = \lim_{\Delta s \to 0} \Delta \boldsymbol{x}/\Delta s$ is a unit vector. Third, and most importantly, we see the arc length $\mathrm{d}s$ is given by

$$(\mathrm{d}s)^2 = \mathrm{d}\boldsymbol{x}\, \mathrm{d}\boldsymbol{x} = \boldsymbol{x}_\kappa \boldsymbol{x}_\lambda\, \mathrm{d}q^\kappa\, \mathrm{d}q^\lambda =: g_{\kappa\lambda}\, \mathrm{d}q^\kappa\, \mathrm{d}q^\lambda. \tag{27}$$

That is to say, arc length on a manifold is governed by the metric tensor $\{g_{\kappa\lambda} = \boldsymbol{x}_\kappa \boldsymbol{x}_\lambda = g_{\lambda\kappa},\ 1 \leqslant \kappa,\ \lambda \leqslant n\}$, a Gramian (Gantmacher, 1977; Horn and Johnson, 1985).

Before proceeding we prove a useful lemma. Its notation will remind most people of relativity theory.

Lemma A. *The metric tensor $g_{\kappa\lambda} = \boldsymbol{x}_\kappa \boldsymbol{x}_\lambda = g_{\lambda\kappa}$ is a positive-definite matrix associated with the basis $\boldsymbol{x}_\kappa$. There exists a unique* reciprocal basis $\boldsymbol{x}^\lambda$ *such that $\boldsymbol{x}_\kappa \boldsymbol{x}^\lambda = \delta_\kappa^\lambda$ where δ_κ^λ is the Kronecker delta, i.e., 1 for $\kappa = \lambda$ and 0 elsewhere. If $g^{\mu\nu} = g^{\nu\mu}$ is the inverse of $g_{\kappa\lambda}$, then $g^{\mu\nu} = \boldsymbol{x}^\mu \boldsymbol{x}^\nu$ and $\boldsymbol{x}^\mu = g^{\mu\nu}\boldsymbol{x}_\nu$ so that $\boldsymbol{x}_\nu = g_{\nu\mu}\boldsymbol{x}^\mu$.*

Proof. By the definition of $g_{\kappa\lambda}$ we have for an arbitrary vector (y^κ) that $y^\kappa g_{\kappa\lambda} y^\lambda = \|y^\kappa \boldsymbol{x}_\kappa\|^2 \geqslant 0$ with equality if and only if $y^\kappa \boldsymbol{x}_\kappa = 0$ and thus $(y^\kappa) = 0$. Hence $(g_{\kappa\lambda})$ is positive-definite, one-to-one, and thus invertible.

As for existence of a reciprocal basis, let us simply define $(g^{\lambda\mu})$ to be the inverse matrix of $(g_{\lambda\mu})$ and put $\boldsymbol{x}^\lambda := g^{\lambda\kappa}\boldsymbol{x}_\kappa$; note the summation convention. Then the $\boldsymbol{x}^\lambda$ with $1 \leqslant \lambda \leqslant n$ are independent, hence a basis, and $\boldsymbol{x}_\mu \boldsymbol{x}^\lambda = g^{\lambda\kappa}\boldsymbol{x}_\kappa \boldsymbol{x}_\mu = g^{\lambda\kappa} g_{\kappa\mu} = \delta_\lambda^\mu$, as required.

Uniqueness follows from the relation $\boldsymbol{x}^\lambda = g^{\lambda\kappa}\boldsymbol{x}_\kappa$ as a consequence of the $\boldsymbol{x}_\kappa$ being a basis, $\boldsymbol{x}^\lambda \boldsymbol{x}_\mu = \delta_\mu^\lambda = g^{\lambda\kappa}\boldsymbol{x}_\kappa \boldsymbol{x}_\lambda = g^{\lambda\kappa} g_{\kappa\mu}$, and the inverse matrix being unique. □

As for uniqueness, the point is that, if there were a second reciprocal basis $\tilde{\boldsymbol{x}}$, then $\tilde{\boldsymbol{x}}^\lambda = \tilde{g}^{\lambda\kappa}\boldsymbol{x}_\kappa$ so that $\delta_\mu^\lambda = \tilde{g}^{\lambda\kappa} g_{\kappa\mu}$ and thus $g = \tilde{g}$. Taking a scalar product with $\boldsymbol{x}^\mu$ and using the defining property of a reciprocal basis we directly find

$$\boldsymbol{x}^\mu \boldsymbol{x}^\lambda = g^{\mu\kappa}\boldsymbol{x}_\kappa \boldsymbol{x}^\lambda = g^{\mu\lambda}. \tag{28}$$

This equation also shows explicitly that the matrix $(g^{\mu\lambda} = g^{\lambda\mu})$ is positive-definite as well.

We return to the problem of determining arc length and area of a curved surface. As for arc length, (27) tells us that for arbitrary parametrization by some t

$$\mathrm{d}s = \mathrm{d}t\,(g_{\kappa\lambda}\,\mathrm{d}_t q^\kappa\,\mathrm{d}_t q^\lambda)^{1/2}. \tag{29}$$

Let us call, whatever the parametrization, $u^\lambda := \mathrm{d}_t q^\lambda$. Then $\mathrm{d}s = \mathrm{d}t\,(u^\kappa g_{\kappa\lambda} u^\lambda)^{1/2}$.

For the area of a curved surface we need a surface measure $\mathrm{d}f$ that can be integrated with respect to the coordinates, or parameters, q^κ. Let us first consider a parallelogram spanned by two vectors $\boldsymbol{a}$ and $\boldsymbol{b}$ in $\mathbb{R}^3$, which have an angle θ in between. Its area is given by the length of their vector product $\|\boldsymbol{a}\|\,\|\boldsymbol{b}\|\sin\theta$ and, thus, is the square root of

$$\|\boldsymbol{a} \times \boldsymbol{b}\|^2 = (\boldsymbol{aa})(\boldsymbol{bb}) - (\boldsymbol{ab})^2 = \det \begin{pmatrix} \boldsymbol{aa} & \boldsymbol{ab} \\ \boldsymbol{ba} & \boldsymbol{bb} \end{pmatrix}. \tag{30}$$

The area of a curved surface is well-approximated by a Riemann sum of small parallelograms spanned by $\Delta q^\kappa \partial_\kappa \boldsymbol{x}$ with $\kappa = 1, 2$. In (30) we therefore take $\boldsymbol{a} := \Delta q^1 \partial_1 \boldsymbol{x}$ and $\boldsymbol{b} := \Delta q^2 \partial_2 \boldsymbol{x}$ so as to find $\det(g_{\mu\nu})(\Delta q^1 \Delta q^2)^2$. In the limit $\Delta q^\kappa \to 0$ we then end up with an infinitesimal surface area

$$\mathrm{d}f = \mathrm{d}q^1 \ldots \mathrm{d}q^n \sqrt{\det g}, \tag{31}$$

which holds equally well for general n (Gantmacher, 1977) as for physical membranes with $n = 2$, where (30) is good for.

Eq. (31) has an immediate physical application since for a membrane with surface tension Σ we find the energy density to be $\Sigma\sqrt{\det g}$. For membranes with negligible bending rigidity, such as soap films, this is already enough to completely describe equilibrium and dynamics (Isenberg, 1992; Oprea, 2000), though a detailed understanding requires a careful analysis of the boundary conditions.

4.4. Curvature

To determine curvature at a point $\boldsymbol{x}$ of a manifold $\mathcal{M}$ we need a curve through $\boldsymbol{x}$ but embedded in the manifold so as to sample $\mathcal{M}$. The curve is parametrized by its arc length s. Before proceeding we take the curve *by itself* and ask how to define its curvature. Differentiating $\mathrm{d}_s \boldsymbol{x}\,\mathrm{d}_s \boldsymbol{x} = 1$ we obtain $\mathrm{d}_s^2 \boldsymbol{x}\,\mathrm{d}_s \boldsymbol{x} = 0$. In other words, the tangent vector $\mathrm{d}_s \boldsymbol{x}$ and $\mathrm{d}_s^2 \boldsymbol{x}$ are orthogonal and we define the curvature $\tilde{\kappa}$ to be $\tilde{\kappa} := \|\mathrm{d}_s^2 \boldsymbol{x}\|$.

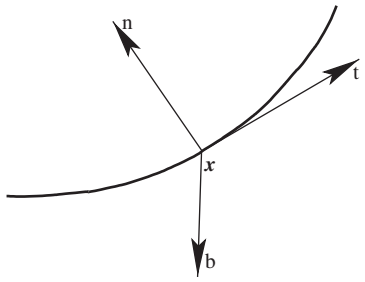

Fig. 6. Darboux triad $\{\mathsf{t}, \mathsf{n}, \mathsf{b}\}$. For the sake of simplicity a curve (solid line) in $\mathbb{R}^3$ is taken to be in the plane of this page. Its curvature $\tilde{\kappa}$ is the arc-rate rotation of the tangent $\mathsf{t} := \mathrm{d}_s \boldsymbol{x}$, a unit vector. That is, $\mathrm{d}_s \mathsf{t} = \mathrm{d}_s^2 \boldsymbol{x} =: \tilde{\kappa} \mathsf{n} \perp \mathsf{t}$ where the orthogonality $\mathsf{n} \perp \mathsf{t}$ is also evident from the geometric construction. The larger the curvature, the faster t changes as we proceed along the curve and, hence, the larger $\tilde{\kappa}$. The vector $\mathsf{b} := \mathsf{t} \times \mathsf{n}$ completes a positively oriented, orthonormal basis in $\mathbb{R}^3$. It is a local one that travels with the beholder along the curve. Since along the above curve b cannot change, there is no torsion, i.e., $\tilde{\tau} = 0$.

Frenet equations. All this is quickly said but not that quickly caught. Let us therefore step back and focus on a single curve at a specific position P, viz., $\boldsymbol{x} \in \mathbb{R}^3$. Intuitively it is plain what *curvature* is: the arc-rate rotation of its tangent. We put $\mathsf{t} := \mathrm{d}_s \boldsymbol{x}$, a unit vector, and $\mathrm{d}_s \mathsf{t} = \mathrm{d}_s^2 \boldsymbol{x} =: \tilde{\kappa} \mathsf{n}$ where n is another unit vector, by construction orthogonal to the tangent t ($0 = \mathrm{d}_s \mathsf{t}^2 = 2\mathsf{t}\mathrm{d}_s \mathsf{t}$) and called the principal normal at position P. By the very nature of t, $\tilde{\kappa}$ is exactly its arc-rate rotation; cf. Fig. 6.

Defining the *bi*normal $\mathsf{b} := \mathsf{t} \times \mathsf{n}$ we arrive at the triad $\{\mathsf{t}, \mathsf{n}, \mathsf{b}\}$ forming a right-handed system of mutually perpendicular unit vectors at P. This system, called the Darboux triad, can be used to specify how a curve "proceeds" in 3-space $\mathbb{R}^3$,

$$\frac{\mathrm{d}\mathsf{t}}{\mathrm{d}s} = \tilde{\kappa}\mathsf{n}, \quad \frac{\mathrm{d}\mathsf{n}}{\mathrm{d}s} = -\tilde{\kappa}\mathsf{t} + \tilde{\tau}\mathsf{b}, \quad \frac{\mathrm{d}\mathsf{b}}{\mathrm{d}s} = -\tilde{\tau}\mathsf{n}. \tag{32}$$

The solution to the linear system (32) is unique, up to translation, viz., of the initial position P, and rotation, viz., of the triad $\{\mathsf{t}, \mathsf{n}, \mathsf{b}\}$. In a self-explanatory notation (32) reappears much more appealing as

$$\frac{\mathrm{d}}{\mathrm{d}s}\begin{pmatrix}\mathsf{t}\\ \mathsf{n}\\ \mathsf{b}\end{pmatrix} = \begin{pmatrix}0 & \tilde{\kappa} & 0\\ -\tilde{\kappa} & 0 & \tilde{\tau}\\ 0 & -\tilde{\tau} & 0\end{pmatrix}\begin{pmatrix}\mathsf{t}\\ \mathsf{n}\\ \mathsf{b}\end{pmatrix}. \tag{33}$$

The above *Frenet* equations were derived by the mathematician J.F. Frenet in his Toulouse dissertation of 1847; they were published in 1852. We are about to check how they arise. The elegance of their present formulation is due to Gaston Darboux (1887). To see their use in physics, one may profitably consult Kamien (2002).

The top line of (33) is nothing but the definition $\mathrm{d}_s \mathsf{t} = \tilde{\kappa}\mathsf{n}$ of the curve's curvature $\tilde{\kappa}$ at P in conjunction with the principal normal n, a unit vector. Next we turn to the bottom line. Since $\mathsf{b}\mathsf{b} = 1$ we have $\mathsf{b}\mathrm{d}_s\mathsf{b} = 0$. In addition, differentiating $\mathsf{t}\mathsf{b} = 0$ we get, taking again advantage of $\mathrm{d}_s \mathsf{t} = \tilde{\kappa}\mathsf{n}$,

$$0 = \mathsf{t}\frac{\mathrm{d}\mathsf{b}}{\mathrm{d}s} + \mathsf{b}\frac{\mathrm{d}\mathsf{t}}{\mathrm{d}s} = \mathsf{t}\mathrm{d}_s\mathsf{b} + \tilde{\kappa}\mathsf{n}\mathsf{b} = \mathsf{t}\mathrm{d}_s\mathsf{b}, \tag{34}$$

where $\mathsf{b}\mathsf{n} = 0$ by construction of the binormal. Hence $\mathrm{d}_s\mathsf{b}$ is perpendicular to both t and b, which together with n span 3-space. That is, $\mathrm{d}_s\mathsf{b} =: -\tilde{\tau}\mathsf{n}$ for some proportionality factor $\tilde{\tau}$, which is called the curve's *torsion* $\tilde{\tau}$ at position P. Both $\tilde{\kappa}$ and $\tilde{\tau}$ may, and in general will, depend on the position P on the curve and, hence, on s. Finally, we differentiate $\mathsf{n} := \mathsf{b} \times \mathsf{t}$ and exploit top and bottom of (33) to get the middle, and key, equation. So we are done.

In words, the Frenet equations (33) tell us that the arc-rate of turning of a curve's tangent is its curvature while the arc-rate of turning of its binormal is its torsion. Since $\mathrm{d}_s\mathsf{n} = -\tilde{\kappa}\mathsf{t} + \tilde{\tau}\mathsf{b}$ the principal normal gives nothing new. What *is* new, however, is the torsion, a consequence of the curve's dangling around in 3- instead of 2-space. The situation is quite similar to mechanics, where one often deals with a rotating coordinate system. That is, if s were time and $\Omega := \tilde{\tau}\mathsf{t} + \tilde{\kappa}\mathsf{b}$, we had the suggestive analogy $\mathrm{d}\boldsymbol{v}/\mathrm{d}s = \boldsymbol{\Omega} \times \boldsymbol{v}$ of a rotating body, $\boldsymbol{v}$ being one of the vectors of the Darboux triad $\{\mathsf{t}, \mathsf{n}, \mathsf{b}\}$.

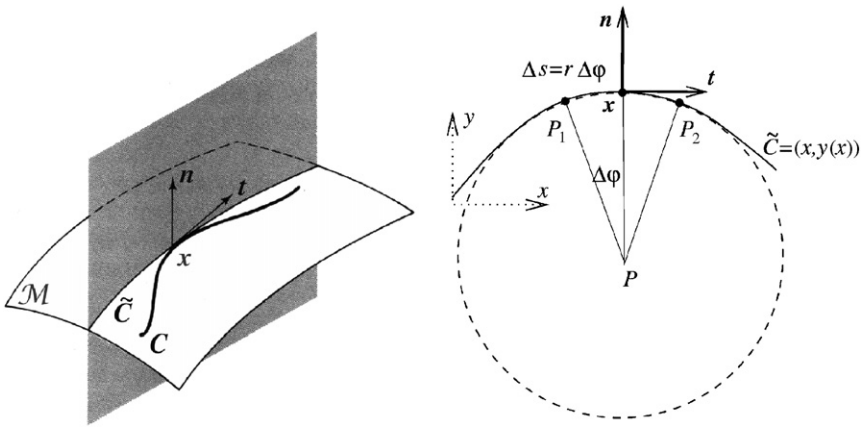

Fig. 7. Curvature and Meusnier's theorem. As is plain to the eye, the manifold $\mathcal{M}$ (left) is curved. It is sampled by a (boldface) curve C at a point $\boldsymbol{x} \in \mathcal{M}$, where we have the tangent vector $\boldsymbol{t} = \mathrm{d}_s\boldsymbol{x}$. The intersection of $\mathcal{M}$ and a plane through $\boldsymbol{t}$ and the normal vector $\boldsymbol{n}$ at $\boldsymbol{x}$ is the curve $\tilde{C}$. As is shown on the right, determining its curvature $\tilde{\kappa} = 1/r$ at $\boldsymbol{x}$ with r as radius of curvature in this vertical plane is as it is done since Huygens (1691) and Bernoulli (1692). By construction, the tangent $\boldsymbol{t} = \mathrm{d}_s\boldsymbol{x}$ along $\tilde{C}$ at $\boldsymbol{x}$ is in the plane and so is $\mathrm{d}_s^2\boldsymbol{x}$, with $\boldsymbol{t} \perp \mathrm{d}_s^2\boldsymbol{x}$. Hence $\theta := \angle(\boldsymbol{n}, \mathrm{d}_s^2\boldsymbol{x}) = 0$ or π. It is convention to take $\boldsymbol{n}$ so that $\theta = 0$; in the figure $\theta = \pi$. The 'osculating circle' (dashed, right) with radius $r := 1/\tilde{\kappa}$ and center P approximates the curve $\tilde{C} = (x, y(x))$ locally up to 2nd order (Thomas, 1972); hence $\Delta s = r\Delta\varphi$ where $\Delta\varphi$ is e.g. the angle between Pp_1 and $P\boldsymbol{x}$. According to (36) and (35), $\tilde{\kappa} = \lim_{\Delta s\to 0}\Delta\varphi/\Delta s = 1/r = \|\mathrm{d}_s(\mathrm{d}_s\boldsymbol{x})\|$; cf. Hilbert and Cohn-Vossen (1964, Section 26). According to Meusnier (see below), the manifold's curvature κ_N at $\boldsymbol{x}$ along C is identical with $\tilde{\kappa}$. We also see that the (boldface) curve C's big "wiggle" *in* the manifold $\mathcal{M}$ tells us nothing about $\mathcal{M}$'s curvature κ_N at $\boldsymbol{x}$.

To see in another way what $\tilde{\kappa}$ means geometrically, we turn to Fig. 7 (right), focus on a curve $\boldsymbol{x} = (x, y(x))$ lying in the plane of this page, and verify that $\tilde{\kappa}$ makes quite a bit of sense as 'curvature'. For a circle of radius r we can easily compute $\tilde{\kappa}$ as, by convention, $\boldsymbol{x} = r\boldsymbol{n}$. Since the tangent vector $\mathrm{d}_s\boldsymbol{x}$ has length 1, we also have $\|\mathrm{d}_s\boldsymbol{n}\| = r^{-1}$ and from $\boldsymbol{n}\mathrm{d}_s\boldsymbol{x} = 0$ we find $\mathrm{d}_s\boldsymbol{n}\mathrm{d}_s\boldsymbol{x} = -\boldsymbol{n}\mathrm{d}_s^2\boldsymbol{x}$. Putting things together, we arrive at

$$\tilde{\kappa} := \|\mathrm{d}_s^2\boldsymbol{x}\| = 1/r. \tag{35}$$

We now go back to an arbitrary curve $\tilde{C} = (x, y(x))$, where φ be the angle between the tangent and the x-axis with $\tan\varphi = \mathrm{d}y/\mathrm{d}x =: y'$; see Fig. 7 (right). Any curve $\tilde{C} = (x, y(x))$ can be approximated locally up to 2nd order by an 'osculating circle' with radius $\varrho = 1/\tilde{\kappa}$ (Thomas, 1972). We therefore define a radius of curvature ϱ to be

$$\varrho := \lim_{\Delta s\to 0}\left|\frac{\Delta s}{\Delta\varphi}\right| = \left|\frac{\mathrm{d}s}{\mathrm{d}\varphi}\right|. \tag{36}$$

So $\tilde{\kappa}$ is a good old friend defined in a way that makes no reference whatsoever to any coordinate system—in clear contrast to the classical expression $\tilde{\kappa} = y''[1 + (y')^2]^{-3/2}$ following from (36) for a curve $y = y(x)$; cf. Thomas (1972).

A manifold's curvature. To exploit (35) for defining a manifold's curvature we note that the basis $\{\boldsymbol{x}_\mu\}$, or $\{\boldsymbol{x}^\kappa\}$, of the tangent space $\mathcal{T}_{\boldsymbol{x}}$ at $\boldsymbol{x} \in \mathcal{M}$ and the normal vector $\boldsymbol{n}$ span all of $\mathbb{R}^{n+1}$. In tangent space

$$\mathbb{P} := |\boldsymbol{x}_\lambda\rangle\langle\boldsymbol{x}^\lambda| = g_{\lambda\mu}|\boldsymbol{x}^\mu\rangle\langle\boldsymbol{x}^\lambda| = |\boldsymbol{x}^\mu\rangle\langle\boldsymbol{x}_\mu| \tag{37}$$

is a decomposition of unity. Here we have used $g_{\lambda\mu} = g_{\mu\lambda}$ and, for the sake of convenience, Dirac's braket notation (Dirac, 1958). By definition, $\boldsymbol{n}\boldsymbol{x}_\mu = 0$ and $\boldsymbol{n}\boldsymbol{n} = 1$ while $\mathbb{P}\boldsymbol{n} = 0$ so that $\mathbb{P} = \mathbb{P}^2 = \mathbb{P}^*$ is the projection onto $\mathcal{T}_{\boldsymbol{x}}$ in $\mathbb{R}^{n+1}$ and $\mathbb{1} = |\boldsymbol{n}\rangle\langle\boldsymbol{n}| + \mathbb{P}$. Accordingly the decomposition

$$\mathrm{d}_s^2\boldsymbol{x} = \boldsymbol{n}(\boldsymbol{n}\mathrm{d}_s^2\boldsymbol{x}) + \mathbb{P}(\mathrm{d}_s^2\boldsymbol{x}) \tag{38}$$

makes sense. It is basic to what follows.

We now return to our manifold, remember from (25) that the unit vector $\mathrm{d}_s\mathbf{x} = \mathbf{x}_\mu u^\mu$ with $u^\mu = \partial_s q^\mu$ is a tangent, and introduce curvature of a manifold at $\boldsymbol{x} \in \mathcal{M}$ by decomposing the curve's $\mathrm{d}_s^2\boldsymbol{x}$ into two parts, one characterizing the

curve's wiggles *in* the manifold, the other sampling the manifold's extrinsic curvature through variation of the normal vector; cf. Fig. 7. To see how this works we start by computing $\mathrm{d}_s^2\boldsymbol{x} = \mathrm{d}_s(\mathrm{d}_s\boldsymbol{x})$ so as to find

$$\mathrm{d}_s(\boldsymbol{x}_\mu u^\mu) = \boldsymbol{x}_{\mu\nu}u^\mu u^\nu + \boldsymbol{x}_\mu \mathrm{d}_s u^\mu. \tag{39}$$

Evidently, $\boldsymbol{x}_{\mu\nu} := \partial_\mu\partial_\nu\boldsymbol{x} = \partial_\nu\partial_\mu\boldsymbol{x} = \boldsymbol{x}_{\nu\mu}$ appears. Whereas $\boldsymbol{x}_\mu$ is in tangent space, its derivative $\boldsymbol{x}_{\mu\nu}$ also has a normal component parallel to the normal vector $\boldsymbol{n}$. Hence we write $\boldsymbol{x}_{\mu\nu} = \mathbb{P}\boldsymbol{x}_{\mu\nu} + \boldsymbol{n}(\boldsymbol{n}\boldsymbol{x}_{\mu\nu})$, take advantage of (37), and obtain the *Gauss formula* (1827)

$$\boldsymbol{x}_{\mu\nu} = \Gamma^\lambda_{\mu\nu}\boldsymbol{x}_\lambda + h_{\mu\nu}\boldsymbol{n}. \tag{40}$$

By definition, $\boldsymbol{n}\boldsymbol{x}_\mu = 0$ and $\boldsymbol{n}\boldsymbol{n} = 1$. A simple calculation then gives

$$\Gamma^\lambda_{\mu\nu} = \boldsymbol{x}^\lambda\boldsymbol{x}_{\mu\nu} = \boldsymbol{x}_{\mu\nu}\boldsymbol{x}_\kappa g^{\kappa\lambda}, \tag{41}$$

$$h_{\mu\nu} = \boldsymbol{x}_{\mu\nu}\boldsymbol{n} = -\boldsymbol{x}_\mu\boldsymbol{n}_\nu. \tag{42}$$

The final equality in (42) is a consequence of differentiating $\boldsymbol{n}\boldsymbol{x}_\mu = 0$ with respect to q^ν. The $\Gamma^\lambda_{\mu\nu}$ are symbols introduced by Christoffel (1869); for illuminating background information concerning Christoffel symbols and Gauss's formula, see Spivak (1979). The tensor $h_{\mu\nu}$ is called the *second fundamental tensor*, the metric one being the first. As matrices, both are symmetric and real.

Substituting the Gauss formula (40) into (39) we can split $\tilde\kappa^2$ into two parts $\tilde\kappa^2 = \kappa_N^2 + \kappa_G^2$ corresponding to (38), with

$$\kappa_N = \boldsymbol{n}\mathrm{d}_s^2\boldsymbol{x} = u^\mu h_{\mu\nu}u^\nu, \tag{43}$$

$$\kappa_G^2 = (\mathrm{d}_s u^\lambda + \Gamma^\lambda_{\nu\mu}u^\mu u^\nu)g_{\lambda\kappa}(\mathrm{d}_s u^\kappa + \Gamma^\kappa_{\nu\mu}u^\mu u^\nu). \tag{44}$$

We can also write $\kappa_G = \|\mathbb{P}\mathrm{d}_s^2\boldsymbol{x}\|$. The quantity $\kappa_N = h_{\mu\nu}u^\mu u^\nu$ represents a surface's "true" curvature, which in a sense is normal to tangent space $\mathcal{T}_{\boldsymbol{x}}$, whereas κ_G takes care of *geodetic* curvature "in" the manifold, i.e., in $\mathcal{T}_{\boldsymbol{x}}$; cf. Fig. 7. Curves in $\mathcal{M}$ with $\kappa_G = 0$ everywhere are called geodesics. They are characterized by

$$0 = \kappa_G \quad\leftrightarrow\quad \mathrm{d}_s u^\lambda + \Gamma^\lambda_{\nu\mu}u^\mu u^\nu = 0, \tag{45}$$

whatever the index λ. For instance, on a sphere with radius R great circles are geodesics. As curves by themselves they have a *non*vanishing curvature in that $\tilde\kappa = 1/R$. So we need something else to characterize what a surface looks like "from the outside", viz., its "extrinsic" or, as it is called, normal curvature κ_N.

The relation $\kappa_N = h_{\mu\nu}u^\mu u^\nu$ with $h_{\mu\nu} = \boldsymbol{x}_{\mu\nu}\boldsymbol{n} = h_{\nu\mu}$ and $\boldsymbol{x}_{\mu\nu} = \partial^2_{\mu\nu}\boldsymbol{x}$ shows explicitly the interplay between a curve and the surface it is living on. We can also see this in a different way by exploiting the Taylor expansion $\boldsymbol{x}(q+\Delta q) - [\boldsymbol{x}(q) + \Delta q^\lambda\partial_\lambda\boldsymbol{x}] = \Delta q^\lambda(\partial^2_{\lambda\mu}\boldsymbol{x})\Delta q^\mu/2$, noting that, after taking a scalar product with the normal vector $\boldsymbol{n}$, the distance (with sign) of $\boldsymbol{x}(q+\Delta q)$ from the tangent plane at $\boldsymbol{x}(q)$ is

$$\boldsymbol{n}[\boldsymbol{x}(q+\Delta q) - \boldsymbol{x}(q)] = \tfrac{1}{2}\Delta q^\lambda(\boldsymbol{n}\partial^2_{\lambda\mu}\boldsymbol{x})\Delta q^\mu = \tfrac{1}{2}\Delta q^\lambda(h_{\lambda\mu})\Delta q^\mu. \tag{46}$$

In other words, $(h_{\lambda\mu})$ measures curvature 'away from', i.e., normal to, the tangent plane and $\kappa \equiv \kappa_N$ is the surface's "true", extrinsic curvature.

The *Weingarten equations* come for free. From $\boldsymbol{n}\boldsymbol{n} = 1$ we obtain by differentiation $\boldsymbol{n}\partial_\lambda\boldsymbol{n} = 0$. We can therefore write $\partial_\lambda\boldsymbol{n} = \eta_{\lambda\kappa}\boldsymbol{x}^\kappa$ and because of (42) we find, taking a scalar product with $\boldsymbol{x}_\mu$, $\eta_{\lambda\mu} = -h_{\lambda\mu}$. Thus we end up with

$$\partial_\lambda\boldsymbol{n} = -h_{\lambda\mu}\boldsymbol{x}^\mu, \tag{47}$$

the Weingarten equations (1861).

4.5. Principal curvature

The idea behind principal curvature is simple but needs some thought in practice. Let us pick a point P, more precisely $\boldsymbol{x}$, on a two-dimensional manifold $\mathcal{M}$, put orthogonal x and y axes in its tangent space $\mathcal{T}_{\boldsymbol{x}}$ with origin at $\boldsymbol{x}$, and take the z axis of our coordinate system parallel to the normal vector $\boldsymbol{n}$. In the neighborhood of $\boldsymbol{x}$ our manifold can be described

to fine approximation by a quadratic surface $z = (x, y)Q(x, y)^{\mathrm{T}}/2$ with respect to the tangent plane at P and with Q as an $n \times n$ matrix, here $n = 2$.

Since Q is real and symmetric, i.e., self-adjoint or also Hermitian, we can diagonalize it and find two orthonormal eigenvectors $\boldsymbol{e}_1$ and $\boldsymbol{e}_2$ in $\mathcal{T}_{\boldsymbol{x}}$ with real eigenvalues, say, κ_1 and κ_2, so that in the new coordinates $z = (\kappa_1 x_1^2 + \kappa_2 x_2^2)/2$. Plainly, the surface is "strongly curved" at P in direction $\boldsymbol{e}_i$, if $|\kappa_i|$ is large. All this is a matter of existence. Doing it in practice and computing the principal curvatures κ_i explicitly is a completely different story, to which we now turn.

To see what principal curvature is in hard daily practice and get a feeling for the n orthogonal principal directions in tangent space $\mathcal{T}_{\boldsymbol{x}}$ of a manifold, we define the linear *Weingarten map* $W(\boldsymbol{x})$ from $\mathcal{T}_{\mathbf{x}}$ into itself by mapping $\boldsymbol{t} = t^\mu \partial_\mu \boldsymbol{x}$ onto

$$W(\boldsymbol{x})(t^\mu \partial_\mu \boldsymbol{x}) := -t^\mu \partial_\mu \boldsymbol{n}. \tag{48}$$

W's dependence upon $\boldsymbol{x}$ is understood. Since $\boldsymbol{n}\partial_\mu \boldsymbol{n} = 0$, the vectors $\boldsymbol{n}_\mu := \partial_\mu \boldsymbol{n}$ are all in tangent space $\mathcal{T}_{\boldsymbol{x}}$ and W is well-defined. The n-dimensional space $\mathcal{T}_{\mathbf{x}} \subset \mathbb{R}^{n+1}$ inherits as such a Euclidean scalar product from $\mathbb{R}^{n+1}$. Using (42) we show that W is self-adjoint with respect to this scalar product,

$$\begin{aligned}(a^\mu \boldsymbol{x}_\mu)[W(b^\nu \boldsymbol{x}_\nu)] &= -a^\mu b^\nu (\boldsymbol{x}_\mu \boldsymbol{n}_\nu) = a^\mu b^\nu h_{\mu\nu} = a^\mu b^\nu h_{\nu\mu} \\ &= [W(a^\mu \boldsymbol{x}_\mu)](b^\nu \boldsymbol{x}_\nu).\end{aligned} \tag{49}$$

By the same token and in conjunction with (43), normal curvature in direction $\boldsymbol{t} = t^\mu \boldsymbol{x}_\mu$ with unit length $\boldsymbol{t}\boldsymbol{t} = 1$ equals $\kappa_N(\boldsymbol{t}) = \boldsymbol{t}W\boldsymbol{t} = t^\mu h_{\mu\nu} t^\nu$, a relation W has been made for.

W's eigenvalues κ_μ and orthonormal eigenvectors $\boldsymbol{t}_\mu$ in $\mathcal{T}_{\boldsymbol{x}}$ follow directly from the eigenvalue equation $W\boldsymbol{t} = \kappa \boldsymbol{t}$,

$$W(t^\nu \boldsymbol{x}_\nu) = \kappa(t^\nu \boldsymbol{x}_\nu) \Rightarrow -t^\nu \boldsymbol{n}_\nu = \kappa t^\nu \boldsymbol{x}_\nu. \tag{50}$$

To simplify notation we have dropped the eigenvector label μ. We take a scalar product with $\boldsymbol{x}_\lambda$, use (42),

$$-t^\nu \boldsymbol{x}_\lambda \boldsymbol{n}_\nu = \kappa \boldsymbol{x}_\lambda \boldsymbol{x}_\nu t^\nu \Rightarrow (h_{\lambda\nu} - \kappa g_{\lambda\nu}) t^\nu = 0, \tag{51}$$

and see we end up with a generalized eigenvalue problem $(h - \kappa g)\vec{t} = 0$ for $\vec{t} := (t_1, \ldots, t_n)$ or equivalently $g^{-1}h\vec{t} = \kappa\vec{t}$, an ordinary one. That is to say, principal directions $t^\nu \boldsymbol{x}_\nu$ are determined by eigenvectors $\vec{t}$ of $g^{-1}h$ and principal curvatures κ are the corresponding eigenvalues of $g^{-1}h\vec{t} = \kappa\vec{t}$.

As a self-adjoint operator, W's eigenvalues are bound to be real. Once we know the matrix equation that determines them, viz., (51), we can also verify this directly. The point is that in general $g^{-1}h$, though real, is not a symmetric matrix and thus one might wonder why principal curvatures are real numbers. This kind of worry, however, can easily be allayed as g^{-1} (with matrix elements $g^{\mu\nu} = \boldsymbol{x}^\mu \boldsymbol{x}^\nu$) is positive-definite so that we can take its square root $g^{-1/2}$ and rewrite the eigenvalue equation as $g^{-1/2}hg^{-1/2}g^{1/2}\vec{t} = \kappa g^{1/2}\vec{t}$. Putting $\vec{v} := g^{1/2}\vec{t}$ we find this to be the eigenvalue equation $g^{-1/2}hg^{-1/2}\vec{v} = \kappa\vec{v}$ for the matrix $g^{-1/2}hg^{-1/2}$. The two fundamental tensors g and h being real-symmetric and thus self-adjoint this also applies to $g^{-1/2}hg^{-1/2}$. Hence its eigenvalues κ are real.

Alternative approach to principal curvature. Instead of decomposing $\mathrm{d}_s^2 \boldsymbol{x}$ one can obtain a manifold's extrinsic, or as we now know normal, curvature directly (Gerretsen, 1962) by focusing on $\mathrm{d}_s \boldsymbol{n} \in \mathcal{T}_{\boldsymbol{x}}$, the wiggles of the *normal* vector $\boldsymbol{n}$ along a given curve in $\mathcal{M}$. Every vector in tangent space $\mathcal{T}_{\boldsymbol{x}}$ can be decomposed uniquely into a component parallel to $\mathrm{d}_s \boldsymbol{x}$, a unit vector, and its orthogonal complement parallel to $\boldsymbol{b}$, another unit vector:

$$\mathrm{d}_s \boldsymbol{n} = -\kappa \mathrm{d}_s \boldsymbol{x} + \tau \boldsymbol{b}, \tag{52}$$

where $\kappa = -\mathrm{d}_s \boldsymbol{n} \mathrm{d}_s \boldsymbol{x}$. We now call κ the 'curvature' of $\mathcal{M}$ at $\boldsymbol{x}$ in the direction $\mathrm{d}_s \boldsymbol{x}$, τ its 'torsion', and say a direction $\mathrm{d}_s \boldsymbol{x}$ is a *principal* one, if $\tau = 0$. That is, when a formula due to *Olinde Rodrigues* (1816) holds, often verified by simple inspection and therefore extremely helpful,

$$\mathrm{d}_s \boldsymbol{n} + \kappa \mathrm{d}_s \boldsymbol{x} = 0. \tag{53}$$

Putting $u^\lambda = \mathrm{d}_s q^\lambda$ and using $\mathrm{d}_s \boldsymbol{n} = \partial_\lambda \boldsymbol{n} u^\lambda$ and $\mathrm{d}_s \boldsymbol{x} = \partial_\lambda \boldsymbol{x} u^\lambda$ in conjunction with Weingarten's relation (47) we obtain

$$\kappa \mathrm{d}_s \boldsymbol{x} = \kappa u^\lambda \partial_\lambda \boldsymbol{x} = -\mathrm{d}_s \boldsymbol{n} = -u^\lambda \partial_\lambda \boldsymbol{n} = \boldsymbol{x}^\kappa h_{\kappa\lambda} u^\lambda.$$

Projecting this onto $\boldsymbol{x}_\mu$ we end up with

$$\kappa g_{\mu\lambda} u^\lambda = h_{\mu\lambda} u^\lambda, \tag{54}$$

a principal direction as specified by (51). In addition, $0 = \mathrm{d}_s(\boldsymbol{n}\mathrm{d}_s\boldsymbol{x}) = \boldsymbol{n}\mathrm{d}_s^2\boldsymbol{x} + \mathrm{d}_s\boldsymbol{n}\mathrm{d}_s\boldsymbol{x}$ gives $\kappa = \kappa_N$ as a combination of $\kappa = -\mathrm{d}_s\boldsymbol{n}\mathrm{d}_s\boldsymbol{x}$ and (44). So it all fits.

The orthonormal triad $\{\boldsymbol{n}, \boldsymbol{t} = \mathrm{d}_s\boldsymbol{x}, \boldsymbol{b}\}$ resembles the Darboux triad $\{\mathsf{n}, \mathsf{t}, \mathsf{b}\}$ of Section 4.4. This is not accidental. Not only does the above definition (52) of a hypersurface's curvature agree with (43), it also ties nicely with the second relation $\mathrm{d}_s\mathsf{n} = -\tilde{\kappa}\mathsf{t} + \tilde{\tau}\mathsf{b}$ of the Frenet equations (34), where $\mathsf{t} = \mathrm{d}_s\boldsymbol{x}$. That is, the notion of torsion can be generalized from curve to hypersurface as well. The new aspect is that $\mathsf{n} \propto \mathrm{d}_s^2\boldsymbol{x}$ whereas, as a normal vector $\boldsymbol{n}$, it refers to the underlying manifold $\mathcal{M}$.

4.6. Meusnier, Euler, and Gauss–Bonnet

The theorems of Euler and Meusnier tie together the principal curvatures and relate them to curvature in a given direction (Euler) and what you think to be "ordinary" curvature (Meusnier); they are all locally defined quantities. On the other hand, Gauss–Bonnet has a global scope.

Meusnier's theorem. Let us return for a moment to a curve embedded in a manifold $\mathcal{M}$, such as C in Fig. 7, and focus on the manifold's curvature $\kappa_N(\boldsymbol{t})$, henceforth simply called the curvature $\kappa(\boldsymbol{t})$, along a given tangent $\boldsymbol{t}$ to this curve at a point $\boldsymbol{x} \in \mathcal{M}$. We may ask: What is the relation between $\mathcal{M}$'s extrinsic curvature $\kappa(\boldsymbol{t})$ and the curve's standard curvature $\tilde{\kappa} = \|\mathrm{d}_s^2\boldsymbol{x}\|$? The answer is given by *Meusnier's Theorem* (1776):

$$\kappa = \tilde{\kappa}\cos\theta \quad \text{where } \theta := \angle(\boldsymbol{n}, \mathrm{d}_s^2\boldsymbol{x}). \tag{55}$$

θ is the angle between $\boldsymbol{n}$ and $\mathrm{d}_s^2\boldsymbol{x}$. In this way we obtain a direct relation between the curvature κ along a curve in a manifold, such as C in Fig. 7, and its inherent curvature $\tilde{\kappa}$ at $\boldsymbol{x}$. For the proof we remember from (35) and (43) that $\tilde{\kappa} = \|\mathrm{d}_s^2\boldsymbol{x}\|$ while $\kappa \equiv \kappa_N = \boldsymbol{n}\mathrm{d}_s^2\boldsymbol{x}$. So we are already done.

There is a direct corollary. In three dimensions one could take the normal vector $\boldsymbol{n}$ at the point $\boldsymbol{x} \in \mathcal{M}$ together with the tangent $\boldsymbol{t} = \mathrm{d}_s\boldsymbol{x}$ and construct the plane through $\boldsymbol{n}$ and $\boldsymbol{t}$. The intersection with $\mathcal{M}$ gives a curve $\tilde{C}$ in a two-dimensional plane ($n = 2$) spanned by $\boldsymbol{n}$ and $\boldsymbol{t}$; cf. Fig. 7 and (35) but now with $\boldsymbol{n}$ pointing downwards. In this plane $\tilde{\kappa} = 1/R$ where R is the radius of the 'osculating circle'. In fact, also $\mathrm{d}_s^2\boldsymbol{x}$ is in the very same plane and $\theta = 0$ so that $\kappa = \tilde{\kappa}$. That is, the two curvatures are identical.

In passing we note that during a rotation of the plane through $\boldsymbol{n}$ and $\boldsymbol{t}$ about the fixed normal vector $\boldsymbol{n}$ the curvature $\tilde{\kappa}$ and, hence $\kappa = \tilde{\kappa}$, assumes a maximum and a minimum. After Euler—see (56) below—these are the two principal curvatures. They are completely *geometrical* constructs, independent of any parametrization. The latter is "only" needed to compute them.

Euler's theorem. The Weingarten map has the spectral representation $W = |\boldsymbol{t}_\mu\rangle\kappa_\mu\langle\boldsymbol{t}_\mu|$ so that $\kappa_N(\boldsymbol{t}) = \boldsymbol{t}W\boldsymbol{t} = \kappa_\mu\langle\boldsymbol{t}_\mu|\boldsymbol{t}\rangle^2$ is a convex combination of the κ_μ's. More explicitly

$$\kappa_N(\boldsymbol{t}) = \sum_{\ell=1}^{n} \kappa_\ell \cos^2\theta_\ell, \tag{56}$$

where θ_ℓ is the angle between the unit vectors $\boldsymbol{t}$ and $\boldsymbol{t}_\ell$. This is *Euler's Theorem* (1760). It has an interesting corollary in $\mathbb{R}^3$, due to Sophie Germain (1821): If κ_1' and κ_2' are the curvatures in two *arbitrary but orthogonal* directions, then

$$\kappa_1' + \kappa_2' = \kappa_1 + \kappa_2. \tag{57}$$

We may call this relation Germain's Lemma. For the proof, which is the original one, we use Euler's theorem, define $\theta_{i\mu}'$ to be the angle between direction i' and eigendirection μ, note that in two dimensions $\theta_{2\mu}' = (\theta_{1\mu}' + \pi/2)$ since the directions we had chosen are orthogonal, and add (summation convention!) $\kappa_1' = \kappa_\mu\cos^2\theta_{1\mu}'$ and $\kappa_2' = \kappa_\mu\cos^2\theta_{2\mu}' = \kappa_\mu\sin^2\theta_{1\mu}'$.

One can generalize the above argument to arbitrary dimension. To this end we take n orthogonal directions $\boldsymbol{d}_\alpha$ in $\mathcal{T}_{\boldsymbol{x}}$ so that $\mathbb{1} = |\boldsymbol{d}_\alpha\rangle\langle\boldsymbol{d}_\alpha|$ in the n-dimensional tangent space $\mathcal{T}_{\boldsymbol{x}}$. By definition, $\kappa_\alpha' = \boldsymbol{d}_\alpha W\boldsymbol{d}_\alpha$ and thus we find, using W's

spectral representation,

$$\sum_{\alpha} \kappa'_{\alpha} = \sum_{\mu\alpha} \kappa_{\mu} \langle \boldsymbol{t}_{\mu} | \boldsymbol{d}_{\alpha} \rangle \langle \boldsymbol{d}_{\alpha} | \boldsymbol{t}_{\mu} \rangle = \sum_{\mu} \kappa_{\mu}. \tag{58}$$

Mean and Gaussian curvature. We finish this section by introducing two invariants, viz., the *mean curvature*

$$\mathbb{H} = \kappa_1 + \cdots + \kappa_n = h^{\mu}_{\mu} = \operatorname{tr} g^{-1} h \tag{59}$$

and the *Gaussian curvature*

$$\mathbb{K} = \kappa_1 \ldots \kappa_n = \det g^{-1} h, \tag{60}$$

where $h = (h_{\mu\nu})$ and $g^{-1} = (g^{\mu\nu})$ is the inverse of the metric tensor $g = (g_{\mu\nu})$. The final equalities in (59) and (60) are a direct consequence of (51). Gaussian curvature $\mathbb{K}$ is geometrically intrinsic in that it is invariant under isometric mappings, i.e., it is a *bending invariant*. As for $\mathbb{K} = \det g^{-1} h = \det h / \det g$, this is quite surprising since the second fundamental tensor h occurs as well. It was Gauss who provided a general proof of $\mathbb{K}$'s invariance in 1826 and dubbed it 'Theorema Egregium' so as to stress its importance. For a succinct proof we refer to the appendix.

It is good to realize that for a two-dimensional manifold in three-dimensional space $\mathbb{H} = \kappa_1 + \kappa_2$ and $\mathbb{K} = \kappa_1 \kappa_2$ are quantities that depend on a manifold's shape only and have nothing to do with the specific parametrization we are using to compute them. Due to Meusnier and Euler, we now see that the κ_i are maximum and minimum of curvatures κ' determined as in Fig. 7. Sophie Germain already proved that one can even take two arbitrary but orthogonal planes through the normal vector, determine the curvatures κ'_i of the intersections, and add them so as to get $\mathbb{H} = \kappa'_1 + \kappa'_2$.

Mean and Gaussian curvature $\mathbb{H}$ and $\mathbb{K}$ are the fundamental geometrical quantities that determine the energy associated with the bending rigidities k_c and k_g of a biomembrane. This becomes obvious by casting a brief look at (16) and the full energy functional (19).

Gauss–Bonnet theorem. Even more than isometric invariance of $\mathbb{K}$ is true. If we integrate $\mathbb{K}$ over a finite *closed* two-dimensional surface $\mathcal{M}$ in $\mathbb{R}^3$ with respect to its natural surface area $\mathrm{d}f = \mathrm{d}q^1 \mathrm{d}q^2 \sqrt{\det g}$ taken from (31) with $n = 2$. Then it can be shown (Gauss, 1827; Bonnet, 1848)

$$\int_{\mathcal{M}} \mathrm{d}f\, \mathbb{K} = 4\pi(1 - p) \tag{61}$$

for a manifold of genus p, that is, the surface of a (generalized) doughnut with p holes or, better, handles; a sphere has $p = 0$ and for a torus $p = 1$, meaning that a torus can be deformed smoothly into, say, a sphere with one handle. To be fair, relation (61) is more 'egregious' in the sense of outstanding than the *Theorema Egregium*. The only important thing is the number of handles, a truly topological invariant. The proof is tricky (Millman and Parker, 1977), or worse, and at least involved (Struik, 1961). For an in-depth analysis regarding physical implications we refer to Kamien (2002).

In spite of its rather involved proof (Millman and Parker, 1977; Struik, 1961), the Gauss–Bonnet formula (61) is nevertheless an extremely helpful tool to investigate the energy functional (19) of a biomembrane. The point is that the integral $\int_{\mathcal{M}} \mathrm{d}f\, \mathbb{K}$, the *curvatura integra* or integral (total) curvature, by which name Gauss introduced it, becomes a topological constant and hence can be dropped as long as no "handles" are added to or removed from the membrane.

5. Nearly flat membrane

It is time for an application that will play a clarifying role. A doughnut or torus would certainly have been a nice equilibrium shape but, since it has inherent curvature, it is not ideal to start with. We therefore take a "torus" with metric tensor $g = \mathbb{1}$, which is just a square of size $L \times L$ with periodic boundary conditions, the academic example of a vesicle.

Monge representation. The nearly flat membrane is ideally parametrized by the simplest representation of a two-dimensional surface $\mathcal{M}$ in three-dimensional space: the Monge representation (1795) reading $\boldsymbol{x} = (x, y, z = \zeta(x, y))$ with parameters $(q^1, q^2) = (x, y)$. We have already met it in example (22). The metric tensor $g = (\boldsymbol{x}_{\mu} \boldsymbol{x}_{\nu})$ with, as

always, $\boldsymbol{x}_\mu = \partial_\mu \boldsymbol{x}$ and the normal vector $\boldsymbol{n}$ at $\boldsymbol{x} \in \mathcal{M}$ readily follow from

$$\boldsymbol{x}_1 = \begin{pmatrix} 1 \\ 0 \\ \partial_x\zeta \end{pmatrix}, \quad \boldsymbol{x}_2 = \begin{pmatrix} 0 \\ 1 \\ \partial_y\zeta \end{pmatrix}, \quad \boldsymbol{x}_1 \times \boldsymbol{x}_2 = \begin{pmatrix} -\partial_x\zeta \\ -\partial_y\zeta \\ 1 \end{pmatrix}.$$

Putting $W := \|\boldsymbol{x}_1 \times \boldsymbol{x}_2\|$ and herewith $\boldsymbol{n} = W^{-1}\boldsymbol{x}_1 \times \boldsymbol{x}_2$, we obtain

$$g = (g_{\mu\nu}) = \begin{pmatrix} 1 + (\partial_x\zeta)^2 & (\partial_x\zeta)(\partial_y\zeta) \\ (\partial_x\zeta)(\partial_y\zeta) & 1 + (\partial_y\zeta)^2 \end{pmatrix} \tag{62}$$

so that $W^2 = 1 + (\partial_x\zeta)^2 + (\partial_y\zeta)^2 = \det g$, the last equality being the result of a simple computation. We henceforth drop W and use the shorthand $\mathrm{g} := \det g$.

The second fundamental tensor is another easy by-product in that $h_{\mu\nu} = \boldsymbol{x}_{\mu\nu}\boldsymbol{n} = \mathrm{g}^{-1/2}\partial^2_{\mu\nu}\zeta$. We now invert g in (62), note (59) and (60), and find after a bit of algebra

$$\mathbb{H} = \mathrm{g}^{-3/2}\{\partial_x^2\zeta + \partial_y^2\zeta + [(\partial_y\zeta)^2\partial_x^2\zeta - 2(\partial_x\zeta)(\partial_y\zeta)\partial_x\partial_y\zeta + (\partial_x\zeta)^2\partial_y^2\zeta]\}, \tag{63}$$

$$\mathbb{K} = \mathrm{g}^{-2}[\partial_x^2\zeta\partial_y^2\zeta - (\partial_x\partial_y\zeta)^2] \tag{64}$$

for the mean and Gaussian curvature $\mathbb{H}$ and $\mathbb{K}$.

The Monge representation is particularly important to membrane physics since a great deal of experimental work is devoted to nearly flat membranes. In the upcoming paragraph we therefore derive energy spectrum and dispersion relation for this experimentally important situation. As we will see, elementary excitations from the flat equilibrium are simple: plane waves.

Undulating flat membrane. Because of (19) and its BCM equivalent, the general energy functional $\mathcal{F}$ reads

$$\mathcal{F} = \frac{1}{2}k_c\int \mathrm{d}f\,\mathbb{H}^2 + \frac{1}{2}k_g\int \mathrm{d}f\,\mathbb{K} + \Sigma A - PV + QM. \tag{65}$$

It is plain that for an initially flat membrane the Monge representation is most natural. The membrane being flat, its volume $V = 0$ vanishes while $\mathbb{H} = \kappa_1 + \kappa_2$ and $M = \int \mathrm{d}f\,\mathbb{H}$ as the integrated mean curvature readily follow from Eq. (62) in conjunction with (63). As we do not want to punch holes and have adopted periodic boundary conditions, i.e., effectively a torus, the Gauss–Bonnet relation (61) tells us that, for a closed surface, $\int \mathrm{d}f\,\mathbb{K}$ is a topological invariant and, therefore, can be dropped beforehand.

Instead of ending up with nonlinear partial differential equations it is for the moment simpler, and also more physical, to first ask whether a sensible approximation is at hand. The answer is affirmative in that we can assume the undulation amplitudes a to be small. In view of derivatives hanging around all over the place, it seems natural to neglect these as well in products of order 3 and higher. We can do so once $a \ll \lambda$ with λ as a typical wavelength; cf. Fig. 1(c). If so, life becomes simple as now $\mathrm{g} = \det g = 1 + (\partial_x\zeta)^2 + (\partial_y\zeta)^2 \approx 1$ so that up to second order in ζ

$$\mathcal{F}(\zeta) = \int\!\!\int \mathrm{d}x\mathrm{d}y\left[\frac{k_c}{2}|\Delta\zeta|^2 + \frac{\Sigma}{2}(\nabla\zeta)^2 + Q\Delta\zeta\right]. \tag{66}$$

Here $\Delta = \partial_x^2 + \partial_y^2$ is a Laplacian. Because of (62) the surface tension Σ is to be accompanied by $\mathrm{d}f = \mathrm{d}x\,\mathrm{d}y\mathrm{g}^{1/2} = \mathrm{d}x\,\mathrm{d}y[1 + (\partial_x\zeta)^2 + (\partial_y\zeta)^2]^{1/2} =: \mathrm{d}x\,\mathrm{d}y[1 + (\nabla\zeta)^2/2]$, where we drop the trivial constant 1 and terms of order three and higher. In a similar vein, Q is related to M and, through (63), to $\mathrm{d}f\,\mathbb{H} = \mathrm{d}x\,\mathrm{d}y\mathrm{g}^{1/2}\mathbb{H} = \mathrm{d}x\,\mathrm{d}y[1 + (\partial_x\zeta)^2 + (\partial_y\zeta)^2)]^{-1}\Delta\zeta = \mathrm{d}x\,\mathrm{d}y\Delta\zeta$.

Embedding our real Hilbert space of quadratically integrable functions $\mathcal{L}^2[-\frac{L}{2}, \frac{L}{2}]^2$ on the square $[-\frac{L}{2}, \frac{L}{2}]^2$ into a complex Hilbert space of exactly the same type we directly find that $\exp(\mathrm{i}\vec{k}\vec{x})$ with $\vec{k} = \frac{2\pi}{L}(m, n)$ and $m, n \in \mathbb{Z}$ are eigenfunctions of all differential operators in sight. For the ensuing arguments we refer to Boal (2002; Chapter 6). Instead we differentiate (66) twice. Being at a minimum ζ_0 we must have

$$\left.\frac{\mathrm{d}\mathcal{F}(\zeta_0 + t\psi)}{\mathrm{d}t}\right|_{t=0} = 0, \quad \left.\frac{\mathrm{d}^2\mathcal{F}(\zeta_0 + t\psi)}{\mathrm{d}t^2}\right|_{t=0} > 0, \tag{67}$$

whatever $\psi \neq 0$. The rest is clear sailing. The first derivative vanishing for all ψ gives $(k_c\Delta^2 - \Sigma\Delta)\zeta_0 = 0$. The self-adjoint operators Δ and Δ^2 have the above $L^{-1}\exp(\mathrm{i}\vec{k}\vec{x})$ as a complete orthonormal set of eigenvectors. Expanding ζ_0 with respect to them we find $(k^2k_c + \Sigma)k^2 = 0$, so that all coefficients vanish, except for $k = 0$. Hence we are left with $\zeta_0 \equiv \mathrm{C}^{\mathrm{st}}$; there is no harm in taking this constant to be 0. The second derivative equals $\delta^2\mathcal{F}(\psi,\psi) = \int \mathrm{d}x\,\mathrm{d}y[k_c(\Delta\psi)^2 + \Sigma(\nabla\psi)^2] = \int \mathrm{d}x\,\mathrm{d}y\psi(k_c\Delta^2 - \Sigma\Delta)\psi \geqslant 0$, a quadratic form associated with the linear operator $\delta^2\mathbb{F} = k_c\Delta^2 - \Sigma\Delta \geqslant 0$. Stability is evident.

Of course one can do without a complex Hilbert space and use $\cos(\vec{k}\vec{x})$ and $\sin(\vec{k}\vec{x})$ instead of $\exp(\mathrm{i}\vec{k}\vec{x})$. The former two are eigenfunctions of the Laplacian Δ but not of ∇. By means of the expansion $\zeta(\vec{x}) = (\sqrt{2}/L)[a_{\vec{k}}\cos(\vec{k}\vec{x}) + b_{\vec{k}}\sin(\vec{k}\vec{x})]$ the energy nevertheless attains the simple form

$$\mathcal{F} = \sum_{\vec{k}\neq 0}[(k_ck^4 + \Sigma k^2)/4](a_{\vec{k}}^2 + b_{\vec{k}}^2). \tag{68}$$

One then considers $a_{\vec{k}}$ and $b_{\vec{k}}$ as new coordinates and applies the equipartition theorem (Huang, 1987) to each of the quadratic terms so as to get, e.g., $(k_ck^4 + \Sigma k^2)\langle a_{\vec{k}}^2\rangle = 2k_{\mathrm{B}}T$ for the thermal average $\langle a_{\vec{k}}^2\rangle$.

A real cell is neither flat nor "nearly" flat but finite in size, even small (10–40 μm), and thus quite curved. Moreover, and in contrast to vesicles, it contains a cytoskeleton stabilizing the cell membrane; cf. Section 3 and in particular (20). Restricting ourselves to normal displacements ζ and forgetting the cell-membrane's curvature for the moment we could add, as pointed out by Gov et al. (Gov et al., 2003; Gov and Safran, 2005), a term $\Gamma\zeta^2/2$ to the integrand of (66). Here the inhomogeneous attachment of the cytoskeleton to the lipid bilayer making up the cell membrane is supposed to give rise to an overall confinement modeled as a harmonic potential $\Gamma\zeta^2/2$. Harmonic potentials are nice as they always give rise to exact solutions; cf. the quadratic form (3) in Section 2, a generic harmonic potential. Instead of (68) we then end up with an energy $\mathcal{F}$ containing one more term,

$$\mathcal{F} = \sum_{\vec{k}\neq 0}[(k_ck^4 + \Sigma k^2 + \Gamma)/4](a_{\vec{k}}^2 + b_{\vec{k}}^2). \tag{69}$$

Accordingly, using the equipartition theorem (Huang, 1987) once again, we find for example the thermal average

$$\langle a_{\vec{k}}^2\rangle = 2k_{\mathrm{B}}T(k_ck^4 + \Sigma k^2 + \Gamma)^{-1}. \tag{70}$$

For $\Gamma > 0$ there is no divergence anymore as, for fixed integers m and n, $\vec{k} = (m,n)2\pi/L \to 0$ for large system size $L \to \infty$. Removing the divergence looks good but is fake as it makes no sense to discuss long-wavelength ($\vec{k} \to 0$) elementary excitations in a finite closed cell membrane with typical diameter of 10–40 μm.

So let's turn to real cells. That is, we then have to do at least two things. First, showing that for a full description of elementary excitations in a biomembrane with inherent curvature *normal* deviations such as ζ suffice. Furthermore, we will have to gain additional insight into the analytical formalism of differential-geometric calculus on a *curved* surface, viz., covariant differentiation, so as to be able to quickly differentiate the energy functional of a curved cell membrane.

6. Why normal deviations suffice

To find the elementary excitations of a (bio)membrane, we proceed as in the case of a harmonic crystal. Instead of the potential V we now have to handle the energy functional $\mathcal{F}$ defined on a smooth manifold. Analogously to $\partial_{\mathbf{q}}V = 0$, we start with an equilibrium shape characterized by $\delta\mathcal{F} = 0$ and, in complete analogy to $\partial_{\mathbf{q}}\partial_{\mathbf{q}}V$, we study its stability and *linearized* dynamics through the (spectrum of the) operator $\delta^2\mathbb{F}$ associated with the second derivative. How to compute all this?

For differentiation we need to subtract but, facing shapes of manifolds, the question is: What? Suppose we are given an equilibrium shape $\mathcal{M}$ with energy $\mathcal{F}_0$. We decompose deviations from equilibrium at the point $\boldsymbol{x} \in \mathcal{M}$ into a tangential part and a normal part proportional to the normal vector $\boldsymbol{n}$. The tangential part does not change energy and only leads to an uninteresting reparametrization so that it will not be considered here any further.

Normal deviations are described by $\psi(\boldsymbol{x})\boldsymbol{n}$ for some smooth real function ψ defined on the manifold. We can add and subtract functions and only have to require that they do not get too unwieldy while being on $\mathcal{M}$ so as to guarantee

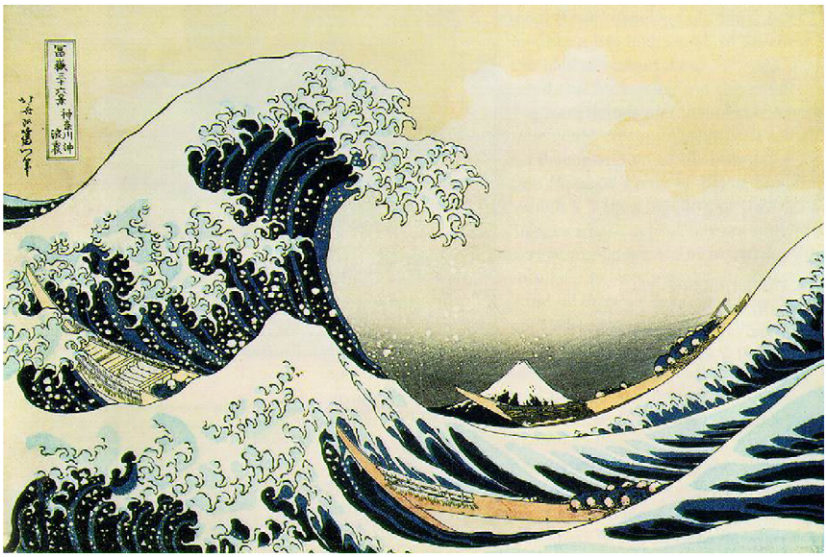

Fig. 8. Katsushika Hokusai (1760–1849): *Under the Wave, off Kanagawa*, woodblock print, 1830–1833. As common as overhanging waves are to our experience of fluids, these shapes are energetically highly improbable on the surfaces of cell membranes. This is particularly true for finer structure like the white curls at the wave crest. Deformations like famous Mount Fuji (background) are equally unlikely because of the kink at the summit.

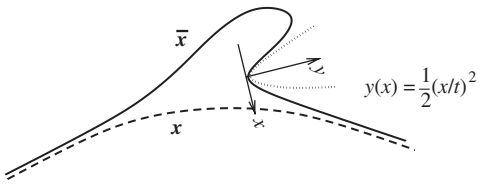

Fig. 9. Small shape fluctuations $\bar{\boldsymbol{x}}$ that cannot be described by normal deviations from the equilibrium form $\boldsymbol{x}$ (dashed line) lead to a divergent energy contribution as $t \to 0$. In this limit, the 'dip' in the overhang is approximated by the parabola $y = (x/t)^2/2$.

a finite energy. Equipped with our surface measure $\mathrm{d}f = \sqrt{\mathrm{g}}\,\mathrm{d}\vec{q}$ with $\mathrm{g} = \det(g_{\mu\nu})$ we therefore require $\delta^2\mathbb{F}$ to live on a suitable domain $\mathcal{D}$ in the real Hilbert space

$$\mathcal{L}^2(\mathcal{M}) = \left\{ \psi \,\middle|\, \int_{\mathcal{M}} \mathrm{d}f\, |\psi(\boldsymbol{x})|^2 < \infty \right\} \tag{71}$$

with scalar product $\langle\varphi|\psi\rangle = \int \mathrm{d}f\, \varphi(\boldsymbol{x})\psi(\boldsymbol{x})$. So the problem is solved. Well, is it?

What actually guarantees that ψ is a *uniquely* defined function on the given manifold $\mathcal{M}$ instead of describing a surface as in Fig. 8 where the overhang needs an at least three-valued ψ? The simple answer is that a single-valued ψ is energetically more favorable. We now prove that life is that simple. In view of (67) we study $\mathcal{F}(\boldsymbol{x} + t\psi\boldsymbol{n})$ with $\boldsymbol{x} \in \mathcal{M}$ and $t \to 0$. There is no harm in restricting the surface to the intersection of the manifold and the plane of the paper, which is the solid line in Fig. 9, and assume translational invariance orthogonal to it.

To estimate the energy it suffices to study $\int \mathrm{d}s\kappa^2(s)$ of the parabola $y = x^2/2$ underneath $y = 1$ and perform the transformation $x \mapsto x/t$ in the limit $t \to 0$; cf. Fig. 9. Using the exact expression for the (radius of) curvature one finds asymptotically $t^{-2}\int \mathrm{d}z(1+z^2)^{-5/2} \sim t^{-2}$, as announced.

That is, we henceforth analyze *normal* variations ψ as smooth functions on $\mathcal{M}$ and study the behavior of the energy functional $\mathcal{F}(\bar{\boldsymbol{x}})$ under normal variations

$$\bar{\boldsymbol{x}} = \boldsymbol{x} + t\psi\boldsymbol{n}. \tag{72}$$

Differentiating $\mathcal{F}(\boldsymbol{x}+t\psi\boldsymbol{n})$ with respect to t once or twice on a given manifold with $\boldsymbol{x}\in\mathcal{M}$ means differentiating $\mathcal{F}$ in the direction ψ. [Technically we obtain a Gâteaux derivative, which is weaker than the Fréchet derivative with respect to the norm. In our Hilbert space (71), however, $(n+1)$ times Gâteaux differentiable means n times Fréchet differentiable (Liusternik and Sobolev, 1961).]

As for stability we finish the argument by noting that the second derivative is of the form $\delta^2\mathcal{F}(\psi,\psi):=\langle\psi|\delta^2\mathbb{F}|\psi\rangle$. In complete analogy to $\boldsymbol{q\Phi q}>0$ for the harmonic crystal we obtain stability, if $\delta^2\mathcal{F}(\psi,\psi)>0$ for all $\psi\neq 0$; in other words, if $\delta^2\mathbb{F}$ is a positive operator on $\mathcal{L}^2(\mathcal{M})$. We are now going to compute $\delta^2\mathbb{F}$. To do this efficiently we need covariant differentiation.

7. Fundamentals of covariant differentiation

In the analysis of undulation phenomena and on several other occasions in physics (Frankel, 1997) an elementary knowledge of covariant differentiation is very helpful. It is therefore explained here. Physical laws should be form-invariant under a coordinate transformation; one also calls this 'covariant'. Covariant differentiation does, so to speak, the job. Furthermore, it brings the derivative of a tangent vector field back into tangent space.

Let us first check the effect of a coordinate transformation $q^\mu\mapsto q^{\mu'}$ on a vector in tangent space,

$$\boldsymbol{a}=a^\mu\partial_\mu\boldsymbol{x}=(a^\mu\partial_\mu q^{\mu'})\partial_{\mu'}\boldsymbol{x}=:a^{\mu'}\partial_{\mu'}\boldsymbol{x}. \tag{73}$$

That is, $a^{\mu'}=a^\mu\partial_\mu q^{\mu'}$. To save space we define $T_\mu^{\mu'}:=\partial_\mu q^{\mu'}$ with, for an n-dimensional manifold, $1\leqslant\mu,\mu'\leqslant n$. Coordinate transformations being invertible, T is invertible as a matrix and its inverse T^{-1} corresponds to the inverse transformation $q^{\mu'}\mapsto q^\mu$. To see why, we use the chain rule and find $\delta_\nu^\mu=\partial_\nu q^\mu(\{q^{\mu'}\})=\partial_{\nu'}q^\mu\partial_\nu q^{\nu'}=T_{\nu'}^\mu T_\nu^{\nu'}$. In summary, we have

$$q^\mu\mapsto q^{\mu'}\to T_\mu^{\mu'}=\partial_\mu q^{\mu'}\quad\Leftrightarrow\quad q^{\mu'}\mapsto q^\mu\to T_{\mu'}^\mu=\partial_{\mu'}q^\mu. \tag{74}$$

A cautionary remark: $T_{\mu'}^\mu$ is *not* $\partial^\mu q_{\mu'}$.

To finish the argument we insert the Gauss formula (40) into (73) and obtain

$$\begin{aligned}\partial_\mu\boldsymbol{a}&=\partial_\mu(a^\nu\boldsymbol{x}_\nu)=(\partial_\mu a^\nu)\boldsymbol{x}_\nu+a^\nu\boldsymbol{x}_{\mu\nu}\\&=(\partial_\mu a^\kappa+\Gamma_{\mu\nu}^\kappa a^\nu)\boldsymbol{x}_\kappa+h_{\mu\nu}a^\nu\boldsymbol{n},\end{aligned} \tag{75}$$

which shows two things. First, Eq. (75) is not covariant. Second, though $\boldsymbol{a}$ is in tangent space, $\partial_\mu\boldsymbol{a}$ in general is not. How, then, can we eliminate these two drawbacks?

Focusing e.g. on the geodesic curvature $\kappa_G=\|\mathbb{P}\mathrm{d}_s^2\boldsymbol{x}\|$ as given by (45), we see a differentiation d_s is followed by a projection $\mathbb{P}$ onto the tangent space $\mathcal{T}_{\boldsymbol{x}}$ at $\boldsymbol{x}\in\mathcal{M}$. Since this order will turn out to be important we define

$$D_\bullet:=\mathbb{P}\mathrm{d}_\bullet\quad\text{with }\mathbb{P}=|\boldsymbol{x}_\mu\rangle\langle\boldsymbol{x}^\mu|=|\boldsymbol{x}^\mu\rangle\langle\boldsymbol{x}_\mu|, \tag{76}$$

projecting onto $\mathcal{T}_{\boldsymbol{x}}$. One calls D a *covariant differentiation*. It puts the final result of differentiation starting in tangent space back into tangent space. Here we take for $\mathrm{d}_\bullet$ either d_s or ∂_μ. For example, we read the coefficients for $D_s\boldsymbol{u}$ with $\boldsymbol{u}=\mathrm{d}_s\boldsymbol{x}=u^\nu\boldsymbol{x}_\nu$ with respect to the basis $\{\boldsymbol{x}^\lambda\}$ from $u^\nu=\mathrm{d}_s q^\nu$ in conjunction with

$$\boldsymbol{x}^\lambda D_s\boldsymbol{u}=\boldsymbol{x}^\lambda\mathrm{d}_s(u^\nu\boldsymbol{x}_\nu)=\mathrm{d}_s u^\lambda+\Gamma_{\nu\mu}^\lambda u^\mu u^\nu. \tag{77}$$

For an arbitrary tangent vector $\boldsymbol{a}=a^\nu\boldsymbol{x}_\nu$ we get

$$\boldsymbol{x}^\lambda D_\mu\boldsymbol{a}=\partial_\mu a^\lambda+\Gamma_{\mu\nu}^\lambda a^\nu. \tag{78}$$

To see all this in an optically different way, we start from the Gauss formula $\boldsymbol{x}_{\mu\nu}=\Gamma_{\mu\nu}^\kappa\boldsymbol{x}_\kappa+h_{\mu\nu}\boldsymbol{n}$ with Christoffel symbol $\Gamma_{\mu\nu}^\lambda=\boldsymbol{x}^\lambda\boldsymbol{x}_{\mu\nu}$ and let $\mathbb{P}$ operate on

$$\begin{aligned}\partial_\mu\boldsymbol{a}&=\partial_\mu(a^\nu\boldsymbol{x}_\nu)=(\partial_\mu a^\nu)\boldsymbol{x}_\nu+a^\nu\boldsymbol{x}_{\mu\nu}\\&=(\partial_\mu a^\kappa+\Gamma_{\mu\nu}^\kappa a^\nu)\boldsymbol{x}_\kappa+h_{\mu\nu}a^\nu\boldsymbol{n}.\end{aligned} \tag{79}$$

Accordingly, the geodesic equation (44) now reads $D_s \boldsymbol{u} = 0$, which is a more precise way of saying that we take a "straight" line on a curved surface.

Geodesics are not a mere mathematical peculiarity. They are in fact of high physical relevance. To see why, we consider a 'fluid' lipid bilayer as a two-dimensional liquid supporting a large variety of proteins floating in this "sea". Proteins are electrically charged or at least are dipoles. Electromagnetic interactions thus strongly influence the motion of proteins on a membrane surface. In contrast, however, to charged particles in vacuo they do not "swim" along straight lines, if they were alone, or follow similar curves that are well-known from classical electrodynamics but follow perturbed geodesics that are determined by the specific *shape* of the membrane they are in.

It is time to list a few properties of covariant differentiation. To this end we consider differentiable vector fields $\boldsymbol{a}$ and $\boldsymbol{b}$ on $\mathcal{M}$, i.e., $\boldsymbol{a}(\boldsymbol{x}), \boldsymbol{b}(\boldsymbol{x}) \in \mathcal{T}_{\boldsymbol{x}}$, and assume φ to be a smooth real function on $\mathcal{M}$.

(i) After a coordinate transformation a covariant derivative in terms of the new coordinates $q^{\mu'}$ reads: $D_{\mu'}\boldsymbol{a} = (\mathbb{P}\partial_{\mu}\boldsymbol{a})T^{\mu}_{\mu'} = T^{\mu}_{\mu'} D_{\mu}\boldsymbol{a}$ where $T^{\mu}_{\mu'} = \partial_{\mu'} q^{\mu}$. This is D's covariant transformation behavior.
(ii) $D_{\mu}(\boldsymbol{a}+\boldsymbol{b}) = D_{\mu}\boldsymbol{a} + D_{\mu}\boldsymbol{b}$, due to linearity of the operators in sight.
(iii) $\partial_{\mu}(\boldsymbol{a}\varphi) = (\partial_{\mu}\boldsymbol{a})\varphi + \boldsymbol{a}\partial_{\mu}\varphi \Rightarrow D_{\mu}(\boldsymbol{a}\varphi) = (D_{\mu}\boldsymbol{a})\varphi + \boldsymbol{a}\partial_{\mu}\varphi$.
(iv) Being a projection operator, $\mathbb{P}$ is self-adjoint, i.e., $\boldsymbol{a}(\mathbb{P}\boldsymbol{b}) = (\mathbb{P}\boldsymbol{a})\boldsymbol{b}$. Furthermore, $\mathbb{P}\boldsymbol{a} = \boldsymbol{a}$, whatever $\boldsymbol{a} \in \mathcal{T}_{\boldsymbol{x}}$. Hence we obtain, for $\boldsymbol{a}$ & $\boldsymbol{b} \in \mathcal{T}_{\boldsymbol{x}}$,

$$\begin{aligned}\partial_{\mu}(\boldsymbol{a}\boldsymbol{b}) &= (\partial_{\mu}\boldsymbol{a})\mathbb{P}\boldsymbol{b} + \mathbb{P}\boldsymbol{b}\boldsymbol{a}(\partial_{\mu}\boldsymbol{b}) = \mathbb{P}(\partial_{\mu}\boldsymbol{a})\boldsymbol{b} + \boldsymbol{a}\mathbb{P}(\partial_{\mu}\boldsymbol{b}) \\ &= (D_{\mu}\boldsymbol{a})\boldsymbol{b} + \boldsymbol{a}(D_{\mu}\boldsymbol{b}).\end{aligned}$$

By construction, covariant differentiation transforms a tangent space into itself. We therefore define its *covariant* and *contravariant* coefficients, transforming under coordinate transformations as ∂_{μ} and ∂^{μ} respectively, by

$$\nabla_{\mu} a^{\nu} := \boldsymbol{x}^{\nu} D_{\mu}\boldsymbol{a} \quad \Leftrightarrow \quad D_{\mu}\boldsymbol{a} = (\nabla_{\mu} a^{\nu})\boldsymbol{x}_{\nu}, \tag{80}$$

$$\nabla_{\mu} a_{\nu} := \boldsymbol{x}_{\nu} D_{\mu}\boldsymbol{a} \quad \Leftrightarrow \quad D_{\mu}\boldsymbol{a} = (\nabla_{\mu} a_{\nu})\boldsymbol{x}^{\nu}. \tag{81}$$

Tensors. In view of (80) and (81) it is timely to introduce the tensor notion. We have seen how tangent vectors $\boldsymbol{a} = a^{\nu}\boldsymbol{x}_{\nu}$ transform under a coordinate transformation. Equation (74) tells us $q^{\nu} \mapsto q^{\nu'} \Rightarrow a^{\nu'} = a^{\nu}\partial_{\nu} q^{\nu'} = T^{\nu'}_{\nu} a^{\nu}$. Referring to this 'covariant' transformation behavior one therefore says a^{ν} is a tensor of rank (1, 0). More generally, a tensor of type (m, n) is a quantity of the form $t^{\nu_1 \ldots \nu_m}_{\mu_1 \ldots \mu_n}$ of which the upper and lower indices *transform* according to

$$t^{\nu'_1 \ldots \nu'_m}_{\mu'_1 \ldots \mu'_n} = T^{\nu'_1}_{\nu_1} \ldots T^{\nu'_m}_{\nu_n} T^{\mu_1}_{\mu'_1} \ldots T^{\mu_n}_{\mu'_n} t^{\nu_1 \ldots \nu_m}_{\mu_1 \ldots \mu_n}.$$

As an illustration we return to (80) and note that, due to (i), we have obtained a tensor of rank (1, 1),

$$\nabla_{\mu'} a^{\nu'} = \boldsymbol{x}^{\nu'} D_{\mu'}\boldsymbol{a} = T^{\nu'}_{\nu} T^{\mu}_{\mu'} \boldsymbol{x}^{\nu} D_{\mu}\boldsymbol{a} = T^{\mu}_{\mu'} T^{\nu'}_{\nu} \nabla_{\mu} a^{\nu}.$$

Invoking (74) and herewith $T^{\mu}_{\nu'} T^{\nu'}_{\nu} = \delta^{\mu}_{\nu}$ we recognize the 'contraction' $\nabla_{\mu} a^{\mu}$ as a quantity that is *invariant* under coordinate transformations, a most valuable property.

Equally natural and hardly more difficult is generalizing covariant differentiation from tangent vectors such as in (80) and (81) to tensors of arbitrary type. To keep our notation simple we stick to type (1, 1), as in g^{μ}_{ν}. A tangent vector $\boldsymbol{t} = t^{\mu}\boldsymbol{x}_{\mu}$, more in particular, t^{μ}, has been declared to be a tensor. We now generalize this through the *tensor product* $\otimes$ as a bilinear (or multilinear) map into product space: $\boldsymbol{a} \otimes (\boldsymbol{b} + \boldsymbol{c}) = \boldsymbol{a} \otimes \boldsymbol{b} + \boldsymbol{a} \otimes \boldsymbol{c}$, $\lambda(\boldsymbol{a} \otimes \boldsymbol{b}) = (\lambda\boldsymbol{a}) \otimes \boldsymbol{b} = \boldsymbol{a} \otimes (\lambda\boldsymbol{b})$, and analogously for $\boldsymbol{a}_1 \otimes \boldsymbol{a}_2 \otimes \cdots \otimes \boldsymbol{a}_m$. A zeroth-order tensor is a scalar $\boldsymbol{t} = t$, invariant under coordinate transformations.

For bases $\boldsymbol{x}_{\mu}$ and $\boldsymbol{x}_{\nu}$ in tangent space $\mathcal{T}_{\boldsymbol{x}}$ we could rewrite the metric tensor $\boldsymbol{g}$, of which we meanwhile know the transformation behavior rather well, in the form $\boldsymbol{g} = g_{\mu\nu}\boldsymbol{x}^{\mu} \otimes \boldsymbol{x}^{\nu}$. We then define a tensor $\boldsymbol{t}$ of type (1, 1) to be the quantity $\boldsymbol{t} = t^{\nu_1}_{\mu_1}\boldsymbol{x}_{\nu_1} \otimes \boldsymbol{x}^{\mu_1}$. It exhibits the "right" behavior under a coordinate transformation and thus is a tensor in the above sense. By the very nature of tensor product we can evaluate $\partial_u[\boldsymbol{a}(u) \otimes \boldsymbol{b}(u)]$ as if it were a normal product, for which the product rule holds. To wit, we can write it as a sum of two terms, $[\boldsymbol{a}(u+h) \otimes \boldsymbol{b}(u+h) - \boldsymbol{a}(u) \otimes \boldsymbol{b}(u+h)]$ and $[\boldsymbol{a}(u) \otimes \boldsymbol{b}(u+h) - \boldsymbol{a}(u) \otimes \boldsymbol{b}(u)]$, divide by h, and send $h \to 0$ so as to get

$$\lim_{h \to 0} \partial_u[\boldsymbol{a}(u) \otimes \boldsymbol{b}(u)]/h = (\partial_u\boldsymbol{a}) \otimes \boldsymbol{b} + \boldsymbol{a} \otimes (\partial_u\boldsymbol{b}). \tag{82}$$

Given the projection operator $\mathbb{P}$, we define the covariant derivative for an arbitrary tensor $\boldsymbol{t}$ to be

$$D_\mu \boldsymbol{t} := \mathbb{P} \otimes \cdots \otimes \mathbb{P}\partial_\mu \boldsymbol{t}. \tag{83}$$

Generalization of the rules (i)–(iv) to a general tensor is straightforward.

After this detour we focus on Christoffel symbols, defined by (41), prove their isometric invariance, and in so doing derive a useful expression for proving Lemma C.

Lemma B. *Christoffel symbols are determined by the* inner *geometry of a manifold*, *i.e.*, *its metric tensor only*,

$$\Gamma^\lambda_{\mu\nu} = g^{\lambda\kappa}(\partial_\mu g_{\kappa\nu} + \partial_\nu g_{\kappa\mu} - \partial_\kappa g_{\mu\nu})/2. \tag{84}$$

In other words, Christoffel symbols are *isometric invariants*. From a classical point of view, a "Riemannian" geometry is defined by its metric tensor $(g_{\mu\nu})$ being positive-definite. According to a modern definition it is a geometry satisfying (84).

Proof. Because of the Gauss formula (40) we get

$$\partial_\kappa g_{\mu\nu} = \boldsymbol{x}_{\mu\kappa}\boldsymbol{x}_\nu + \boldsymbol{x}_\mu \boldsymbol{x}_{\nu\kappa} = g_{\nu\lambda}\Gamma^\lambda_{\mu\kappa} + g_{\mu\lambda}\Gamma^\lambda_{\nu\kappa}.$$

A cyclic permutation of the indices then gives

$$\partial_\mu g_{\nu\kappa} = g_{\kappa\lambda}\Gamma^\lambda_{\nu\mu} + g_{\nu\lambda}\Gamma^\lambda_{\kappa\mu}, \quad \partial_\nu g_{\kappa\mu} = g_{\mu\lambda}\Gamma^\lambda_{\kappa\nu} + g_{\kappa\lambda}\Gamma^\lambda_{\mu\nu}.$$

We add the final two and subtract the first equation, multiply by $g^{\kappa\lambda}$, and find (84). □

Lemma C (*Ricci, 1888*). *The covariant derivative commutes with the metric tensor*, $[\nabla_\kappa, g_{\mu\nu}] = [\nabla_\kappa, g^{\mu\nu}] = 0$, *and even stronger* $\nabla_\kappa g_{\mu\nu} = \nabla^\kappa g_{\mu\nu} = 0$.

Proof. The proof is a simple consequence of (80) and (81),

$$g_{\mu\nu}\nabla_\kappa a^\nu = g_{\mu\nu}\boldsymbol{x}^\nu D_\kappa \boldsymbol{a} = \nabla_\kappa a_\mu = \nabla_\kappa(a^\nu g_{\mu\nu}).$$

Vanishing of $\nabla^\kappa g_{\mu\nu}$ is now obvious since

$$0 = g_{\mu\nu}\nabla_\kappa a^\nu - \nabla_\kappa(g_{\mu\nu}a^\nu) = -(\nabla_\kappa g_{\mu\nu})a^\nu$$

for vectors $\boldsymbol{a} \neq 0$. □

As we have seen in (78), covariant differentiation transforms a tangent vector $a^\nu \boldsymbol{x}_\nu$ into

$$\nabla_\mu a^\nu = \partial_\mu a^\nu + \Gamma^\nu_{\mu\kappa} a^\kappa. \tag{85}$$

In a similar vein, $a_\nu \boldsymbol{x}^\nu$ gives rise to

Lemma D. *The covariant derivative of tensor coordinates with lower index is given by*

$$\nabla_\mu a_\nu = \partial_\mu a_\nu - \Gamma^\kappa_{\mu\nu} a_\kappa. \tag{86}$$

Proof. To understand why, we start by computing $\partial_\mu g_{\lambda\nu} = \partial_\mu(\partial_\lambda \boldsymbol{x}\partial_\nu \boldsymbol{x}) = \Gamma^\kappa_{\mu\lambda} g_{\nu\kappa} + \Gamma^\kappa_{\mu\nu} g_{\kappa\lambda}$, and obtain

$$\partial_\mu a_\nu = \partial_\mu(a^\lambda g_{\lambda\nu}) = \underline{(\partial_\mu a^\lambda) g_{\lambda\nu}} + a^\lambda \Gamma^\kappa_{\mu\lambda} g_{\nu\kappa} + \Gamma^\kappa_{\mu\nu} a_\kappa.$$

Lemma C and (85) provide us with

$$\nabla_\mu a_\nu = (\nabla_\mu a^\lambda) g_{\lambda\nu} = \underline{(\partial_\mu a^\lambda) g_{\lambda\nu}} + \Gamma^\lambda_{\mu\kappa} a^\kappa g_{\nu\lambda} = \partial_\mu a_\nu - \Gamma^\kappa_{\mu\nu} a_\kappa - (a^\lambda \Gamma^\kappa_{\mu\lambda} g_{\nu\kappa} - \Gamma^\lambda_{\mu\kappa} a^\kappa g_{\nu\lambda}).$$

An interchange of the dummy indices κ and λ in the final term finishes the argument. □

Covariant differentiation of tensors. Using Lemma D in conjunction with (85), (80), (81), and (82) we find for a (1, 1) tensor $D_\kappa t^\nu_\mu = \partial_\kappa t^\nu_\mu + \Gamma^\nu_{\kappa\lambda} t^\lambda_\mu - \Gamma^\lambda_{\kappa\mu} t^\nu_\lambda$, and with a bit more work for an (m, n) tensor

$$D_\kappa t^{\nu_1\dots\nu_n}_{\mu_1\dots\mu_m} = \partial_\kappa t^{\nu_1\dots\nu_n}_{\mu_1\dots\mu_m} + \sum_{i=1}^{n} \Gamma^{\nu_i}_{\kappa\lambda} t^{\nu_1\dots\lambda\dots\nu_n}_{\mu_1\dots\mu_m} - \sum_{j=1}^{m} \Gamma^{\lambda}_{\kappa\mu_j} t^{\nu_1\dots\nu_n}_{\mu_1\dots\lambda\dots\mu_m}. \tag{87}$$

Lemma E. *Let us define* $\mathrm{g} := \det g = \det(g_{\mu\nu})$. *Then a* '*contraction*' *of the Christoffel symbols gives*

$$\Gamma^\kappa_{\kappa\mu} = \frac{\partial_\mu \sqrt{\mathrm{g}}}{\sqrt{\mathrm{g}}} \Rightarrow \partial_\mu(\sqrt{\mathrm{g}} a^\mu) = \sqrt{\mathrm{g}} \nabla_\mu a^\mu. \tag{88}$$

Proof. To convince oneself of the truth of this statement, it is best to start on the left and verify differentiation of a determinant first. Let adj(g) denote the adjugate matrix (Horn and Johnson, 1985) of $g = (g_{\mu\kappa})$. Writing out its key property $g\,\mathrm{adj}(g) = \mathrm{g}\mathbb{1}$ in terms of components, we get $g_{\mu\kappa}\mathrm{adj}(g)^{\kappa\nu} = \mathrm{g}\delta^\nu_\mu$ and thus, since $\mathrm{adj}(g)^{\kappa\nu}$ does not depend on $g_{\mu\kappa}$,

$$\frac{\partial \mathrm{g}}{\partial g_{\mu\nu}} = \mathrm{adj}(g)^{\mu\nu} = \mathrm{g} g^{\mu\nu}. \tag{89}$$

A direct consequence is

$$\frac{\partial_\mu \sqrt{\mathrm{g}}}{\sqrt{\mathrm{g}}} = \frac{1}{2} g^{\kappa\nu} \partial_\mu g_{\kappa\nu} = \frac{1}{2} g^{\kappa\nu} (g_{\lambda\nu} \Gamma^\lambda_{\kappa\mu} + g_{\lambda\kappa} \Gamma^\lambda_{\mu\nu}) = \frac{1}{2} (\Gamma^\kappa_{\kappa\mu} + \Gamma^\nu_{\mu\nu}).$$

By the very nature of a Christoffel symbol $\Gamma^\lambda_{\mu\nu} = \boldsymbol{x}^\lambda \boldsymbol{x}_{\mu\nu}$, it is symmetric in the lower indices. This, then, gives the first half of (88). To finish the argument we insert (85) into $\partial_\mu(\sqrt{\mathrm{g}} a^\mu) = \sqrt{\mathrm{g}}(\partial_\mu a^\mu + \Gamma^\kappa_{\kappa\mu} a^\mu) = \sqrt{\mathrm{g}} \nabla_\mu a^\mu$ and are done. □

The last equality in (89) is of particular importance since, due to $\mathrm{d}f = \sqrt{\mathrm{g}}\,\mathrm{d}q^1\,\mathrm{d}q^2$, it assures Green's integral equations to apply to curved surfaces as well. One has to realize, however, that for surfaces with boundaries the boundary terms have to be multiplied by $\sqrt{\mathrm{g}}$ in order to take into account the length changes induced by curvature; see, for example, Struik (1961, p. 153).

8. Gradient, divergence, Laplace–Beltrami operator

We are going to introduce gradient, divergence, and Laplace–Beltrami operator as physically covariant quantities that are independent of the specific coordinate system we are working with. Finally, we will see how *integrated* expressions such as (19) and (120) below are invariant under conformal transformations.

Gradient. A scalar function $\Phi : \mathcal{M} \mapsto \mathbb{R}$ assigns a real number to each point on the manifold. It is evidently form-invariant as long as we do not disrupt $\mathcal{M}$. Taking such a function Φ we define its *gradient* to be a vector in tangent space $\mathcal{T}_{\boldsymbol{x}}$ such that

$$\mathrm{grad}\,\Phi \equiv \nabla\Phi := (\partial_\mu \Phi)\boldsymbol{x}^\mu. \tag{90}$$

A function Φ on $\mathcal{M}$ is meant to be $\Phi(\boldsymbol{x}(\{q^\mu\}))$, so effectively a function of the q^μ. We now take a curve $C := \{\boldsymbol{x}(\{q^\mu(s)\})\} \subset \mathcal{M}$ and compute the derivative of Φ in the direction of the tangent vector $\boldsymbol{e} = \mathrm{d}_s \boldsymbol{x} = \boldsymbol{x}_\mu \mathrm{d}_s q^\mu =: \boldsymbol{x}_\mu e^\mu$, a unit vector (Section 4.3),

$$\mathrm{d}_s \Phi(\boldsymbol{x}(\{q^\mu(s)\})) = (\partial_\mu \Phi)\mathrm{d}_s q^\mu = \boldsymbol{e}\,\mathrm{grad}\,\Phi. \tag{91}$$

While traveling along the manifold $\mathcal{M}$, we see that Φ changes most when $\nabla\Phi$ and $\boldsymbol{e}$ are parallel, a coordinate-independent property.

Divergence. Using covariant derivatives we define the divergence of a vector field in tangent space to be

$$\mathrm{div}\,\boldsymbol{v} := \nabla_\mu v^\mu. \tag{92}$$

As a contraction of a (1, 1) tensor it is coordinate-invariant. In addition, we get through (78) and (88)

$$\nabla_\mu v^\mu = \partial_\mu v^\mu + \Gamma^\mu_{\lambda\mu} v^\lambda = \partial_\mu v^\mu + (\partial_\lambda \sqrt{g}/\sqrt{g}) v^\lambda = (\sqrt{g}\partial_\mu v^\mu + v^\mu \partial_\mu \sqrt{g})/\sqrt{g},$$

and hence a most useful expression for partial integration in the style of Green, as is exemplified by (94) below,

$$\operatorname{div} \boldsymbol{v} = \frac{1}{\sqrt{g}} \partial_\mu (\sqrt{g} v^\mu). \tag{93}$$

Laplace–Beltrami operator. Following Beltrami (1864) we construct the symmetric bilinear function $\nabla\Phi\nabla\Psi = (\partial_\mu \Phi) g^{\mu\nu} (\partial_\nu \Psi)$ out of two tangent vectors $\nabla\Phi$ and $\nabla\Psi$. Performing a partial integration with respect to q^μ and starting with $\mathrm{d}f = \mathrm{d}\vec{q}\sqrt{g}$ we find the Laplace–Beltrami Operator Δ,

$$\begin{aligned} -\int \mathrm{d}f \nabla\Phi\nabla\Psi &= -\int \mathrm{d}\vec{q}\sqrt{g}(\partial_\mu \Psi) g^{\mu\nu} (\partial_\nu \Phi) \overset{\mathrm{NB}}{=} \int \mathrm{d}f \Phi \left[\frac{1}{\sqrt{g}} \partial_\mu (\sqrt{g} g^{\mu\nu} \partial_\nu) \Psi \right] \\ &=: \int \mathrm{d}f \Phi \Delta \Psi \end{aligned} \tag{94}$$

provided there are *no* boundary terms, as on a vesicle surface. Throughout what follows, this condition is denoted by NB. Though the above expression for Δ looks forbiddingly complicated, it is not. First, it is an old friend. In $\mathbb{R}^3$ with $g = \mathbb{1}$ it is the usual Laplacian $\Delta = \partial_\nu \partial^\nu$. Equation (94) also tells us that, on a unit sphere with spherical coordinates θ and ϕ, Δ is nothing but another old friend, the angular momentum operator $\hbar^{-2}\mathbf{L}^2 = -(\sin\theta)^{-1}\partial_\theta(\sin\theta\partial_\theta) - (\sin\theta)^{-2}\partial_\phi^2$ with $(2l+1)$-fold degenerate eigenvalues $l(l+1)$, $l = 0, 1, 2, \ldots$ and the spherical harmonics Y_{lm}, $-l \leqslant m \leqslant l$, as eigenfunctions (Dirac, 1958, Section 38). In general the following lemma holds.

Lemma F. The Laplace–Beltrami operator Δ looks the same in all coordinate systems, viz.,

$$\Delta = (\sqrt{g})^{-1} \partial_\mu [\sqrt{g} g^{\mu\nu} \partial_\nu] = \operatorname{div} \operatorname{grad} = \nabla_\mu \nabla^\mu. \tag{95}$$

Proof. For a tangent vector $\boldsymbol{v} := \nabla\Phi = \Phi_\mu \boldsymbol{x}^\mu$ we have $v_\mu = \partial_\mu \Phi = \Phi_\mu$ or, if desired, $v^\mu = g^{\mu\nu}\partial_\mu \Phi$. Lemmas C and D give in conjunction with definition (92) that $\operatorname{divgrad}\Phi = \nabla_\mu g^{\mu\nu} \Phi_\nu$ equals

$$\operatorname{div}(\nabla\Phi) = g^{\mu\nu}\nabla_\mu \Phi_\nu = g^{\mu\nu}(\partial_{\mu\nu}\Phi - \Gamma^\kappa_{\mu\nu}\partial_\kappa \Phi), \tag{96}$$

which is a handy expression for performing explicit calculations. We now return to (95) and invoke (93) to directly verify that (div grad) equals Δ as defined by (94) and showing up in (95) on the left. Putting $a_\mu := \partial_\mu \Phi \equiv \nabla_\mu \Phi$ & $\partial^\mu \Phi \equiv \nabla^\mu \Phi$ and combining (96) with Lemma D we find $\operatorname{div}(\nabla\Phi) = g^{\mu\nu}\nabla_\mu a_\nu = \nabla_\mu g^{\mu\nu} a_\nu = \nabla_\mu a^\mu = (\nabla_\mu \nabla^\mu)\Phi$. □

The Laplace–Beltrami operator Δ and the mean curvature $\mathbb{H} = \operatorname{tr} g^{-1} H$ are closely related: $\Delta \boldsymbol{x} = \mathbb{H}\boldsymbol{n} \Leftrightarrow \mathbb{H} = \boldsymbol{n}\Delta\boldsymbol{x}$. To see why, we combine (96) with Lemma D once again and use the Gauss formula (40) reading $\partial_\mu \boldsymbol{x}_\nu = \Gamma^\lambda_{\mu\nu}\boldsymbol{x}_\lambda + h_{\mu\nu}\boldsymbol{n}$ so as to get $\Delta\boldsymbol{x} = g^{\mu\nu}\nabla_\mu \boldsymbol{x}_\nu = g^{\mu\nu}(\partial_\mu \boldsymbol{x}_\nu - \Gamma^\lambda_{\mu\nu}\boldsymbol{x}_\lambda) = g^{\mu\nu}h_{\mu\nu}\boldsymbol{n} = \mathbb{H}\boldsymbol{n}$.

9. Conformal invariance of energy functionals

The integral $\int \mathrm{d}f\, \mathbb{H}^2$ occurring in many energy functionals of membranes is invariant under conformal transformations, i.e., angle-preserving mappings (Willmore, 1982). Translations and rotations in $\mathbb{R}^3$ are angle-preserving and so are constant scale-factor transformations. Translations, rotations, and constant scale-factor transformations are called *similarities*. In addition to similarities, in $\mathbb{R}^3$ and more generally in $\mathbb{R}^n$ with $n \geqslant 3$ *only* inversions, viz., reflections, in spheres are conformal; cf. Fig. 10. Since the classic proof of Liouville (1850) for the $n = 3$ case, which is what interests us here, does not give too much insight we will skip it and simply refer to Blair (2000). Instead we clarify why inversions are conformal transformations.

Let $S_a(\boldsymbol{x}_0) = \{\boldsymbol{x} \in \mathbb{R}^n \,|\, \|\boldsymbol{x} - \boldsymbol{x}_0\| = a\}$ be the sphere centered at $\boldsymbol{x}_0$ with radius a. The *inversion* in $S_a(\boldsymbol{x}_0)$ is the mapping $\imath : \mathbb{R}^n \backslash \boldsymbol{x}_0 \mapsto \mathbb{R}^n$ defined by

$$\imath(\boldsymbol{x}) := \boldsymbol{x}_0 + a^2 \frac{\boldsymbol{x} - \boldsymbol{x}_0}{\|\boldsymbol{x} - \boldsymbol{x}_0\|^2}. \tag{97}$$

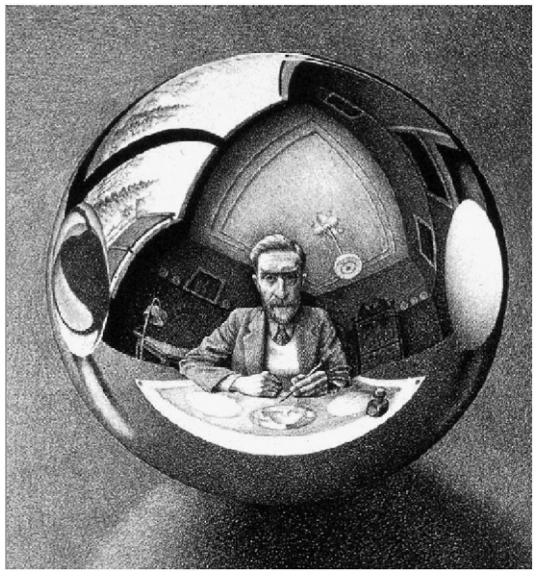

Fig. 10. Inversion in a sphere is a conformal transformation preserving angles. In this lithograph by, and of, the Dutch artist Escher (1946), one discerns how the artist is positioned mid-sphere on the weakly reflecting surface of a desk and joined on the right and left by two more reflecting spheres. Though distances are distorted, it is clearly seen that inversion in a sphere is angle-preserving. Taken from M.C. Escher's "Three Spheres II"

We note that $\boldsymbol{x}$ and $\imath(\boldsymbol{x})$ are on the same ray starting from $\boldsymbol{x}_0$, that the product of the distances of $\boldsymbol{x}$ and $\imath(\boldsymbol{x})$ from $\boldsymbol{x}_0$ equals a^2, and that $\imath^2$ is the identity. In addition, there is no harm in assuming that $\boldsymbol{x}_0 = 0$ is not on our manifold $\mathcal{M}$ so that the map $\imath$ from $\mathcal{M}$ onto $\tilde{\mathcal{M}} := \imath(\mathcal{M})$ is one-to-one and we may identify the parameters describing $\boldsymbol{x}$ and $\imath(\boldsymbol{x})$. Finally, we will simplify the notation further by calling $\tilde{\boldsymbol{x}} := \imath(\boldsymbol{x})$ so that with $r := \|\boldsymbol{x}\|$ Eq. (97) reappears in the form $\tilde{\boldsymbol{x}} := a^2\boldsymbol{x}/r^2$.

Following Willmore (1982) we start with an arbitrary variation of $\tilde{\boldsymbol{x}} := \imath(\boldsymbol{x})$ with $\boldsymbol{x} \in \mathcal{M}$,

$$\mathrm{d}\tilde{\boldsymbol{x}} = \frac{a^2}{r^2}\mathrm{d}\boldsymbol{x} - \frac{2a^2}{r^3}\mathrm{d}r\,\boldsymbol{x} \tag{98}$$

where $\boldsymbol{x}\,\mathrm{d}\boldsymbol{x} = r\,\mathrm{d}r$. Hence the scalar product reads

$$\mathrm{d}\tilde{\boldsymbol{x}}\,\mathrm{d}\tilde{\boldsymbol{x}} = \frac{a^4}{r^4}\,\mathrm{d}\boldsymbol{x}\,\mathrm{d}\boldsymbol{x} - \frac{4a^4}{r^5}\,\mathrm{d}r\,\boldsymbol{x}\,\mathrm{d}\boldsymbol{x} + \frac{4a^4}{r^6}r^2\,\mathrm{d}r^2. \tag{99}$$

Since the last two terms on the right in (99) cancel we are left with

$$\mathrm{d}\tilde{\boldsymbol{x}}\,\mathrm{d}\tilde{\boldsymbol{x}} = \frac{a^4}{r^4}\,\mathrm{d}\boldsymbol{x}\,\mathrm{d}\boldsymbol{x} \Rightarrow \mathrm{d}\tilde{f} = \frac{a^4}{r^4}\mathrm{d}f. \tag{100}$$

In so doing we have related the surface elements $\mathrm{d}\tilde{f}$ and $\mathrm{d}f$ as well; cf. (31) and (102) below.

After inversion the normal vector is given by

$$\tilde{\boldsymbol{n}} = \frac{2}{r^2}(\boldsymbol{n}\boldsymbol{x})\boldsymbol{x} - \boldsymbol{n} \tag{101}$$

as one verifies by simple inspection using (98): $\tilde{\boldsymbol{n}}$ is orthogonal to any $\mathrm{d}\tilde{\boldsymbol{x}}$. Moreover, $\tilde{\boldsymbol{n}}\tilde{\boldsymbol{n}} = 1$. From (98) we can derive the tangential basis $\tilde{\boldsymbol{x}}_\mu = a^2/r^2\boldsymbol{x}_\mu - 2a^2/r^4(\boldsymbol{x}\boldsymbol{x}_\mu)\boldsymbol{x}$. By means of (28) we then easily determine the first fundamental tensor

$$\tilde{g}_{\mu\nu} = \tilde{\boldsymbol{x}}_\mu\tilde{\boldsymbol{x}}_\nu = \frac{a^4}{r^4}g_{\mu\nu} \tag{102}$$

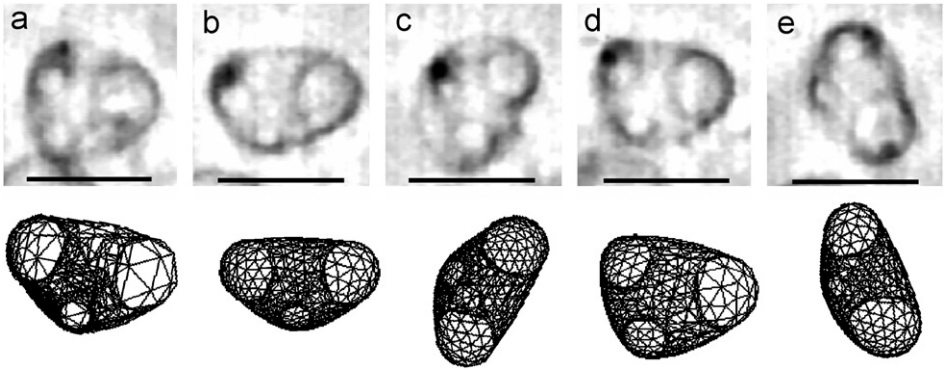

Fig. 11. Conformal deformation of a genus-2 vesicle with two handles, as observed in experiment (top). As time proceeds by steps of 30 s the vesicle evolves at no cost of energy through the conformal deformation (a) → (e), a "conformal diffusion" (Jülicher et al., 1993). The horizontal scale bar stands for 10 μm. In the bottom row numerical shapes belonging to the corresponding family of absolute minimal surfaces are shown. They strongly resemble their experimental counterparts. Picture based on that of Michalet and Bensimon (1995, Fig. 5).

and its inverse

$$\tilde{g}^{\mu\nu} = \frac{r^4}{a^4} g^{\mu\nu}.$$

After straightforward differentiation of (101) and applying $\boldsymbol{x}_\nu \boldsymbol{n} = 0$ we arrive at the somewhat unwieldy expression

$$\partial_\nu \tilde{\boldsymbol{n}} = -\partial_\nu \boldsymbol{n} + \frac{2}{r^2}\left[\boldsymbol{x}_\nu(\boldsymbol{n}\boldsymbol{x}) + \boldsymbol{x}(\partial_\nu \boldsymbol{n}\boldsymbol{x}) - \frac{2}{r^2}\boldsymbol{x}(\boldsymbol{n}\boldsymbol{x})(\boldsymbol{x}\boldsymbol{x}_\nu)\right],$$

which as a reward directly gives the second fundamental form

$$\tilde{h}_{\mu\nu} = -\tilde{\boldsymbol{x}}_\mu \partial_\nu \tilde{\boldsymbol{n}} = -\frac{a^2}{r^2}\left[h_{\mu\nu} - \frac{2}{r^2}(\boldsymbol{n}\boldsymbol{x}) g_{\mu\nu}\right]$$

as it follows from (42); equivalently,

$$\tilde{h}^\mu_\nu = \tilde{g}^{\mu\lambda}\tilde{h}_{\lambda\nu} = -\frac{r^2}{a^2}\left[h^\mu_\nu - \frac{2}{r^2}(\boldsymbol{n}\boldsymbol{x})\delta^\mu_\nu\right].$$

Taking advantage of (59) and (60) for a two-dimensional manifold we then find

$$\tilde{\mathbb{H}}^2 - 4\tilde{\mathbb{K}} = \frac{r^4}{a^4}(\mathbb{H}^2 - 4\mathbb{K}) \tag{103}$$

and because of (100) we end up with

$$(\tilde{\mathbb{H}}^2 - 4\tilde{\mathbb{K}})\mathrm{d}\tilde{f} = (\mathbb{H}^2 - 4\mathbb{K})\mathrm{d}f. \tag{104}$$

Integrating (104) over $\mathcal{M}$ and its mirror image $\tilde{\mathcal{M}}$ and invoking the Gauss–Bonnet Theorem (61) we obtain the desired invariance $\int_{\tilde{\mathcal{M}}} \mathrm{d}\tilde{f}\tilde{\mathbb{H}}^2 = \int_{\mathcal{M}} \mathrm{d}f\,\mathbb{H}^2$.

For interesting physical applications we refer to Jülicher et al. (1993) and Seifert (1997, Section 5). A rather surprising experimental confirmation of *conformal diffusion* as introduced by the former paper is due to Michalet and Bensimon (1995); see Fig. 11.

The problem of minimizing $\int_{\mathcal{M}} \mathrm{d}f\,\mathbb{H}^2$ for a closed surface $\mathcal{M}$ is meanwhile a famous one; solutions $\mathcal{M}$ are called Willmore surfaces. Jülicher (1996) discusses conformal invariance in the context of this Willmore problem, which we will soon turn to. Before doing so we make a small detour to get a better understanding of the invariance properties of energy functionals used to describe conformal diffusion and a wealth of other phenomena such as those depicted in Figs. 1–3.

10. Models of energy functionals and their invariances

In this section we reconsider the three energy functionals of Section 3 as we now have good reasons for doing so. The two more involved ones are going to be derived in greater detail and discussed in the new light of conformal invariance. Let us therefore return to Section 3, Eq. (19), from which we find the energy of a membrane surface to be described by the functional

$$\mathcal{F} = \frac{1}{2}k_c \int_{\mathcal{M}} \mathrm{d}f(\mathbb{H} - \kappa_0)^2 + \Sigma A - PV. \tag{105}$$

Here, $\mathbb{H} = \kappa_1 + \kappa_2$ is the local mean curvature and A is the total area, which is taken to be constant in time, so that the surface tension Σ plays the role of a Lagrange multiplier (Segel, 1977) for fixing the total area of the manifold $\mathcal{M}$ describing, say, our cell membrane. In a similar vein we have taken a constant volume into account by adding $-PV$ to (105) with V as volume and P as pressure. Finally, the term $\int_{\mathcal{M}} \mathrm{d}f\,\mathbb{K}$ containing the Gaussian curvature $\mathbb{K} = \kappa_1\kappa_2$ has been dropped from (19) as we assume no additional holes and thus "handles" are introduced so that the Gauss–Bonnet theorem (61) holds and the integral stays constant, whatever $\mathcal{M}$. Then the resulting functional (105) is that of Helfrich (1973) with κ_0 as fit parameter, called "spontaneous curvature". The model represented by (105) is henceforth named *spontaneous-curvature model*. As we have seen near (17), for $\kappa_0 = \Sigma = P = 0$ it dates back to Thomson and Tait (1878).

Bilayer coupling model (BCM). Evans (1974) was the first to note that a biomembrane is a lipid *bi*layer with the inner leaf of the lipid bilayer being slightly different from the outer one so that their areas may well differ by $\Delta A \neq 0$. For instance, by fixing the distance between the two leaves to be $\psi := \ell$ we find from (128) below that $\Delta A := A(\ell) - A(0) = \ell \int \mathrm{d}f\,\mathbb{H}$. In other words, by fixing ΔA we get the *bilayer coupling model* (BCM)

$$\mathcal{F}_{\mathrm{BCM}} = \frac{1}{2}k_c \int_{\mathcal{M}} \mathrm{d}f\,\mathbb{H}^2 + QM + \Sigma A + PV \tag{106}$$

with vanishing spontaneous curvature $\kappa_0 = 0$ but with an extra term QM instead, which is to be added to (105) with Q as Lagrange multiplier and $M = \int_{\mathcal{M}} \mathrm{d}f\,\mathbb{H}$ as integrated mean curvature. In view of the derivation of (16) in Section 3 this argument is quite appealing. In both cases, Helfrich's spontaneous curvature model and BCM, we have a bunch of (fit) parameters and by writing out (105) and redubbing them we can directly prove equivalence of the two models (105) and (106).

There is also an interesting scale invariance of (106) and, thus, (105). Though $\int \mathrm{d}f\,\mathbb{H}^2$ is invariant under whatever similarity, the quantities M, A, and V are not if we perform the scale transformation $\boldsymbol{x} \mapsto \lambda\boldsymbol{x}$ with $\lambda \neq 1$. We then find

$$M \mapsto \lambda M, \quad A \mapsto \lambda^2 A, \quad V \mapsto \lambda^3 V. \tag{107}$$

The functional (105) stays invariant if Q, Σ, and P transform according to

$$Q \mapsto \frac{Q}{\lambda}, \quad \Sigma \mapsto \frac{\Sigma}{\lambda^2}, \quad P \mapsto \frac{P}{\lambda^3}. \tag{108}$$

If, accordingly, $\boldsymbol{x}(q^1, q^2)$ is a solution to the variational problem of minimizing (105) for given (M, A, V), then $\lambda\boldsymbol{x}(q^1, q^2)$ is another solution for $(\lambda M, \lambda^2 A, \lambda^3 V)$. To characterize the solution it therefore suffices to work with only *two*, dimensionless, parameters. Say we put $R_0 := \sqrt{A/4\pi}$ and

$$m := M/(4\pi R_0), \quad v := V/(4\pi R_0^3/3) \tag{109}$$

so that for a sphere $m = v = 1$. Reducing a three-dimensional parameter space given by (M, A, V) to a two-dimensional one given by (m, v) we are left with a degeneracy characterized by a one-dimensional manifold, i.e., a line.

Using the above scale invariance of (106) we can understand the conformal diffusion that has been found by Jülicher et al. (1993) and is based upon an idea of Seifert (1991). In the present context 'conformal diffusion' means that the system wanders along the line of degeneracy in parameter space at no cost of energy. In so doing it is thermally driven but, because such a process requires a global change of shape and, hence, of fluid contained therein, it will evolve on a long hydrodynamic time scale of tens of seconds. The time elapsed between the different (top row) images of Fig. 11

is 30 s and in clear contrast to the fast *sub*second thermal fluctuations of the cell membrane, the key issue of the next section. We now turn to the mathematics underlying conformal diffusion.

First we note that $\int_{\mathcal{M}} \mathrm{d}f\,\mathbb{H}^2$ is invariant under *any* conformal mapping so that we can concentrate on the other terms in (106). Let us call a transformation (97) with $a=1$ and $\boldsymbol{x}_0=0$ a 'simple' inversion; it is simply a reflection in the unit sphere at the origin. A special conformal transformation $\mathrm{SCT}_{\boldsymbol{t}}$ is defined to be a composition of a simple inversion, a translation by $\boldsymbol{t}$, and again a simple inversion. That is,

$$\mathrm{SCT}_{\boldsymbol{t}}(\boldsymbol{x}) = (\boldsymbol{x}/r^2+\boldsymbol{t})/(\boldsymbol{x}/r^2+\boldsymbol{t})^2 \tag{110}$$

with $r^2 := \|\boldsymbol{x}\|^2 = \boldsymbol{x}^2$. We now start with some free-energy minimum for a given parameter vector $\boldsymbol{p}_0=(m_0, v_0)$ in (106) and compute the change under $\mathrm{SCT}_{\boldsymbol{t}}$ with $\boldsymbol{t}\to 0$. This gives the Taylor expansion

$$\Delta\boldsymbol{p} := \boldsymbol{p}_{\boldsymbol{t}} - \boldsymbol{p}_0 = \mathbb{A}\boldsymbol{t} \tag{111}$$

for some 2×3 matrix $\mathbb{A}$. Calling the row vectors of $\mathbb{A}$, which are 3-vectors, $\boldsymbol{a}_m$ and $\boldsymbol{a}_v$ and realizing we are at a minimum and want to stay there, we thus have to require $\mathbb{A}\boldsymbol{t}=0$ as $\boldsymbol{t}\to 0$. The line of degeneracy can be characterized by its length s and we have $\mathrm{d}\boldsymbol{t} = (\mathrm{d}\boldsymbol{t}/\mathrm{d}s)\,\mathrm{d}s$ where $\mathrm{d}\boldsymbol{t}/\mathrm{d}s$ is the tangent vector

$$\mathrm{d}\boldsymbol{t}/\mathrm{d}s = \boldsymbol{a}_m \times \boldsymbol{a}_v \tag{112}$$

pointing into the direction of degeneracy of the energy functional, i.e., where $(m, v)=(m_0, v_0)$ does not change. Here $\times$ denotes a vector product so that $\boldsymbol{a}_m\times\boldsymbol{a}_v$ is orthogonal to both $\boldsymbol{a}_m$ and $\boldsymbol{a}_v$. Finding an explicit expression for the two vectors $\boldsymbol{a}_1$ and $\boldsymbol{a}_2$, though straightforward, is a bit of work but the result is easy to formulate (Seifert, 1991). If we define the "centers of mass"

$$\begin{aligned}\boldsymbol{R}_A &:= A^{-1}\int_{\mathcal{M}} \mathrm{d}f\,\boldsymbol{x}, \quad \boldsymbol{R}_M := M^{-1}\int_{\mathcal{M}} \mathrm{d}f\,\mathbb{H}\boldsymbol{x},\\ \boldsymbol{R}_V &:= V^{-1}\int_{\{\mathcal{M}\}} \mathrm{d}V\,\boldsymbol{x},\end{aligned} \tag{113}$$

where $\{\mathcal{M}\}$ indicates the region enclosed by $\mathcal{M}$ and $\mathrm{d}V$ an infinitesimal volume element therein, then we obtain

$$\boldsymbol{a}_m = 2(\boldsymbol{R}_A-\boldsymbol{R}_M), \quad \boldsymbol{a}_v = 6(\boldsymbol{R}_A-\boldsymbol{R}_V). \tag{114}$$

These vectors are now substituted into (112) and by integrating the resulting expression we directly find the trajectory of conformal diffusion.

Area-difference elasticity (*ADE*) *model*. The third model, the so-called area-difference elasticity (ADE) model, is based on the idea (Miao et al., 1994, Appendix A) that the total area may well be taken to be constant (in decent approximation) but area *differences* need not be because of elasticity. The primary assumption is that certain (small) pieces of area a_h and a_t of the membrane surface are assigned to each lipid molecule's head and tail, respectively, and that the total energy can be expressed in terms of these variables. Local curvatures, described by $\mathbb{H}$ and $\mathbb{K}$, modulate both area portions a_h and a_t so as to give a Taylor expansion

$$a_{h/t} = a_0(1 - z_{h/t}\mathbb{H} + z_{h/t}^2\mathbb{K}). \tag{115}$$

Here $z_{h/t}$ denotes the position of heads and tails above or below the neutral plane in the direction of the normal; see Fig. 4 and Eqs. (128) and (137) below with $\psi := h$ constant and thus $\psi_\mu \equiv 0$. Equation (115) can then be inserted into an ansatz for the free-energy density f of a lipid *mono*layer, which assumes a quadratic dependence upon the differences between the $a_{h/t}$ and their "equilibrium" values $a_{h/t,0}$ so as to give

$$f(a_h, a_t) = \frac{1}{2}\sum_{\imath=h,t} k_\imath a_{\imath,0}(a_\imath/a_{\imath,0}-1)^2 \tag{116}$$

with $k_\imath$ as area-stretching elasticities and $a_{\imath,0}$ with $\imath = h$ or t (head or tail) as preferred areas dangling in the background.

Eq. (116) already looks plausible and is in principle easy to understand, the more so if we remember the sandwich plate of (18) in Section 3. The idea behind (116) dates back to Helfrich (1973, Section II) and has been extended slightly by Marčelja (1974). As we have seen, a biomembrane is a lipid bilayer consisting of two sheets with the hydrophobic,

lipid, CH-tails or chains (c) inside and the hydrophilic polar groups or heads (h) outside. We now focus on one sheet, consider it as a sandwich with heads and tails and nothing in between, and apply the elasticity theory of Section 3 to each of them with their neutral plane in between. Being fluid they are also homogeneous and no direction in a sheet is preferred.

If a sheet were flat and in equilibrium, a_h and a_t equal $a_{h/t,0}$, respectively. By bending it we stretch one side and squeeze the other. This was the essence of Section 3 leading to the functional (19) with $\kappa_0 = 0$. We now proceed somewhat differently so as to allow a final, tangential, stretching of mono- and bilayers as well. That is, we bend and stretch the head and tail layer separately. For small changes the monolayer tension σ, this time not to be confused with the Poisson ratio, is supposed to be linear in the relative *area* per polar head (h) or lipid tail (t),

$$\sigma(a_{h/t}) = \sigma_{h/t,0} + k_{h/t}(a_{h/t}/a_{h/t,0} - 1). \tag{117}$$

We note that Eq. (117) can be considered as a *higher*-order correction to the usual surface tension, the latter being a simple consequence of $\sigma_{h/t,0}$. An energy change ΔE corresponding to an area change Δa is of the form $\Delta E = \sigma\Delta a$; here σ has the dimension N/m and Δa that of m^2 so that the dimension of $\sigma\Delta a$ is Nm, exactly that of an energy. To wit, pull at a piece of membrane, a layer, along a bar of length L and called $\mathcal{L}$. Because of the sheet's homogeneity, the force we have to exert is *normal* to $\mathcal{L}$ and the work to be done so as to shift $\mathcal{L}$ by a distance Δs along the normal to $\mathcal{L}$ is $\sigma L\Delta s =: \sigma\Delta A$ where $\Delta A := L\Delta s$ is the area change. Thus the work is $\sigma\Delta a$ in the present units.

Starting with $\sigma_{h/t,0}$ and integrating we obtain the free-energy densities ($\imath = h/t$)

$$f(a_\imath) = \sigma_{\imath,0}(a_\imath - a_{\imath,0}) + \frac{k_\imath}{2}a_{\imath,0}(a_\imath/a_{\imath,0} - 1)^2. \tag{118}$$

We finally apply Occam's razor in that we make the physically simplest choice of putting $\sigma_{h/t,0} := \Sigma$ with Σ as Lagrange multiplier accompanying the surface area $A = N(a_h + a_t)/2$ in (119) below, where constants can be dropped and N as the total number of molecules in a monolayer is fixed on time scales we are interested in. In (118) we can therefore put $\sigma_{h/t,0} = 0$. The total (free) energy $f(a_h, a_t) = f(a_h) + f(a_t)$ of two head and tail layers that are bent and constitute a monolayer or 'leaf' then equals that of (116).

The rest of the ADE scenario is quite simple in principle but requires a bit of algebra, which we will skip. The idea is this. We start with (116) as the energy of a *mono*layer, brush it up, and then compose two of these monolayers so as to form a bilayer. In a similar vein to the BCM model, we fix the total distance between the two leaves to be D so that $\Delta A := A(D) - A(0) = D\int \mathrm{d}f\,\mathbb{H} := DM$ due to (128) below, and allow ΔA to change because of tangential elasticity. Collecting terms we end up with a free-energy functional of the form (Miao et al., 1994, Appendix A, esp (A17))

$$\mathcal{F}_{\mathrm{ADE}} = \frac{1}{2}k_c\int_{\mathcal{M}}\mathrm{d}f(\mathbb{H} - \kappa_0)^2 + \frac{\bar{Q}}{2A}(M - M_0)^2 + \Sigma A + PV, \tag{119}$$

where κ_0, M_0, and $\bar{Q}$ are independent quantities that depend on $a_{h/t,0}$ and $k_{h/t}$ and can be treated as fit parameters. Furthermore, $M := \int_{\mathcal{M}}\mathrm{d}f\,\mathbb{H}$ while, in view of (116), the second term on the right in (119), with prefactor $\bar{Q}/A$, represents the area-difference elasticity,

$$\frac{\bar{Q}}{2AD^2}(\Delta A - \Delta A_0)^2,$$

hence the name of the model. The ADE model is quite successful in explaining transitions of vesicle forms from, e.g., prolate to pear-shaped, and even to budding (Miao et al., 1994). As we have seen in Section 1, it also explains quite intricate phenomena such as a red blood cell's full stomatocyte–discocyte–echinocyte transition, part of which has been depicted in Fig. 3. It was as early as 1948 that Ponder precisely identified the discocyte to echinocyte transition.

11. Differential geometry of elementary excitations

The energy functional describing a cell, or any other, membrane is given by (19) or, more generally, by an integrated version of (20) and formulated in terms of quantities that are determined by the membrane *shape* only. To wit, here we will study the functional

$$\mathcal{F} = \int \mathrm{d}f\left(\frac{1}{2}k_c\mathbb{H}^2 + k_g\mathbb{K}\right) + \Sigma A - PV + Q\int \mathrm{d}f\,\mathbb{H}, \tag{120}$$

where $A = \int \mathrm{d}f$ is the surface area and V the volume of a cell whose membrane surface constitutes the manifold $\mathcal{M}$ under consideration. We have to differentiate the functional (120) twice. The first derivative vanishing gives us the equilibrium shape of the membrane whose energy is given by (120). The second derivative tells us whether or not this equilibrium is stable and what its elementary excitations look like. It may well be that a stable equilibrium shape has a certain symmetry, say, it is rotationally invariant, but in performing our first and second derivative we are not allowed to assume any symmetry since small deviations from symmetry need not have any symmetry. That is, we are facing the problem of differentiating (120) *without any* further symmetry assumption. As we will see in Section 11.3, already by itself the problem of differentiating (120) is a neat challenge whose solution will pay off fully since we will obtain a solution that is good for *any* membrane shape. Moreover, the extra money we pay is none.

We follow the notation of Section 6, viz., consider normal variations ψ of an unperturbed surface $\{\boldsymbol{x} \in \mathcal{M}\}$ so that $\{\bar{\boldsymbol{x}} = \boldsymbol{x} + t\psi\boldsymbol{n} | \boldsymbol{x} \in \mathcal{M}\}$ is the "perturbed" one. Since t is "small" the perturbed and unperturbed manifold can be described by the *same* coordinates or parameters. We also define, as in (67), $\delta^n\mathcal{F} := (\mathrm{d}^n\mathcal{F}/\mathrm{d}t^n)|_{t=0}$ and require that at a minimum $\delta\mathcal{F} = 0$ while for stability $\delta^2\mathcal{F} > 0$. As a second derivative, the bilinear form $\delta^2\mathcal{F}(\varphi, \psi) =: \langle\varphi|\delta^2\mathbb{F}|\psi\rangle$ in the Hilbert space (71) is symmetric (Liusternik and Sobolev, 1961) so that the operator $\delta^2\mathbb{F}$ is automatically symmetric too. With a bit more work (Buser, 1992) one can show it is (essentially) self-adjoint; cf. as an illustration, $\delta^2\mathbb{F} = k_c\Delta^2 - \Sigma\Delta \geqslant 0$ in Section 5. Not only does it look awfully Hermitian, it actually also is.

Before proceeding it may be well to put things in a historical perspective. The first publications presenting the solution to the variational problems associated with (120) in full generality are due to Peterson (1985); see also Peterson et al. (1992). In addition, we ought to mention Ou-Yang and Helfrich (1989); further references will be given as we proceed.

The analysis below has been inspired by the wonderful Chapter 7 of Tom Willmore's *Riemannian Geometry* (1993). This chapter is devoted to the 'Willmore problem' of finding the infimum of $\int_{\mathcal{M}} \mathrm{d}f\,\mathbb{H}^2$ for closed surfaces $\mathcal{M}$ of genus p (Section 4.6) and without self-intersections (as in the Klein bottle). For $p = 0$ a sphere does the job whereas for $p = 1$ the stereographic projection of the Clifford torus seems to be the solution; at least a 200-page proof has been submitted. For each fixed value of the genus $p > 1$, it is unknown what the minimizer is. That is, the problem is open since 1965.

One of the fruitful ideas practiced by Willmore (1993) is the observation that, as is suggested by (67), 'variation' can be reduced to ordinary differentiation of functions in an integrand. As a consequence *the ordinary algebra generated by product rule and chain rule holds*. The first and second derivative of expressions in the integrand of $\mathcal{F}(\boldsymbol{x} + t\psi\boldsymbol{n})$ with respect to t at $t = 0$ will be denoted by δ and δ^2, respectively; for instance, $\delta h_{\mu\nu}$.

11.1. Differentiating once: equilibrium shapes

We start with the first derivative and in so doing with what we will call the Willmore functional,

$$\mathcal{F}_W = \int \mathrm{d}f \left(\frac{1}{2}k_c\mathbb{H}^2 + k_g\mathbb{K}\right). \tag{121}$$

According to the Gauss-Bonnet theorem (61) $\int \mathrm{d}f\,\mathbb{K}$ will not change as long as the manifold's genus p does not change. Even for surfaces *with* border $\delta\mathbb{K}$ will not provide a contribution (Nitsche, 1989) so that we can safely drop $\mathbb{K}$ and concentrate on $\int \mathrm{d}f\,\mathbb{H}^2$,

$$\delta\mathcal{F}_W = \frac{k_c}{2}\left[\int (\delta\mathrm{d}f)\mathbb{H}^2 + \int \mathrm{d}f\, 2\mathbb{H}\delta\mathbb{H}\right]. \tag{122}$$

We know from (51) that $\mathbb{H} = \mathrm{tr}\,g^{-1}h = g^{\mu\nu}h_{\mu\nu}$. Since we need both $\delta\mathrm{d}f = d\vec{q}\,\delta\sqrt{g}$ and $\delta\mathbb{H} = \delta g^{\mu\nu}h_{\mu\nu} + g^{\mu\nu}\delta h_{\mu\nu}$ we have to differentiate the first as well as the second fundamental form $g_{\mu\nu} = \boldsymbol{x}_\mu\boldsymbol{x}_\nu$ and $h_{\mu\nu} = -\boldsymbol{x}_\mu\boldsymbol{n}_\nu$ where, as usual, $\boldsymbol{x}_\mu$ means $\partial_\mu\boldsymbol{x}$, etc.; cf. Sections 4.3 and 4.4 for where g and h come from. For what follows, the *third fundamental form* $k_{\mu\nu} := \boldsymbol{n}_\mu\boldsymbol{n}_\nu$ is also helpful.

11.1.1. Metric tensor, surface area, and volume

As we have seen in Section 6, normal variations $\bar{\boldsymbol{x}} = \boldsymbol{x} + t\psi\boldsymbol{n}$ suffice and thus

$$\partial_\mu\bar{\boldsymbol{x}} = \partial_\mu\boldsymbol{x} + t(\psi_\mu\boldsymbol{n} + \psi\partial_\mu\boldsymbol{n}) \tag{123}$$

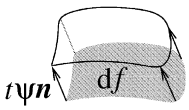

Fig. 12. For volume variations a certain distance $t\psi$ along the normal vector $\boldsymbol{n}$ is to be specified, where ψ is a function on the manifold $\mathcal{M}$. With height $t\psi$ and base $\mathrm{d}f$ the first normal variation of a volume element is given by $\psi\,\mathrm{d}f$. In view of $\delta\,\mathrm{d}f = -\psi\mathbb{H}\,\mathrm{d}f$ leading to (128), the second-order term is then $\psi\delta\,\mathrm{d}f = -\psi^2\mathbb{H}\,\mathrm{d}f$.

gives the modified metric tensor

$$\bar{g}_{\mu\nu} = g_{\mu\nu} - 2t\psi h_{\mu\nu} + t^2(\psi_\mu\psi_\nu + \psi^2 k_{\mu\nu}). \tag{124}$$

We differentiate both (123) and (124) once with respect to t at $t = 0$ and get

$$\begin{aligned}\delta\partial_\mu\boldsymbol{x} &= \psi_\mu\boldsymbol{n} + \psi\partial_\mu\boldsymbol{n},\\ \delta\partial^2_{\mu\nu}\boldsymbol{x} &= \psi_{\mu\nu}\boldsymbol{n} + \psi_\mu\partial_\nu\boldsymbol{n} + \psi_\nu\partial_\mu\boldsymbol{n} + \psi\partial^2_{\mu\nu}\boldsymbol{n},\end{aligned} \tag{125}$$

as well as

$$\delta g_{\mu\nu} = -2\psi h_{\mu\nu}, \tag{126}$$

a key result. We obtain the derivative of the inverse metric $g^{\mu\nu}$ through $\delta^\mu_\nu = g^{\mu\lambda}g_{\lambda\nu}$ in the form $0 = (\delta g^{\mu\nu})g_{\lambda_\nu} + g^{\mu\nu}(\delta g_{\lambda\nu})$ and, using (126), end up with

$$\delta g^{\mu\nu} = -g^{\mu\lambda}(\delta g_{\lambda\kappa})g^{\kappa\nu} = 2\psi h^{\mu\nu}. \tag{127}$$

Eq. (126) tells us how to compute $\delta\mathrm{d}f$ and hereby the surface variation δA for $A = \int_{\mathcal{M}}\mathrm{d}f = \int_{\mathcal{M}}\mathrm{d}\vec{q}\sqrt{\mathrm{g}}$ where $\mathrm{g} = \det(g)$. Because of (89), differentiating g is easy: $\partial\sqrt{\mathrm{g}}/\partial g_{\kappa\lambda} = \sqrt{\mathrm{g}}g^{\kappa\lambda}/2$. Since $\delta\sqrt{\mathrm{g}} = (\partial_{g_{\mu\nu}}\sqrt{\mathrm{g}})\delta g_{\mu\nu}$ we get $\delta\,\mathrm{d}f = -\psi\mathbb{H}\,\mathrm{d}f$, which is equivalent to

$$\delta A = -\int \mathrm{d}f\psi\mathbb{H}. \tag{128}$$

Variation of surface area, a geometric quantity, can therefore be expressed in terms of other coordinate-independent quantities such as the mean curvature $\mathbb{H}$ and the normal variation of the height ψ. In passing we note that under normal circumstances $\boldsymbol{n}$ is to point outwards (cf. Fig. 5) so that $\psi > 0$ corresponds to an area *in*crease at positions where the surface is locally convex ($\mathbb{H} < 0$) and an area *de*crease for concave ($\mathbb{H} > 0$) parts of the surface. If locally the mean curvature vanishes, there is no contribution to an area change, e.g., as is the case for lifting a flat piece of paper.

There is an interesting application of (128). For a lipid bilayer the distance ℓ between the inner and the outer leaf is about constant so that we can take $\psi \equiv \ell$, which is much smaller than the inverse surface curvature, and obtain $\Delta A := A(\ell) - A(0) = \ell\int\mathrm{d}f\,\mathbb{H} = M$. Requiring this to be fixed means that one puts $\kappa_0 = 0$ in (19) and adds a term QM with Lagrange multiplier Q, as advertised in deriving the 'bilayer coupling model' (BCM) at the end of Section 3.

Computing volume variations is algebraically quite nasty. It is, however, simpler and also more physical to glance Fig. 12 so as to conclude that normal (= height) variations give rise to $\delta V = \int_{\mathcal{M}}\mathrm{d}f\psi$.

11.1.2. Differentiating mean curvature

Once we have obtained δg, computing the variation of the mean curvature $\mathbb{H} = \mathrm{tr}\,g^{-1}h$ means analyzing $h_{\mu\nu} = (\partial^2_{\mu\nu}\boldsymbol{x})\boldsymbol{n}$ in this way we are led to both $\partial^2_{\mu\nu}\boldsymbol{x} = \Gamma^\kappa_{\mu\nu}\partial_\kappa\boldsymbol{x} + h_{\mu\nu}\boldsymbol{n}$, which is the Gauss formula (40), and the normal vector $\boldsymbol{n}$, a unit vector.

For $\boldsymbol{n}$ life is easy. Since $\boldsymbol{n}\boldsymbol{n} = 1$ we get $\boldsymbol{n}\delta\boldsymbol{n} = 0$ and $\boldsymbol{n}\partial_\mu\boldsymbol{n} = 0$ so that both $\delta\boldsymbol{n}$ and $\partial_\mu\boldsymbol{n}$ are bound to be in tangent space $\mathcal{T}_{\boldsymbol{x}}$ and $\delta(\boldsymbol{n}\partial_\mu\boldsymbol{x}) = 0$. Thus, the effect of δ being a differentiation, $(\delta\boldsymbol{n})\partial_\mu\boldsymbol{x} = -\boldsymbol{n}\delta\partial_\mu\boldsymbol{x}$. Inserting $\delta\partial_\mu\boldsymbol{x}$ from (125) we get $\delta\boldsymbol{n}$'s components $(\delta\boldsymbol{n})\partial_\mu\boldsymbol{x} = -\boldsymbol{n}\delta\partial_\mu\boldsymbol{x} = -\psi_\mu$ with respect to the basis $\partial_\mu\boldsymbol{x} = \boldsymbol{x}_\mu$ and hereby the extremely

simple result

$$\delta \boldsymbol{n} = -\psi_\mu \boldsymbol{x}^\mu = -\psi^\mu \boldsymbol{x}_\mu. \tag{129}$$

So far, so good. We now turn to $\mathbb{H} = g^{\mu\nu} h_{\mu\nu}$.

Starting this time with (125) and (129) we get

$$\delta h_{\mu\nu} = \partial^2_{\mu\nu} \boldsymbol{x} \delta \boldsymbol{n} + (\delta \partial^2_{\mu\nu} \boldsymbol{x}) \boldsymbol{n} = -\Gamma^\kappa_{\mu\nu} \psi_\kappa + \psi_{\mu\nu} + \psi \boldsymbol{n} \partial^2_{\mu\nu} \boldsymbol{n},$$

where the Christoffel symbols $\Gamma^\kappa_{\mu\nu} = \boldsymbol{x}^\kappa \boldsymbol{x}_{\mu\nu}$ have been introduced in (41). We now remember (127) and the covariant derivative $\nabla_\mu \psi_\nu = \psi_{\mu\nu} - \Gamma^\kappa_{\mu\nu} \psi_\kappa$ from (86) of Lemma D, note that differentiating $\boldsymbol{n} \partial_\mu \boldsymbol{n} = 0$ gives $\boldsymbol{n} \partial^2_{\mu\nu} \boldsymbol{n} = -\partial_\mu \boldsymbol{n} \partial_\nu \boldsymbol{n} = -k_{\mu\nu}$, where the final equality is just the definition of the *third* fundamental form $k_{\mu\nu}$, and uncover the already fancy looking expression

$$\delta h_{\mu\nu} = \nabla_\mu \psi_\nu - \psi k_{\mu\nu}. \tag{130}$$

We now note $\mathbb{H} = g^{\mu\nu} h_{\mu\nu}$, differentiate this, and conjoin (130) and (127) so as to get

$$\delta \mathbb{H} = g^{\mu\nu} \delta h_{\mu\nu} + \delta g^{\mu\nu} h_{\mu\nu} = g^{\mu\nu} \nabla_\mu \psi_\nu + \psi(-g^{\mu\nu} k_{\mu\nu} + 2 h^{\mu\nu} h_{\mu\nu}).$$

Combining the Laplace–Beltrami expression $\Delta\psi = 1/\sqrt{g} \partial_\mu [\sqrt{g} g^{\mu\nu} \partial_\nu \psi] = g^{\mu\nu} \nabla_\mu \psi_\nu$, which is (95) of Lemma F, with the observation of $k_{\mu\nu} = h_{\mu\lambda} g^{\lambda\kappa} h_{\kappa\nu}$ implying $g^{\mu\nu} k_{\mu\nu} = h^{\mu\nu} h_{\mu\nu} = \mathrm{tr}(g^{-1} h)^2 = \sum_{h=1}^n \kappa_h^2$, which we check in a minute, we are left with a truly appealing expression containing geometric (i.e., coordinate-independent) quantities only,

$$\delta \mathbb{H} = \Delta\psi + \psi \sum_{h=1}^n \kappa_h^2. \tag{131}$$

In particular, for the undulation case with $n = 2$ we have $\mathrm{tr}(g^{-1} h)^2 = \kappa_1^2 + \kappa_2^2 = \mathbb{H}^2 - 2\mathbb{K}$. To finally see why $k_{\mu\nu} = h_{\mu\lambda} g^{\lambda\kappa} h_{\kappa\nu}$ holds we return to the Weingarten equations (47), viz., $\partial_\lambda \boldsymbol{n} = -h_{\lambda\mu} \boldsymbol{x}^\mu$ and use the third fundamental form's definition $k_{\mu\nu} := \boldsymbol{n}_\mu \boldsymbol{n}_\nu$, insert the Weingarten equations, find $k_{\mu\nu} = h_{\mu\lambda} \boldsymbol{x}^\lambda \boldsymbol{x}^\kappa h_{\kappa\nu}$, and note we are done since $\boldsymbol{x}^\lambda \boldsymbol{x}^\kappa = g^{\lambda\kappa}$ because of Lemma A.

11.1.3. Equation characterizing a Willmore surface

If a closed surface $\mathcal{M}$ of genus p minimizes the functional (121) of the Willmore problem, what equation characterizes it? We can exhibit this equation by invoking the condition $\delta \mathcal{F}_W = 0$ for arbitrary ψ, as alluded to in the introduction to this section. We now combine $\delta \mathrm{d}f = -\psi \mathbb{H} \mathrm{d}f$ from (128) and $\delta \mathbb{H}$ from (131) so as to find

$$\delta \mathcal{F}_W = \frac{k_c}{2} \left(\int \delta \mathrm{d}f \mathbb{H}^2 + \int \mathrm{d}f 2\mathbb{H} \delta \mathbb{H} \right) = \frac{k_c}{2} \int \mathrm{d}f [-\mathbb{H}^3 + 2\mathbb{H}(\Delta + \mathbb{H}^2 - 2\mathbb{K})] \psi. \tag{132}$$

Assuming as before that no boundary terms (NB) arise during partial integration we obtain the condition

$$\delta \mathcal{F}_W \overset{\mathrm{NB}}{=} \frac{k_c}{2} \int \mathrm{d}f \psi [2\Delta \mathbb{H} + \mathbb{H}(\mathbb{H}^2 - 4\mathbb{K})] = 0,$$

for any ψ and thus

$$\Delta \mathbb{H} + \tfrac{1}{2} \mathbb{H}(\mathbb{H}^2 - 4\mathbb{K}) = 0, \tag{133}$$

where Δ is the Laplace–Beltrami operator of the Willmore surface under consideration.

The history of Eq. (133) is interesting (Pinkall and Stirling, 1987; Willmore, 1993). It dates back to at least 1922 appearing in a footnote of a paper by Thomsen (1924), who used a different representation and had to admit that Schadow had outdone him two years earlier. Nothing is known, however, about the person who first discovered this highly nonlinear equation. A 'minimal' surface characterized by $\mathbb{H} = 0$ provides a solution but is in general not closed.

Poisson had already derived (133) in 1812 as solution to the first derivative of (121) vanishing (i.e., as an Euler equation) but in a truly clumsy form; after all, Beltrami wasn't born before 1835. According to Pinkall and Stirling

(1987), Sophie Germain used $\int \mathrm{d}f k_c \mathbb{H}^2/2$, the main term in (121), as the virtual work in a study of vibrating curved plates as early as 1810; cf. (15) and (16). It is still unclear "whether she carried this program through". Poisson did so *in extenso* two years later.

11.1.4. General membrane equilibrium

To finish our argument and derive the full equation characterizing membrane equilibrium in general and without any recourse to symmetry, we return to the functional (120). The first part, $\mathcal{F}_W$ in (121), gives rise to (133). The terms with prefactor P and Σ have been taken care of by Fig. 12 together with (128) and (131) while the first variation of the integrated mean curvature $\delta M = \int[(\delta \mathrm{d}f)\mathbb{H} + \mathrm{d}f(\delta\mathbb{H})]$ is an easy application of both equations. Putting all terms together we get the following partial differential equation containing *geometric* quantities only,

$$2\Delta\mathbb{H} + \mathbb{H}(\mathbb{H}^2 - 4\mathbb{K}) - \frac{2\Sigma}{k_c}\mathbb{H} - \frac{4Q}{k_c}\mathbb{K} - \frac{2P}{k_c} = 0. \tag{134}$$

In membrane physics *all* terms must be present (Seifert, 1995). In view of (133) we nevertheless think it is fair to call (134) the *Poisson–Schadow* equation since Schadow was the first to derive the essential part of this coordinate-independent equation, which Poisson forecasted in 1812 and Willmore rediscovered in the early sixties of the last century. We will analyze an amusing application of (134) in Section 11.3.1 below. First we are going to compute the second derivative of the full energy functional (120).

11.2. Differentiating twice: undulations

Of course the Willmore functional (121) is the main dish. We differentiate (122) once more and find

$$\delta^2\mathcal{F}_W = \frac{k_c}{2}\left\{\int(\delta^2\mathrm{d}f)\mathbb{H}^2 + 2\int(\delta\mathrm{d}f)2\mathbb{H}\delta\mathbb{H} + \int \mathrm{d}f\, 2[(\delta\mathbb{H})^2 + \mathbb{H}\delta^2\mathbb{H}]\right\}. \tag{135}$$

So "all" we need is $\delta^2\mathrm{d}f$ and $\delta^2\mathbb{H}$; the rest is already at our disposal.

11.2.1. Metric tensor, surface area and volume once more

Taking advantage of (124) we directly get

$$\delta^2 g_{\mu\nu} = 2(\psi_\mu\psi_\nu + \psi^2 k_{\mu\nu}), \tag{136}$$

where $k_{\mu\nu}$ is the third fundamental form; so this is done. We now return to (128) and rewrite $\delta\,\mathrm{d}f = -\psi\mathbb{H}\,\mathrm{d}f$,

$$\delta\mathrm{d}f = \mathrm{d}\vec{q}\,\delta\sqrt{\mathrm{g}} = \mathrm{d}\vec{q}/(2\sqrt{\mathrm{g}})\delta\mathrm{g} = \mathrm{d}f g^{\mu\nu}\delta g_{\mu\nu}/2.$$

Using (126), (127), and (136) and allowing δ to operate only on the argument directly following it, we write the second derivative $\delta^2\mathrm{d}f$

$$\begin{aligned}\delta^2\mathrm{d}f &= \frac{1}{2}(\delta\mathrm{d}f g^{\mu\nu}\delta g_{\mu\nu} + \mathrm{d}f\delta g^{\mu\nu}\delta g_{\mu\nu} + \mathrm{d}f g^{\mu\nu}\delta^2 g_{\mu\nu})\\ &= \frac{\mathrm{d}f}{2}[2\psi^2\mathbb{H}^2 - 4\psi^2 h^{\mu\nu}h_{\mu\nu} + 2(\psi^\mu\psi_\mu + \psi^2 k^\mu_\mu)].\end{aligned}$$

For a two-dimensional manifold ($n = 2$) in $\mathbb{R}^3$ we have $\mathrm{tr}(g^{-1}h)^2 = k^\mu_\mu = h^{\mu\nu}h_{\mu\nu} = \sum_{h=1}^n \kappa_h^2 = \mathbb{H}^2 - 2\mathbb{K}$ so that in the experimentally relevant case we end up with

$$\delta^2\mathrm{d}f = \mathrm{d}f(2\mathbb{K}\psi^2 + \psi^\mu\psi_\mu). \tag{137}$$

For a volume element $\mathrm{d}V$ the argument leading to the second derivative is a continuation of $\delta V = \int \mathrm{d}f\psi$ as illustrated by Fig. 12. Differentiating twice we now get $\delta^2 V = \int(\delta\mathrm{d}f)\psi$ and hence

$$\delta^2 V = -\int \mathrm{d}f\mathbb{H}\psi^2. \tag{138}$$

Alternatively, one can take $V = \int \mathrm{d}\boldsymbol{x} = 1/3\int \mathrm{d}\boldsymbol{x}\,\mathrm{div}\,\boldsymbol{x} = 1/3\int \mathrm{d}f\boldsymbol{n}\boldsymbol{x}$, which is a consequence of Gauss' theorem, as a starting point—and continue.

11.2.2. Differentiating the mean curvature twice

We will have to devote most of our time to evaluating

$$\delta^2\mathbb{H} = \delta^2 h_{\mu\nu} g^{\mu\nu} + 2\delta h_{\mu\nu}\delta g^{\mu\nu} + h_{\mu\nu}\delta^2 g^{\mu\nu}. \tag{139}$$

We first turn to $\delta^2 h_{\mu\nu}$ and $\delta^2 g^{\mu\nu}$. Before doing so, however, it is worth our while to focus on $\partial^2_{\mu\nu}\boldsymbol{n} =: \boldsymbol{n}_{\mu\nu}$, which stems from (125), and prove another useful lemma.

Lemma G. *A second partial derivative $\partial^2_{\mu\nu}\boldsymbol{n}$ of the normal vector $\boldsymbol{n}$ is of the form*

$$\boldsymbol{n}_{\mu\nu} = (-\partial_\nu h_{\mu\kappa} + \Gamma^\lambda_{\kappa\nu} h_{\mu\lambda})\boldsymbol{x}^\kappa - k_{\mu\nu}\boldsymbol{n}.$$

Proof. We first compute the normal, then the tangential part of $\boldsymbol{n}_{\mu\nu}$, and finally put things together. That is,

(i) Weingarten's equations (47) tell us $\boldsymbol{n}_\nu = -\boldsymbol{x}^\kappa h_{\kappa\nu}$.
(ii) Differentiating $\boldsymbol{n}\boldsymbol{n} = 1$ we get $\boldsymbol{n}_\mu \boldsymbol{n} = 0$ and then, proceeding as in the argument following (131), $\boldsymbol{n}_{\mu\nu}\boldsymbol{n} = -\boldsymbol{n}_\mu \boldsymbol{n}_\nu = -h_{\mu\kappa}h^\kappa_\nu = -k_{\mu\nu}$.
(iii) Differentiating (42), i.e., $\boldsymbol{n}_\mu \boldsymbol{x}_\kappa = -h_{\mu\kappa}$, we obtain

$$\boldsymbol{n}_{\mu\nu}\boldsymbol{x}_\kappa = -\partial_\nu h_{\mu\kappa} - \boldsymbol{n}_\mu \boldsymbol{x}_{\kappa\nu} = -\partial_\nu h_{\mu\kappa} - \Gamma^\lambda_{\kappa\nu}\boldsymbol{n}_\mu \boldsymbol{x}_\lambda = -\partial_\nu h_{\mu\kappa} + \Gamma^\lambda_{\kappa\nu} h_{\lambda\mu}.$$

Since $\mathbb{P} = |\boldsymbol{x}_\mu\rangle\langle\boldsymbol{x}^\mu|$ projects onto tangent space $\mathcal{T}_{\boldsymbol{x}}$, $\boldsymbol{n}$ is a unit vector orthogonal to $\mathcal{T}_{\boldsymbol{x}}$, and thus $\mathbb{1} = \mathbb{P} + |\boldsymbol{n}\rangle\langle\boldsymbol{n}|$, $\boldsymbol{n}_{\mu\nu} = \mathbb{P}\boldsymbol{n}_{\mu\nu} + \boldsymbol{n}(\boldsymbol{n}\boldsymbol{n}_{\mu\nu})$ is a direct consequence. □

Computing $(\delta^2 h_{\mu\nu})g^{\mu\nu}$. Exploiting (42) this time in the form $h_{\mu\nu} = \boldsymbol{n}\partial^2_{\mu\nu}\boldsymbol{x}$ together with $\delta^2\partial^2_{\mu\nu}\boldsymbol{x} = 0$ as a consequence of (123), we see

$$\delta^2 h_{\mu\nu} = 2\delta\boldsymbol{x}_{\mu\nu}\delta\boldsymbol{n} + \boldsymbol{x}_{\mu\nu}\delta^2\boldsymbol{n} \tag{140}$$

and concentrate on $\delta^2\boldsymbol{n}$.

Second derivatives of (123) w.r.t. t always vanish, hence $\delta^2\boldsymbol{x}_\mu = 0$ too. The normal part of $\delta^2\boldsymbol{n}$ follows from $\boldsymbol{n}\boldsymbol{n} = 1 \Rightarrow \boldsymbol{n}\delta\boldsymbol{n} = 0 \Rightarrow \delta^2\boldsymbol{n}\boldsymbol{n} = -(\delta\boldsymbol{n})^2 = -\psi^\mu\psi_\mu$ while its tangential part originates from (125) and (129): $\boldsymbol{n}\boldsymbol{x}_\mu = 0 \Rightarrow (\delta\boldsymbol{n})\boldsymbol{x}_\mu = -\boldsymbol{n}\delta\boldsymbol{x}_\mu$ and thus, after a bit of algebra,

$$\boldsymbol{x}_\mu\delta^2\boldsymbol{n} = -2\delta\boldsymbol{n}\delta\boldsymbol{x}_\mu - \boldsymbol{n}\delta^2\boldsymbol{x}_\mu = 2\psi\psi^\nu\delta\boldsymbol{n}\delta\boldsymbol{x}_\mu = -2\psi\psi^\nu h_{\mu\nu}.$$

Pasting the two parts together according to $\mathbb{1} = \mathbb{P} + |\boldsymbol{n}\rangle\langle\boldsymbol{n}|$ we obtain

$$\delta^2\boldsymbol{n} = -2\psi\psi_\nu h^{\nu\mu}\boldsymbol{x}_\mu - \psi^\mu\psi_\mu\boldsymbol{n}. \tag{141}$$

Combining (140) and (141) with the expression (125) for $\delta\boldsymbol{x}_{\mu\nu}$ we get a fairly unwieldy result,

$$\delta^2 h_{\mu\nu} = 2(\psi_{\mu\nu}\boldsymbol{n} + \boldsymbol{n}_\mu\psi_\nu + \boldsymbol{n}_\nu\psi_\mu + \psi\boldsymbol{n}_{\mu\nu})(-\psi^\lambda\boldsymbol{x}_\lambda) - (\Gamma^\lambda_{\mu\nu}\boldsymbol{x}_\lambda + h_{\mu\nu}\boldsymbol{n})(\boldsymbol{n}\psi^\mu\psi_\mu + \psi_\nu h^{\nu\mu}\boldsymbol{x}_\mu),$$

which, however, is simplified by Lemma G so as to read

$$\delta^2 h_{\mu\nu} = 2\psi^\lambda(\psi_\mu h_{\lambda\nu} + \psi_\nu h_{\lambda\mu}) + 2\psi\psi^\lambda(h_{\lambda\mu} - \Gamma^\kappa_{\lambda\mu}h_{\kappa\nu} - \Gamma^\kappa_{\lambda\nu}h_{\kappa\mu}) - h_{\mu\nu}\psi^\kappa\psi_\kappa.$$

According to (87), the second term between brackets on the right is the covariant derivative $\nabla_\nu h_{\lambda\mu}$ so that

$$\delta^2 h_{\mu\nu} g^{\mu\nu} = 4\psi_\mu\psi_\nu h^{\mu\nu} + 2\psi\psi_\mu\nabla_\nu h^{\mu\nu} - \psi^\mu\psi_\mu\mathbb{H}. \tag{142}$$

We are now practically done. The rest is clear sailing.

Computing $h_{\mu\nu}\delta^2 g^{\mu\nu}$. According to (127), $\delta g^{\mu\nu} = -g^{\mu\kappa}\delta g_{\kappa\lambda} g^{\lambda\nu}$. Differentiating this once more we get

$$\delta^2 g^{\mu\nu} = -\delta g^{\mu\kappa}\delta g_{\kappa\lambda} g^{\lambda\nu} - g^{\mu\kappa}\delta^2 g_{\kappa\lambda} g^{\lambda\nu} - g^{\mu\kappa}\delta g_{\kappa\lambda}\delta g^{\lambda\nu}.$$

Collecting terms from (126), (127), and (137) we end up with

$$h_{\mu\nu}\delta^2 g^{\mu\nu} = 6\psi^2 \operatorname{tr}(g^{-1}h)^3 - 2\psi_\mu \psi_\nu h^{\mu\nu}. \tag{143}$$

As always in two dimensions ($n = 2$), $\operatorname{tr}(g^{-1}h)^3 = \sum_{h=1}^n \kappa_h^3 = \mathbb{H}^3 - 3\mathbb{K}\mathbb{H}$; cf. Section 4.5.

Computing $\delta^2\mathbb{H}$. We now return to (139), use (130) and (127), conclude

$$2\delta h_{\mu\nu}\delta g^{\mu\nu} = 4\psi h^{\mu\nu}\nabla_\nu\psi_\mu - 4\psi^2 \operatorname{tr}(g^{-1}h)^3,$$

and add this to (142) and (143),

$$\delta^2\mathbb{H} = 2\psi\psi_\mu\nabla_\nu h^{\mu\nu} + 4\psi h^{\mu\nu}\nabla_\nu\psi_\mu + 2h^{\mu\nu}\psi_\mu\psi_\nu + 2\psi^2\sum_{h=1}^n \kappa_h^3 - \mathbb{H}\psi^\mu\psi_\mu. \tag{144}$$

11.2.3. Undulating Willmore surface

We started with (135) and are now in a position to finish our main dish, collecting all the terms that contribute to $\delta^2\mathcal{F}_W$,

$$\delta^2\mathcal{F}_W = \frac{k_c}{2}\int \mathrm{d}f\,[\mathbb{A}\psi^2 + \mathbb{B}^\mu\psi_\mu\psi + \mathbb{C}^{\mu\nu}\psi_\mu\psi_\nu + \mathbb{D}^{\mu\nu}(\nabla_\mu\psi_\nu)\psi + 2(\Delta\psi)^2]. \tag{145}$$

This would describe an undulating Willmore surface characterized by $\delta\mathcal{F}_W = 0$. For our two-dimensional manifold the coefficients $\mathbb{A} - \mathbb{D}$ read

$$\mathbb{A} = 2(\mathbb{H}^2 - \mathbb{K})(\mathbb{H}^2 - 4\mathbb{K}), \tag{146}$$
$$\mathbb{B}^\mu = 4\mathbb{H}\nabla_\kappa h^{\mu\kappa}, \tag{147}$$
$$\mathbb{C}^{\mu\nu} = 4\mathbb{H}h^{\mu\nu} - \mathbb{H}^2 g^{\mu\nu}, \tag{148}$$
$$\mathbb{D}^{\mu\nu} = 8(\mathbb{H}h^{\mu\nu} - \mathbb{K}g^{\mu\nu}). \tag{149}$$

Though (145) should be a self-adjoint bilinear form, the terms containing $\mathbb{B}$ and $\mathbb{D}$ do not look very symmetric yet. We now check they are. Applying the divergence equation (93) in the form $\mathrm{d}\vec{q}\,\partial_\mu(\sqrt{g}v^\mu) = \mathrm{d}f\,\nabla_\mu v^\mu$ to $\mathbb{D}$ as it occurs in (145) we see, through a partial integration that should give no boundary (NB) terms, that $\int \mathrm{d}f\,\psi\mathbb{D}^{\mu\nu}\nabla_\nu\psi_\mu$ is transformed into

$$\int \mathrm{d}f\,\psi\nabla_\nu(\mathbb{D}^{\mu\nu}\psi_\mu) - \int \mathrm{d}f\,\psi(\nabla_\nu\mathbb{D}^{\mu\nu})\psi_\mu \overset{\mathrm{NB}}{=} -\int \mathrm{d}f\,\psi_\nu\mathbb{D}^{\mu\nu}\psi_\mu - \int \mathrm{d}f\,\psi\psi_\mu(\nabla_\nu\mathbb{D}^{\mu\nu}).$$

The first term on the right is already symmetric and the second has the very same structure as the $\mathbb{B}^\mu$ term in (145). So we are left with the latter. Defining $\tilde{\mathbb{C}}^{\mu\nu} := \mathbb{C}^{\mu\nu} - \mathbb{D}^{\mu\nu}$, $\tilde{\mathbb{B}}^\mu := \mathbb{B}^\mu - \nabla_\kappa\mathbb{D}^{\mu\kappa}$, and $\tilde{\mathbb{A}} := \mathbb{A} - \nabla_\mu/2\tilde{\mathbb{B}}^\mu$, invoking (93) once more, and performing another partial integration that should give no boundary (NB) terms either,

$$\int \mathrm{d}f\psi\tilde{\mathbb{B}}^\mu\psi_\mu \overset{\mathrm{NB}}{=} -\frac{1}{2}\int \mathrm{d}f\psi^2(\nabla_\mu\tilde{\mathbb{B}}^\mu)^2,$$

we arrive at a symmetric form of (145),

$$\delta^2\mathcal{F}_W \overset{\mathrm{NB}}{=} \int \mathrm{d}f\,[\tilde{\mathbb{A}}\psi^2 + \tilde{\mathbb{C}}^{\mu\nu}\psi_\mu\psi_\nu + 2(\Delta\psi)^2]. \tag{150}$$

The symmetry is evident, except for $\int \mathrm{d}f(\Delta\psi)^2]$. Remembering, however, that the Laplace–Beltrami operator Δ is as self-adjoint as you can wish as long as there are no boundary terms in partial integration, we are effectively done.

More explicitly, applying Lemma F and (93) to the second and third term on the right in (150) we obtain the Willmore operator $\delta^2\mathbb{F}_W$ belonging to $\delta^2\mathcal{F}_W := \langle\psi|\delta^2\mathbb{F}_W|\psi\rangle = \int \mathrm{d}f\psi(\delta^2\mathbb{F}_W)\psi$,

$$\delta^2\mathbb{F}_W = [\tilde{\mathbb{A}} - \nabla_\mu\tilde{\mathbb{C}}^{\mu\nu}\nabla_\nu + 2\Delta^2], \tag{151}$$

under the proviso that no boundary terms occur, as we have indicated explicitly by means of NB accompanying all equality signs where we had to invoke this condition.

11.2.4. Energy of an undulating membrane surface

The full energy $\mathcal{F}$ one has to consider in studying a cell, or any other, membrane is given by (120). Stationary configurations are characterized by $\delta\mathcal{F} = 0$ and, hence, by the Poisson–Schadow equation (134). To be a minimum, and herewith stable, we need its associated 'Hamilton operator' $\delta^2\mathbb{F}$ to be positive. That is to say, the energy $\delta^2\mathcal{F}_W := \langle\psi|\delta^2\mathbb{F}_W|\psi\rangle$ for an arbitrary, though smooth, undulation ψ is to be positive; see Fig. 1 for what ψ looks like as real time proceeds.

The Willmore part (151) being at our disposal, we collect the terms related to Σ, P, and Q, and see it is advantageous to redefine $\tilde{\mathbb{A}} \to \check{\mathbb{A}}$ and $\tilde{\mathbb{C}} \to \check{\mathbb{C}}^{\mu\nu}$ in (150) and (151) so as to get

$$\begin{aligned}\check{\mathbb{A}} &:= \frac{k_c}{2}\tilde{\mathbb{A}} + P\mathbb{H} + 2\Sigma\mathbb{K} + Q\left[\mathbb{H}^3 - 2\mathbb{H}\mathbb{K} + \frac{1}{2}\Delta\mathbb{H}\right],\\ \check{\mathbb{C}}^{\mu\nu} &:= \frac{k_c}{2}\tilde{\mathbb{C}}^{\mu\nu} + \Sigma g^{\mu\nu} + Q(\mathbb{H}g^{\mu\nu} - 2h^{\mu\nu}).\end{aligned} \tag{152}$$

Relation (86) of Lemma D and Mainardi-Codazzi (173) derived in the appendix are both helpful in verifying the first equation. In this way we get, for example, $\nabla_\mu h^\mu_\nu = \nabla_\nu\mathbb{H}$.

Furthermore, the stability of a closed membrane surface described by (120) is governed by the condition $\delta^2\mathcal{F} = t^2\langle\psi|\delta^2\mathbb{F}|\psi\rangle > 0$ for all fluctuations $t\psi$, and thus by its Hamilton operator

$$\delta^2\mathbb{F} = \check{\mathbb{A}} - \nabla_\mu\check{\mathbb{C}}^{\mu\nu}\nabla_\nu + k_c\Delta^2 \tag{153}$$

being positive. General abstract sense (Buser, 1992; Schoen and Yau, 1994) tells us that the operator $\delta^2\mathbb{F}$ is self-adjoint (we did not say > 0) and that on a finite smooth manifold its spectrum consists of isolated *eigenvalues of finite multiplicity* only. Since the spectral analogy between a general closed manifold $\mathcal{M}$ and a sphere hits the eye, we denote the eigenvalues by E_l with $l = 0, 1, 2, \ldots$, and the associated eigenfunctions by Φ_{lm} with $m > 0$ labeling the different, orthogonal, eigenfunctions in case E_l is degenerate; this being understood, we simply drop the m.

Eqs. (153) and (152) indicate that a membrane shape could become unstable as, for instance, P changes. In Section 11.3.2 we will see that for spherical vesicles there may indeed exist a critical P_c such that they loose their stability for $P > P_c$.

Finally, for a given elementary excitation ψ of a stable configuration ($t := 1$) we have found its (positive) energy $\mathcal{F}(\psi)$ is given by

$$\mathcal{F}(t\psi) - \mathcal{F}(0) = \frac{1}{2}\langle\psi|\delta^2\mathbb{F}|\psi\rangle = \frac{1}{2}\sum_l E_l|\langle\psi|\Phi_l\rangle|^2.$$

As indicated at the end of Section 5, we consider the right-hand side as a Hamilton function determined by (153), diagonalize it, i.e, consider the coefficients $c_l := \langle\psi|\Phi_l\rangle$ as new coordinates and perform a canonical transformation from continuous ψ to denumerable c_l for this (linear) system. The equipartition theorem (Huang, 1987, Section 6.4) then determines the thermal average $\langle c_l^2\rangle$ to be given by $E_l\langle c_l^2\rangle = k_\mathrm{B}T$ where T is the temperature; we will work out the details in the next subsection. The coefficients c_l follow from, e.g., light-scattering experiments.

11.3. Applications

Having the appropriate formalism at one's disposal work on membrane physics becomes straightforward. The classical Hamilton operator (153) is certainly a good example since its derivation was long considered to be an extremely hard task. The literature shows why. We have now seen how to proceed—in fact, without taking recourse

to any overly abstract or complicated mathematics. As further illustrations we will consider equilibrium shapes of rotationally invariant vesicles and the undulating sphere. The former problem has been solved in full generality by Seifert et al. (1991) in a beautiful and elaborate paper, the latter problem attained its solution rather early through Safran (1983); see also Milner and Safran (1987).

It is good to realize, though, that rotational invariance may well but need not occur. A nice illustration is provided by a red blood cell undergoing the stomatocyte–discocyte–echinocyte transition of Fig. 3. It passes through a sequence of shapes that initially may well be taken rotationally invariant (top-left) but soon break this symmetry. The general situation of no symmetry is taken care of by the formalism of Section 11. As for the red blood cell, one starts with a surface of revolution (Peterson, 1992) in the top-left corner but soon ends up with manifolds depicted by the rest of Fig. 3 and explained in detail by Wortis and coworkers (Lim et al., 2002; Mukhopadhyay et al., 2002).

11.3.1. Rotationally invariant equilibrium shapes

Let us assume our manifold $\mathcal{M}$ is rotationally invariant about the z-axis. In this case it suffices to specify its intersection with the x–z plane; more precisely, we take $0 < x =: \rho$. Following Peterson (1985) we adopt the arc length s as measured from the "top" of $\mathcal{M}$ and the rotation angle ϕ as coordinates. Then points on $\mathcal{M}$ are given by

$$\boldsymbol{x}(s,\phi) = \begin{pmatrix} \rho(s)\cos(\phi) \\ \rho(s)\sin(\phi) \\ z(s) \end{pmatrix}, \tag{154}$$

where $(x, y)=(\rho(s)\cos(\phi), \rho(s)\sin(\phi))$. We put $\dot{}=\mathrm{d}/\mathrm{d}s$ so that $\dot{z}^2+\dot{\rho}^2=1$. Since ϕ and s are orthogonal coordinates the metric tensor is the diagonal matrix $g=\mathrm{diag}(1,\rho^2)$. A simple computation using (154) gives $g^{-1}h=\mathrm{diag}(-\ddot{\rho}/\dot{z}, \dot{z}/\rho)$ and, hence, mean and Gaussian curvature,

$$\mathbb{H} = \mathrm{tr}(g^{-1}h) = \frac{\dot{z}^2 - \ddot{\rho}\rho}{\rho\dot{z}}, \quad \mathbb{K} = \det(g^{-1}h) = -\frac{\ddot{\rho}}{\rho}. \tag{155}$$

Except for $\Gamma^{\phi}_{\phi s} = \dot{\rho}/\rho$ and $\Gamma^{s}_{\phi\phi} = -\dot{\rho}\rho$ the Christoffel symbols all vanish. Using (95) of Lemma F we readily find the Laplace–Beltrami operator,

$$\Delta = g^{\mu\nu}\nabla_\mu\nabla_\nu = \partial^2_{ss} + \dot{\rho}\rho^{-1}\partial_s + \rho^{-2}\partial^2_{\phi\phi}. \tag{156}$$

The Poisson–Schadow equation (134) then reads

$$2(\partial^2_{ss} + \dot{\rho}\rho^{-1}\partial_s)\mathbb{H} + \mathbb{H}(\mathbb{H}^2 - 4\mathbb{K}) - (2\Sigma/k_c)\mathbb{H} - (4Q/k_c)\mathbb{K} - (2P/k_c) = 0. \tag{157}$$

Altogether this is a nonlinear fourth-order differential equation for ρ, provided we eliminate $\dot{z}$ from $\mathbb{H}$ appearing in (155). In principle this is easy since $\dot{z}^2 + \dot{\rho}^2 = 1$ gives $\dot{z} = \pm(1-\dot{\rho}^2)^{1/2}$ where the sign of $\dot{z}$ depends on the situation at hand. Even for an 8-shaped intersection $\dot{z}$ does not change sign; it is and stays $\leqslant 0$.

To gain contact with the existing literature (Seifert et al., 1991) and reduce the order of the differential equation (157) we introduce three auxiliary variables, as is fair enough for a 4th-order equation: k_1, k_2, and ϑ. First we define ϑ and k_1 through

$$\dot{\rho} = \cos(\vartheta), \quad \dot{\vartheta} = k_1 \tag{158}$$

and find, using e.g. the Rodrigues formula (53) and Meusnier's Theorem (Section 4.6), that $\mathbb{H}$ and $\mathbb{K}$ can be expressed without any derivative occurring,

$$\mathbb{H} = k_1 + \sin(\vartheta)/\rho, \quad \mathbb{K} = k_1\sin(\vartheta)/\rho.$$

We then introduce k_2 through

$$k_2 := \partial_s\mathbb{H} = -\rho^{-2}\cos(\vartheta)\sin(\vartheta) + k_1\rho^{-1}\cos(\vartheta) + \dot{k_1},$$

which is de facto a first-order differential equation for k_1,

$$\dot{k_1} = k_2 + \rho^{-2}\cos(\vartheta)\sin(\vartheta) - k_1\rho^{-1}\cos(\vartheta). \tag{159}$$

It looks as if the first-order differential equation $\dot{k}_2 = f(\rho, \vartheta, k_1, k_2)$ for k_2 is still missing. Appearances are deceiving, however, since this is our friend (157) reappearing in the form

$$\dot{k}_2 = -\frac{\cos\vartheta}{\rho}k_2 - \frac{1}{2}\left[\mathbb{H}(\mathbb{H}^2 - 4\mathbb{K}) - \frac{2\Sigma}{k_c}\mathbb{H} - \frac{4Q}{k_c}\mathbb{K} - \frac{2P}{k_c}\right]. \tag{160}$$

Eqs. (158)–(160) constitute a system of four coupled first-order differential equations, as advertised. They fully describe the equilibrium shape of rotationally invariant vesicles, such as the ones in Fig. 2.

11.3.2. The undulating sphere

For a sphere with radius R in $\mathbb{R}^3$, a two-sphere, the two principal curvatures are $\kappa_1 = \kappa_2 = 1/R$. The mean curvature is simply $\mathbb{H} = 2/R$ and the Gaussian one equals $\mathbb{K} = 1/R^2$. The natural coordinates are the spherical ones, $(q^1, q^2) = (\theta, \phi)$, despite a few indeterminacy problems, e.g. at the poles. They are orthogonal, viz., $g_{12} = \boldsymbol{x}_1\boldsymbol{x}_2 = 0$. Hence the metric tensor is $g = \mathrm{diag}(R^2, R^2\sin^2\theta)$. Moreover, since $\kappa_1 = \kappa_2 = 1/R$ are the principal curvatures and thus eigenvalues of $g^{-1}h$, i.e., of the matrix h^ν_κ, and principal directions are orthogonal, we have $h^\nu_\kappa = \delta^\nu_\kappa/R = g^\nu_\kappa/R$ and thus $h_{\nu\mu} = g_{\nu\mu}/R$.

Substituting all this into Eqs. (146)–(149), (152) and finally into (153) while taking into account $\nabla_\kappa h^{\mu\nu} = 0$, we obtain

$$\delta^2\mathbb{F} = C_\Delta - (\Sigma - 2k_c/R^2)\Delta + k_c\Delta^2. \tag{161}$$

Here we have put $C_\Delta := (2P/R + 2\Sigma/R^2 + 4Q/R^3)$. For experimental work on the above system exhibiting thermally excited amplitudes corresponding to flickering as shown in Fig. 1 and confirming our formalism we refer to Peterson et al. (1992), Zilker et al. (1987, 1992) and Zeman et al. (1990). The recent work of Marx et al. (2002) is more general in that it also takes into account the substrate a vesicle is on.

As we already noted in Section 7 below (94), Δ is well-known as angular momentum operator of quantum mechanics,

$$\Delta = -(\hbar R)^{-2}\mathbf{L}^2 = [(\sin\theta)^{-1}\partial_\theta(\sin\theta\partial_\theta) + (\sin\theta)^{-2}\partial^2_\phi]$$

with $(2l+1)$-fold degenerate eigenvalues $l(l+1)/R^2$, $l = 0, 1, 2, \ldots$ and the spherical harmonics Y_{lm}, $-l \leqslant m \leqslant l$, as eigenfunctions (Dirac, 1958, Section 38). It is therefore an easy exercise to compute the $(2l+1)$-fold degenerate eigenvalues E_l of $\delta^2\mathbb{F}$ belonging to the eigenfunctions Y_{lm},

$$E_l = \frac{2P}{R} + \frac{\Sigma}{R^2}[2 + l(l+1)] + \frac{4Q}{R^3} + \frac{k_c}{R^4}l(l+1)(l^2 + l - 2).$$

The eigenfunctions, e.g., for $l = 1$ the $Y_{10}(\theta, \phi) = \sqrt{3/4\pi}\cos\theta$, and $Y_{11}(\theta, \phi) = -\sqrt{3/8\pi}\exp(\mathrm{i}\phi)\sin\theta = (-1)^{m=1}Y^*_{1,-1}$, tell us something on *how* the spherical shape would change, if $E_l(P, Q, \Sigma)$ becomes negative as one of the parameters P, Q, or Σ is varied.

Because we start with equilibrium we use the Poisson–Schadow equation (134) to verify that for a sphere $P/2R + \Sigma/R^2 + Q/R^3 = 0$, which gives a quadratic equation to determine the radius $R_\circ$. We can now eliminate Σ and are left with

$$E_l = \frac{1}{2}[l(l+1) - 2]\left[\frac{k_c}{R^4_\circ}l(l+1) - \frac{Q}{R^3_\circ} - \frac{P}{2R_\circ}\right]. \tag{162}$$

Interestingly, $E_1 = 0$. The explanation is simple. We take *normal* deviations from the sphere so that $r = R_\circ + \psi$ with, e.g., $\psi = \varepsilon Y_{10}$ and $0 < \varepsilon/R_\circ \ll 1$. It is a bit of work to show this ψ is equivalent to a uniform translation of the sphere along the z-axis, which of course costs no energy. Corresponding to 3 independent directions of translation in $\mathbb{R}^3$, the degeneracy is 3 (Peterson, 1989).

This is also true in general and allows a construction of the corresponding eigenfunctions as well. Eq. (153) originates from a variational problem with the translationally invariant energy functional (120). By a Noether-type theorem Eq. (153) is bound to have a *three*-fold degenerate eigenvalue $E = 0$. Since this kind of excitation has no physical meaning it is to be excluded.

Because of (162), $E_1 = 0$, $E_0 = (Q/R^2_\circ + P)/R_\circ$ while for $l \geqslant 2$ we have $E_l \geqslant E_2$ as long as $\mathrm{sgn}(E_2) = \mathrm{sgn}(6k_c/R^3_\circ - Q/R^2_\circ - P/2) \geqslant 0$. Let us suppose $P \,\&\, Q > 0$ and consequently $\Sigma < 0$. Q is fixed by the lipid bilayer under consideration.

P on the other hand is experimentally at our disposal. We see that E_2 changes sign and becomes negative, if $P > P_c$ with P_c given by

$$(6k_c/R_\circ^3 - Q/R_\circ^2 - P_c/2) = 0. \tag{163}$$

For $P > P_c$ we get a bifurcation of the shape in the direction of the eigenspace spanned by the $\{Y_{2m}; -2 \leqslant m \leqslant 2\}$.

One could object that for a normal balloon ($k_c = Q = 0$), a children's toy, this never happens. Indeed, from the point of view of energy here $P < 0$ and its volume is to increase until it is compensated by the surface tension $\Sigma > 0$, which wants to make it smaller. Nevertheless $E_0 < 0$. This argument is faulty, however, since P and Σ are considered to be Lagrange parameters and not quantities related to the radius R through an equation of state. The radius, however, changes if fluctuations have a component along Y_{00}.

11.3.3. Experimental verification

Is curvature really important and do we see it in experiment? As has been pointed out by Peterson et al. (1992) and Zilker et al. (1992) the answer is a univocal yes. Let us try to see why this is so and, to this end, return to the nearly flat membrane of Section 5. It has no intrinsic curvature and, hence, the metric tensor $\mathbb{1}$. As a consequence of (68) in conjunction with the equipartition theorem we have obtained $(k_c k^4 + \Sigma k^2)\langle a_{\vec{k}}^2 \rangle = 2k_B T$ for the thermal average $\langle a_{\vec{k}}^2 \rangle$ of an undulation amplitude $a_{\vec{k}}$.

For a finite square of size $L \times L$ we get $k \geqslant \pi/L$ whereas distances less than a molecular diameter a are meaningless so that $k \leqslant \pi/a$. In a real vesicle curvature is not felt for *small enough* wavelengths λ and thus for large enough k so that asymptotically $\langle a_{\vec{k}}^2 \rangle \sim (2k_B T/k_c)k^{-4}$ with information about the bending rigidity k_c coming for free (Zilker et al. 1992, Fig. 3). The timescale of undulations in cell membranes is typically 0.1 s and less whereas molecular motors in the cytoplasm operate on a timescale of 1s and more so that we can handle the latter through an adiabatic treatment. In passing we note that, as a consequence of fluctuation analysis, both Peterson et al. (1992) and Zilker et al. (1992) favor the bilayer coupling model (BCM) and shear-free deformations—the latter in agreement with the arguments of Section 3.

On the other hand, for small enough wave vector length k the quadratic k-dependence of $\langle a_{\vec{k}}^2 \rangle$ is illusory and undulations are eigenstates of (153), or linear combinations thereof. The Hamiltonian operator (153) holds for *any* closed smooth surface one can think of; e.g., that of (161), a sphere, and we can expect something like (162), which shows explicitly how and why curvature is important. That is, equipped with (153) life has now become simple: the low-lying excitation energies E_l as eigenvalues of a well-defined Hamiltonian operator are discrete, rather far apart, and thus their distance cannot become arbitrarily small; there are only finitely many of them in any neighborhood of $E = 0$. Accordingly, there are no singularities in the total energy (and hence there is no need for $k \geqslant \pi/L$ either so as to avoid a logarithmic divergence). The computation of the eigenvalues E_l of (153) is straightforward in principle but may be somewhat involved in practice. Nevertheless elementary excitations of freely moving vesicles and cells are henceforth completely understood.

As an illustration we take a rotationally invariant, discocytic erythrocyte (Peterson et al., 1992) with equilibrium form depicted in Fig. 13(a), which directly corresponds to Fig. 2 (left) and, more in particular, to the red blood cell in Fig. 3 (top-left). As follows from a more detailed analysis (Peterson et al., 1992), the membrane itself is a two-dimensional fluid. The horizontal x-axis is a symmetry axis so that a plot of the upper half of the figure suffices. The cell's diameter length is $2R = 7.8\,\mu\text{m}$, corresponding to cell borders at $x = \pm 3.9\,\mu\text{m}$; see Peterson et al. (1992) for all other physical parameters.

The normal variation at a certain site $\boldsymbol{x}$ on the manifold $\mathcal{M}$ at time t is given by a positive or negative deviation $\psi(\boldsymbol{x}, t)$ along the normal vector $\boldsymbol{n}$. Throughout what follows $\cdot$ denotes a dummy variable; e.g., $\boldsymbol{x}$ as integration variable. We write

$$\psi(\boldsymbol{x}, t) = \sum_l \Phi_l(\boldsymbol{x})\langle \Phi_l(\cdot)|\psi(\cdot, t)\rangle, \tag{164}$$

where the inner product $\langle \Phi_l(\cdot)|\psi(\cdot, t)\rangle$ is an integral over $\boldsymbol{x}$. This inner product, which still depends on the time t, equals the simple decomposition into real and imaginary parts,

$$\langle \Phi_l(\cdot)|\psi(\cdot, t)\rangle = a_l(t) + \mathrm{i}b_l(t). \tag{165}$$

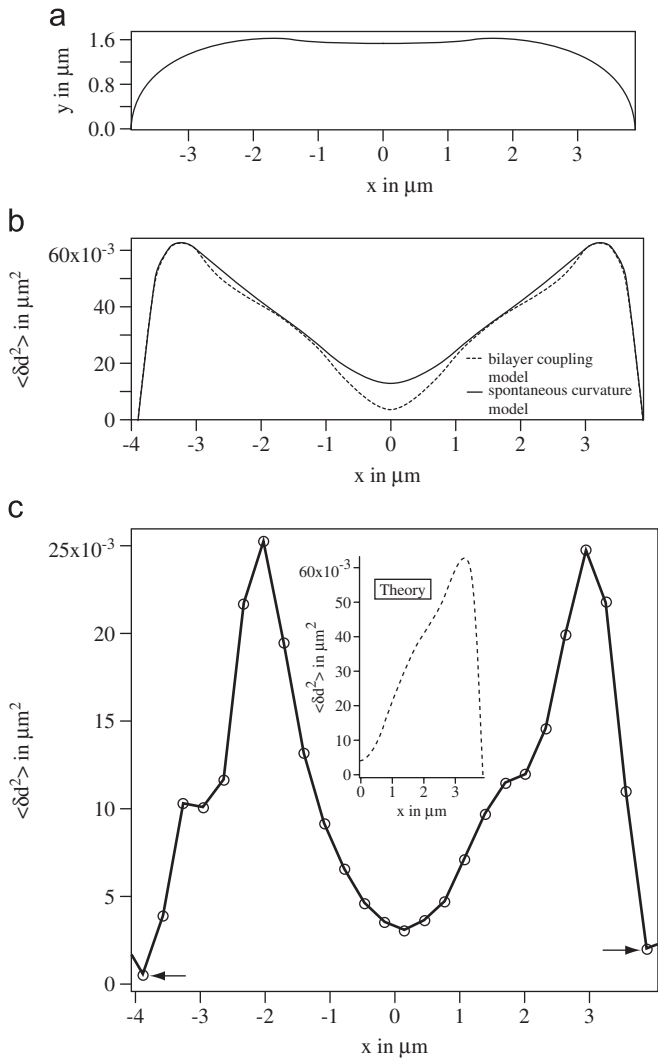

Fig. 13. Erythrocyte fluctuations: (a) Equilibrium form of the upper half of a model cell shape, a red blood cell of fixed area 135 μm^2 and volume 115 μm^3; see also Fig. 3 (top-left). The cell is rotationally invariant about the vertical y-axis through the origin at $x = 0$; (b) Flicker amplitude-squared profile $\langle \delta d^2 \rangle$, a time average of the normal fluctuations squared, as a function of x, along the diameter of the cell. The solid line is a prediction due to the spontaneous-curvature model (105), the dashed one follows from the bilayer-coupling model (106), also nicknamed BCM; (c) Experimental check of the flicker-amplitude profile $\langle \delta d^2 \rangle$, favoring BCM. The horizontal arrows indicate the cell borders. The above plots (a)–(c) are based on data of Peterson et al. (1992).

According to (153) the energy of a small normal fluctuation ψ equals $\langle \psi | \delta^2 \mathbb{F} | \psi \rangle / 2$. Expanding $\psi = \sum_l \Phi_l \langle \Phi_l | \psi \rangle$ in terms of the eigenfunctions Φ_l of $\delta^2 \mathbb{F}$ as in (164), and noting $|\langle \Phi_l | \psi \rangle|^2 = a_l^2 + b_l^2$ because $\langle \Phi_l | \psi \rangle = a_l + \mathrm{i} b_l$ according to (165), we end up with an energy of the form

$$E = \sum_l (a_l^2 + b_l^2) E_l / 2. \tag{166}$$

It is nothing but a *quadratic* expression in the real coordinates a_l and b_l. We can therefore write the energy in terms of a Hamilton function $\mathcal{H} = \sum_l (a_l^2 + b_l^2) E_l / 2$ and interpret a_l and b_l as independent coordinates; cf. Sections 2 and 5.

Because of rotational invariance, we can invoke (158), (159), and (160) to determine the eigenvalues E_l of $\delta^2 \mathbb{F}$. Furthermore, (166) is the direct equivalent of (68) with a plain l replacing the index $\vec{k}$ in (68). Here too we can apply

the equipartition theorem (Huang, 1987) to each of the quadratic terms so as to get, e.g., $E_l\langle a_l^2\rangle_\beta = k_\mathrm{B}T$ for the thermal average $\langle\dots\rangle_\beta$ at inverse temperature β; the latter equals the temporal average due to ergodicity of the ergodic component the system is in (van Enter and van Hemmen, 1984). We see from Fig. 13(b) and (c) that BCM gives rise to a better fit than Helfrich's spontaneous-curvature model.

What can be measured experimentally is the time average of $|\psi(\boldsymbol{x},t)|^2$. Let us define Φ_m^* to be the complex conjugate of the eigenfunction Φ_m of $\delta^2\mathbb{F}$. Exploiting (164) and (165) in conjunction with the ergodicity of the thermodynamic equilibrium the system is in, at least on the undulation time scales we are interested in, viz., < 0.1s, we will obtain the local mean-square fluctuations $\langle\delta d^2\rangle$ at a site $\boldsymbol{x}$ in Fig. 13(b) and (c), viz.,

$$\langle\delta d^2\rangle := \lim_{T\to\infty}\frac{1}{T}\int_0^T \mathrm{d}t\,|\psi(\boldsymbol{x},t)|^2. \tag{167}$$

We simply note that because of (164) and (165)

$$\psi(\boldsymbol{x},t) = \sum_l \Phi_l(\boldsymbol{x})\langle\Phi_l(\cdot)|\psi(\cdot,t)\rangle = \sum_l \Phi_l(\boldsymbol{x})[a_l(t) + \mathrm{i}b_l(t)], \tag{168}$$

where $\boldsymbol{x}$ and t have been separated, and substitute this into the right-hand side of (167) so as to find

$$\begin{aligned}\langle\delta d^2\rangle &= \sum_{l,m}\Phi_l(\boldsymbol{x})\Phi_m^*(\boldsymbol{x})\langle(a_l+\mathrm{i}b_l)(a_m-\mathrm{i}b_m)\rangle_\beta\\ &= 2k_\mathrm{B}T\sum_l |\Phi_l(\boldsymbol{x})|^2/E_l\end{aligned} \tag{169}$$

since time average equals the canonical-ensemble average $\langle\dots\rangle_\beta$ with respect to the Hamilton function $\mathcal{H} = \sum_l(a_l^2 + b_l^2)E_l/2$ of (166) at inverse temperature β and

$$\langle a_l b_m\rangle_\beta = 0, \quad \langle a_l a_m\rangle_\beta = \langle b_l b_m\rangle_\beta = \delta_{lm}k_\mathrm{B}T/E_l. \tag{170}$$

Eq. (170) is another consequence of the equipartition theorem (Huang, 1987) with a_l and b_m being independent variables. Finally, we note (Buser, 1992; Schoen and Yau, 1994) $\lim_{l\to\infty}1/E_l = 0$ so that (169) makes sense, in contrast to $\sum_l|\Phi_l(\boldsymbol{x})|^2$ itself. Because of $\sum_l|\Phi_l\rangle\langle\Phi_l| = \mathbb{1}$ the sum $\sum_l\Phi_l(\boldsymbol{x})\Phi_l^*(\boldsymbol{y}) = \delta(\boldsymbol{x}-\boldsymbol{y})$ produces mathematical nonsense for $\boldsymbol{x}=\boldsymbol{y}$. Adding, however, the multiplicative factor $1/E_l$ we cancel the divergence. That is, we get a weighted sum of $|\Phi_l(\boldsymbol{x})|^2$ and the larger l, the less important these terms become. It is good to realize as well that $|\Phi_l(\boldsymbol{x})|^2$ reflects the nature of the cell-surface shape *at the site* $\boldsymbol{x}$.

To see why, and how, all this works, we turn to the simple case of a sphere with radius R. It is so to speak the opposite of the (nearly) flat membrane of Section 5 but typical to any cell membrane. So let us now focus on $\sum_l|\Phi_l(\boldsymbol{x})|^2/E_l$ on the sphere. We have to estimate the eigenvalues E_l of $\delta^2\mathbb{F}$ as $l\to\infty$. Hence it suffices to study those of the dominating term $k_c\Delta^2$, i.e., Δ^2 where $-\Delta$ on a sphere of radius R equals $\boldsymbol{L}^2/R^2$ with $\boldsymbol{L}$ as angular momentum operator. For the present estimate we drop k_c. The spherical harmonics Y_{lm} with $-l\leqslant m\leqslant l$ for a given l are eigenfunctions of the Laplace–Beltrami operator $-\Delta = \boldsymbol{L}^2/R^2$ on the sphere with eigenvalue $l(l+1)/R^2$. Using (Messiah, 1961)

$$\sum_{m=-l}^{l}|Y_{lm}|^2 = \frac{2l+1}{4\pi}$$

and dropping a prefactor R^4 together with the term $l=0$ as they are irrelevant for the present estimate we are left with a sum à la (169) of the form

$$\sum_{l\neq0,m}|Y_{lm}|^2[l(l+1)]^{-2} = \sum_{l=1}^{\infty}\frac{2l+1}{4\pi[l(l+1)]^2}.$$

The argument on the right being $\sim l^{-3}$ the sum is quite convergent, as claimed.

Because of the high symmetry of a sphere its fluctuation profile $\langle \delta d^2 \rangle$ does not depend on the position $\boldsymbol{x}$. For less symmetric manifolds, however, such as the one in Fig. 13, this is of course no longer true. Quite to the contrary, the mean-square fluctuations $\langle \delta d^2 \rangle$ clearly depend on $\boldsymbol{x} \in \mathcal{M}$, the position on the manifold $\mathcal{M}$ describing the cell membrane.

It is noteworthy that the fluctuation profile in Fig. 13(b) and (c) is *low* at the center of the cell and *high* near the periphery, contrary to any first guess. Because of alignment problems in the microscope the experimental profile in Fig. 13(c) is slightly asymmetric with respect to the y-axis. Comparison with (b) shows the bilayer-coupling model (106) gives a better fit than Helfrich's spontaneous-curvature model (105); in particular, near the center. Experimental fluctuation amplitudes at the periphery are expected to be far greater than what is indicated in Fig. 13(c) because of the 'finite focus depth effect' cutting off fluctuations far away from the focus plane. So it is fair to say that the mean fluctuation amplitude varies between 2 nm at the center and 8 nm at the periphery, as follows from Fig. 13(b) displaying $\langle \delta d^2 \rangle$.

Fig. 14 shows explicitly that biomembranes *on a substrate* also experience undulations and, in so doing, open new avenues leading to as yet unknown vistas. The underlying undulations govern the extent to which adhesion works. Computing them will be a fascinating challenge for some time to come.

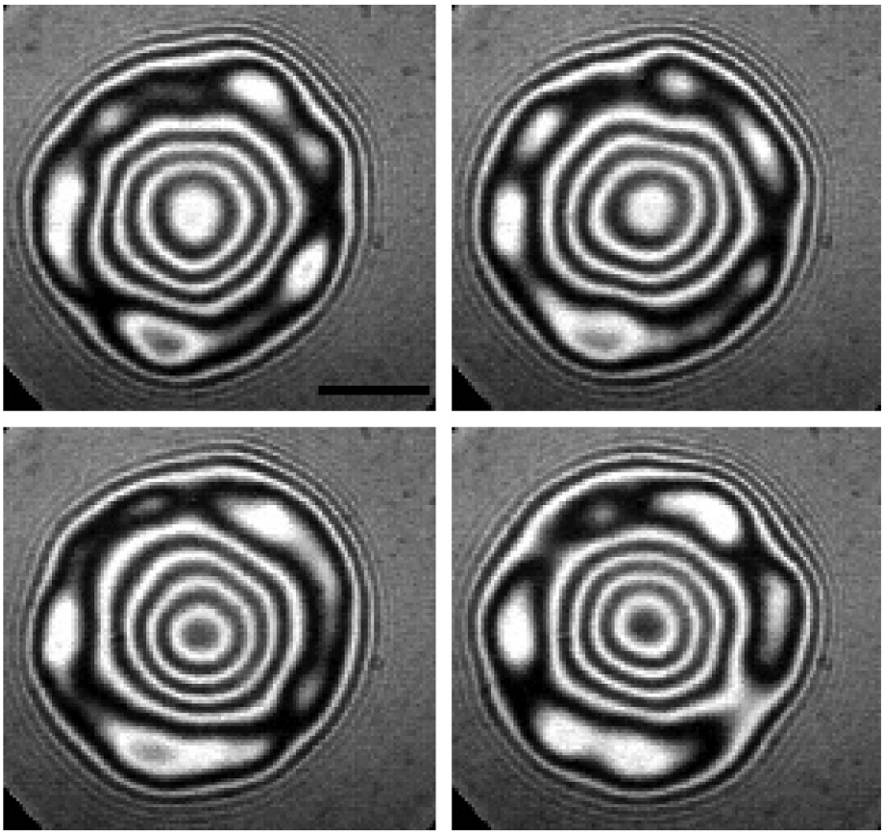

Fig. 14. Contrast-enhanced pictures of thermally excited surface undulations of a DMPC-cholesterol vesicle provided by dynamic reflection interference contrast microscopy (RICM). Temporal distance between the pictures (left-right, top-bottom) is 1 s. The black horizontal bar (top left) represents 5μm. The vesicle is embedded in an aqueous solution and weakly bound to an underlying glass plate through adhesion. The horizontal contact area has a circular shape, the thick outer rim, and the membrane is curved upwards in between—a kind of buckling, which is not understood yet. The interaction between adhesion and gravitation on the one hand and undulations on the other determines how well a vesicle is bound to the substrate. The vertical distance between two consecutive black and white Newtonian rings is 100 nm = 0.1 μm. Picture courtesy of Barbara Lorz.

12. Outlook

We have analyzed undulations as elementary excitations of a flexible membrane such as that of a cell. In so doing we have used continuum mechanics since it is both general and versatile. Principal curvatures (Section 4.6) of cell shapes and undulation wavelengths (Section 11.3) being much bigger than typical intermolecular distances, a continuum mechanics description makes quite a bit of sense and neatly reduces biomembranes to 'shapes' governed by an energy functional in terms of inherently geometric quantities. We are then left with plain *shapes*, which may be of *any* form, and we have seen that classical differential geometry is ideally suited to handle the problem of finding minimal configurations of the energy functional and determining their stability.

For cells and vesicles on a substrate, governed by adhesion, the above setup is all the more important. For instance, the explanation of the typical buckling of a cell on a substrate as shown in Fig. 14 is still an open problem. In contrast to a freely moving cell one now has to take into account boundary conditions of the membrane on the substrate, which give rise to new phenomena. In the above derivations we have already indicated where boundary conditions are important, as denoted by NB in some of the equations.

Furthermore, the arguments remain valid if we include the cytoskeleton as a flexible medium inside a cell but interacting with the cell membrane since the former's changes are adiabatic with respect to latter's undulations. Cell adhesion in conjunction with undulation is highly relevant to biotechnical applications.

Finally, the geometric, nearly picturesque, techniques of classical differential geometry presented here may also aid more general applications in soft-matter physics where form and shape are important constituents of how and in what direction processes evolve.

Acknowledgments

The authors thank Philip Brownell, Ulrich Hillenbrand, Jürgen Jost, Johannes Nitsche, Bennett Palmer, Mark Peterson, Erich Sackmann, and Bruce Young for helpful suggestions and Wenzel Schürmann for technical assistance. This paper has benefited greatly in its final version from constructive criticisms made by Ranjan Mukhopadhyay and Ted Steck.

Appendix Gauss and Mainardi-Codazzi

We prove Mainardi-Codazzi by making a detour via Gauss' Theorema Egregium. The aim is to see slightly better how, and why, it all works. We start with the Gauss formula (40) in the form $\partial_{\beta\mu}\boldsymbol{x} = \Gamma^{\nu}_{\beta\mu}\partial_{\nu}\boldsymbol{x} + h_{\beta\mu}\boldsymbol{n}$ and differentiate this with respect to q^{λ},

$$\partial_{\beta\mu\lambda}\boldsymbol{x} = \Gamma^{\nu}_{\beta\mu}\partial_{\nu\lambda}\boldsymbol{x} + \partial_{\kappa}\boldsymbol{x}\partial_{\lambda}\Gamma^{\kappa}_{\beta\mu} + h_{\beta\mu}\partial_{\lambda}\boldsymbol{n} + \boldsymbol{n}\partial_{\lambda}h_{\beta\mu}. \tag{171}$$

Taking a scalar product with $\partial_{\alpha}\boldsymbol{x}$ and remembering the metric tensor $g_{\alpha\kappa} = \boldsymbol{x}_{\alpha}\boldsymbol{x}_{\kappa}$ from Lemma A we get

$$\partial_{\alpha}\boldsymbol{x}\partial_{\beta\mu\lambda}\boldsymbol{x} = g_{\alpha\kappa}[\Gamma^{\kappa}_{\nu\lambda}\Gamma^{\nu}_{\beta\mu} + \partial_{\lambda}\Gamma^{\kappa}_{\beta\mu}] - h_{\alpha\lambda}h_{\beta\mu},$$

which looks complicated. This does not last for long, if we interchange λ and μ, use the symmetry of $\partial_{\beta\mu\lambda}\boldsymbol{x}$, and subtract the two equations so as to find the essence of Gauss' *Theorema Egregium*

$$h_{\alpha\lambda}h_{\beta\mu} - h_{\alpha\mu}h_{\beta\lambda} = g_{\alpha\kappa}\mathcal{R}^{\kappa}_{\beta\lambda\mu} = \mathcal{R}_{\alpha\beta\lambda\mu} \tag{172}$$

where $\mathcal{R}^{\kappa}_{\beta\lambda\mu}$ is the famous Riemann tensor,

$$\mathcal{R}^{\kappa}_{\beta\lambda\mu} := \partial_{\lambda}\Gamma^{\kappa}_{\beta\mu} - \partial_{\mu}\Gamma^{\kappa}_{\beta\lambda} + \Gamma^{\kappa}_{\nu\lambda}\Gamma^{\nu}_{\beta\mu} - \Gamma^{\kappa}_{\nu\mu}\Gamma^{\nu}_{\beta\lambda}.$$

On the left in (172) we have the second fundamental form, on the right the metric tensor and its derivatives, bending invariant. It is time to harvest some corollaries.

First, let us take $\alpha=\lambda=1$ and $\beta=\mu=2$ for a two-dimensional manifold $\mathcal{M}$ in $\mathbb{R}^3$. Eq. (172) reads $\det h = h_{11}h_{22} - h_{12}^2 = \mathcal{R}_{1212}$ so that $\mathbb{K} = \kappa_1\kappa_2 = \det h/\det g = \mathcal{R}_{1212}/\det g$ is a bending invariant, as announced by Gauss.

Second, we return to (171), interchange λ and μ in $\boldsymbol{n}\partial_{\beta\mu\lambda}\boldsymbol{x} = \Gamma^{\nu}_{\beta\mu}h_{\nu\lambda} + \partial_{\lambda}h_{\beta\mu}$, use the symmetry of $\partial_{\beta\mu\lambda}\boldsymbol{x}$, and subtract the two equations so as to find the equations due to Mainardi (1856) and D. Codazzi (1860),

$$\partial_{\lambda}h_{\kappa\mu} - \Gamma^{\nu}_{\kappa\lambda}h_{\nu\mu} = \partial_{\mu}h_{\kappa\lambda} - \Gamma^{\nu}_{\kappa\mu}h_{\nu\lambda}. \tag{173}$$

In terms of covariant differentiation and Lemma D Eq. (173) would read $\nabla_{\lambda}h_{\kappa\mu} = \nabla_{\mu}h_{\kappa\lambda}$.

The Gauss formula (40) and the Mainardi-Codazzi equations (173) are so-called integrability conditions. If they hold and g & h are symmetric matrices with g positive-definite, then (Gerretsen, 1962; Millman and Parker, 1977; Struik, 1961) there is a two-dimensional surface in $\mathbb{R}^3$, unique up to position in space, realizing them. Bonnet was the first to pose and solve this problem in 1867.

References

Anderson, P.W., 1963. Concepts in Solids. Benjamin, Reading, MA. (Chapter 3).
Berndl, K., Käs, J., Lipowsky, R., Sackmann, E., Seifert, U., 1990. Europhys. Lett. 13, 659.
Blair, D.E., 2000. Inversion Theory and Conformal Mapping. American Mathematical Society, Providence, RI.
Boal, D., 2002. Mechanics of the Cell. Cambridge University Press, Cambridge. (Chapter 6).
Boal, D., Seifert, U., Shillcock, J.C., 1993. Phys. Rev. B 48, 4274.
Boruvka, L., Neumann, A.W., 1977. J. Chem. Phys. 66, 5464.
Boulbitch, A., et al., 2000. Phys. Rev. E 62, 3974.
Bowick, M., Cacciuto, A., Thorleifsson, G., Travesset, A., 2001. Phys. Rev. Lett. 87, 148103.
Brochard, F., Lennon, J.F., 1975. J. Phys. (Paris) 36, 1035.
Brouricz, E., 1890. Zbl. Med. Wiss. 28, 625.
Bruinsma, R., Sackmann, E., 2001. C.R. Acad. Sci. Paris 2/Sér. IV, 803.
Buser, P., 1992. Geometry and Spectra of Compact Riemann Surfaces. Birkhäuser, Boston.
Canham, P.B., 1970. J. Theor. Biol. 26, 61.
Coombs, D., Huber, G., Kessler, J.O., Goldstein, R.E., 2002. Phys. Rev. Lett. 89, 118102.
De Jeu, W.H., Ostrovskii, B.I., Shalaginov, A.N., 2003. Rev. Mod. Phys. 75, 181.
Deuling, H.J., Helfrich, W., 1976. J. Phys. (Paris) 37, 1335.
Döbereiner, H.-G., Evans, E., Kraus, M., Seifert, U., Wortis, M., 1997. Phys. Rev. E 55, 4458.
Dirac, P.A.M., 1958. The Principles of Quantum Mechanics. fourth ed. Oxford University Press, Oxford.
Duplantier, B., 1990. Physica A 168, 179.
Duplantier, B., Goldstein, R.E., Romero-Rochin, V., Pesci, A.I., 1990. Phys. Rev. Lett. 65, 508.
Duwe, H.P., Sackmann, E., 1990. Physica A 163, 410.
Engelhardt, H., Duwe, H.P., Sackmann, E., 1985. J. Phys. (Paris) Lett. 46, L395.
van Enter, A.C.D., van Hemmen, J.L., 1984. Phys. Rev. A 29, 355(especially, Sections II–III C and the appendix).
Evans, E.A., 1974. Biophys. J. 14, 923.
Frankel, Th., 1997. The Geometry of Physics: An Introduction. Cambridge University Press, Cambridge.
Gantmacher, F.R., 1977. The Theory of Matrices, vol. 1. Chelsea, New York. (IX. Sections 3 and IX. Section 5).
Gauss, C.F., 1827. Disquisitiones Generales circa Supervicies Curvas. in: Comm. soc. regiae sci. Gott. recentiores, vol. VI, pp. 1823–1827; translation Allgemeine Flächentheorie, 1900 (Engelmann, Leipzig) (See also Spivak (1979) Chapter 3).
Gerretsen, J.C.H., 1962. Lectures on Tensor Calculus and Differential Geometry. Noordhoff, Groningen.
Goldstein, R.E., Powers, T.R., Wiggins, C.H., 1998. Phys. Rev. Lett. 80, 5232.
Goldstein, R.E., Goriely, A., Huber, G., Wolgemuth, C.W., 2000. Phys. Rev. Lett. 84, 1631.
Gov, N., Zilman, A.G., Safran, S., 2003. Phys. Rev. Lett. 90, 228101.
Gov, N., Safran, S., 2005. Biophys. J. 88, 1859.
Guttenberg, Z., Lorz, B., Sackmann, E., Boulbitch, A., 2001. Europhys. Lett. 54, 826.
Head, D.A., Levine, A.J., MacKintosh, F.C., 2003. Phys. Rev. Lett. 91, 108102.
Helfrich, W., 1973. Z. Naturf. C 28, 693.
Hilbert, D., Cohn-Vossen, S., 1964. Geometry and the Imagination. Chelsea, New York. (Sections 26– 29).
Hildebrandt, S., Tromba, A., 1996. The Parsimonious Universe: Shape and Form in the Natural World. Springer, New York.
Horn, R.A., Johnson, C.R., 1985. Matrix Analysis. Cambridge University Press, Cambridge. (Sections 0.8.2 and 7.2.10).
Huang, K., 1987. Statistical Mechanics. second ed. Wiley, New York. (Section 6.4).
Hyde, S., et al., 1997. The Language of Shape: The Role of Curvature in Condensed Matter. Elsevier, Amsterdam.
Isenberg, C., 1992. The Science of Soap Films and Soap Bubbles. Dover, Mineola, NY. (Chapters 5 and 6).
Jülicher, F., 1996. J. Phys. II France 6, 1797.
Jülicher, F., Seifert, U., Lipowsky, R., 1993. Phys. Rev. Lett. 71, 452.
Kamien, R.D., 2002. Rev. Mod. Phys. 74, 953.

Kenmotsu, K., 2003. Surfaces with Constant Mean Curvature. American Mathematical Society, Providence, RI.
Kleman, M., Lavrentovich, O.D., 2002. Soft Matter Physics: An Introduction. Springer, New York.
Komura, S., Andelman, D., 2000. Eur. Phys. J. E 3, 259.
Kuzman, D., Svetina, S., Waugh, R.E., Žekš, B., 2004. Eur. Biophys. J. 33, 1.
Lakes, R., 2001. Nature 414, 503.
Landau, L.D., 1941. J. Phys. U.S.S.R. 5, 71.
Landau, L.D., Lifshitz, E.M., 1986. Theory of Elasticity. third ed. Pergamon, Oxford.
Lim, G.H.W., Wortis, M., Mukhopadhyay, R., 2002. Proc. Natl. Acad. Sci. USA 99, 16766.
Lipowsky, R., 1991. Nature 349, 475.
Liusternik, L.A., Sobolev, V.J., 1961. Elements of Functional Analysis. Ungar, New York.
Marčelja, S., 1974. Biochim. Biophys. Acta 367, 165(see in particular the appendix).
Marx, S., Schilling, J., Sackmann, E., Bruinsma, R., 2002. Phys. Rev. Lett. 88, 138102.
Messiah, A., 1961. Quantum Mechanics, vol. I. North-Holland, Amsterdam. (Chapter V; Section 18, Chapter IX, Section 2), esp. (IX.9); Appendix B, Sections 9–11 esp. (B.98) and (B.81).
Miao, L., Seifert, U., Wortis, M., Döbereiner, H.-G., 1994. Phys. Rev. E 49, 5389.
Michalet, X., Bensimon, D., 1995. Science 269, 666.
Millman, R.S., Parker, G.D., 1977. Elements of Differential Geometry. Prentice-Hall, Englewood Cliffs, NJ.
Milner, S.T., Safran, S.A., 1987. Phys. Rev. A 36, 4371.
Milnor, J.W., 1997. Topology from the Differentiable Point of View. Princeton University Press, Princeton, NJ. (Section 1).
Misner, C.W., Thorne, K.S., Wheeler, J.A., 1973. Gravitation. Freeman, San Francisco.
Mukhopadhyay, R., Lim, G.H.W., Wortis, M., 2002. Biophys. J. 82, 1756.
Nelson, D., Piran, T., Weinberg, S. (Eds.). 1989. Statistical Mechanics of Membranes and Surfaces. World Scientific, Singapore.
Nitsche, J.C.C., 1989. Lectures on Minimal Surfaces, vol. 1. Cambridge University Press, Cambridge.
Oprea, J., 2000. The Mathematics of Soap Films: Exploration with Maple. American Mathematical Society, Providence, RI.
Ou-Yang, Z., Helfrich, W., 1989. Phys. Rev. A 39, 5280.
Peliti, L., 1996. In: David, F., Ginsparg, P., Zinn-Justin, J. (Eds.), Les Houches LXII: Fluctuating Geometries in Statistical Mechanics and Field Theory. North-Holland, Amsterdam.
Peterson, M.A., 1985. J. Math. Phys. 26, 711Peterson, M.A., 1985. J. Appl. Phys. 57, 1739; Mol. Cryst. Liq. Cryst. 127, 159 and 257.
Peterson, M.A., 1988. Phys. Rev. Lett. 61, 1325.
Peterson, M.A., 1989. Phys. Rev. A 39, 2643.
Peterson, M.A., 1992. Phys. Rev. A 45, 4116.
Peterson, M.A., Strey, H., Sackmann, E., 1992. J. Phys. II France 2, 1273.
Pinkall, U., Stirling, I., 1987. Math. Intell. 9, 38.
Ponder, E., 1948. Hemolysis and Related Phenomena. Grune and Stratton, New York.
Rayleigh, J.W.S., 1894. The Theory of Sound, second ed., vol. 1. Macmillan, London (Vol. 2 appeared two years later and both were republished by Dover (New York, 1945). For present purposes, see e.g. Sections 214 and 235 b. The convention of using h for the thickness of an elastic sheet goes back at least to Lord Rayleigh. His insight and clarity are amazing. We note that Rayleigh's thickness is $2h$ whereas ours is h).
Reissner, E., 1947. Quart. Appl. Math. 5, 55.
Sackmann, E., 1994. FEBS Lett. 346, 3.
Sackmann, E., Bausch, A.R., Vonna, L., 2002. In: Flyvbjerg, H., Jülicher, F., Ormos, P., David, F. (Eds.), Les Houches LXXV. EDP Sciences, Les Ulis and Springer, Berlin, pp. 237–284.
Safran, S.A., 1983. J. Chem. Phys. 78, 2073.
Safran, S.A., 1994. Statistical Thermodynamics of Surfaces, Interfaces, and Membranes. Addison-Wesley, Reading, MA.
Schäfer, M., 1952. Z. Angew. Math. Mech. 32, 162.
Segel, L.A., 1977. Mathematics Applied to Continuum Mechanics. Macmillan, New York. (Chapter 11).
Schoen, R., Yau, S.-T., 1994. Lectures on Differential Geometry. International Press, Cambridge, MA. (in particular, Chapter III).
Seifert, U., 1991. J. Phys. A: Math. Gen. 24, L573and Phys. Rev. Lett. 66, 2404.
Seifert, U., 1995. Z. Phys. B 97, 299.
Seifert, U., 1997. Adv. Phys. 46, 13.
Seifert, U., Berndl, K., Lipowsky, R., 1991. Phys. Rev. A 44, 1182.
Seifert, U., Lipowsky, R., 1990. Phys. Rev. A 42, 4768.
Sheetz, M.P., Singer, S.J., 1974. Proc. Natl. Acad. Sci. USA 71, 4457.
Spivak, M., 1979. A Comprehensive Introduction to Differential Geometry, second ed., vol. II. Publish or Perish, Berkeley, CA. (Chapters 3 and 4).
Stephani, H., 1990. General Relativity: An Introduction to the Theory of the Gravitational Field. Cambridge University Press, Cambridge.
Strey, H., Peterson, M., Sackmann, E., 1995. Biophys. J. 69, 478.
Struik, D.J., 1961. Lectures on Classical Differential Geometry. second ed. Addison-Wesley, Reading, MA. (1988, reprint, Dover, New York).
Svetina, S., Žekš, B., 1989. Eur. Biophys. J. 17, 101.
Thomas, G.B., 1972. Calculus and Analytic Geometry. third ed. Addison-Wesley, Reading, MA. (Sections 12.6, and 14.1–6).
Thomsen, G., 1924. Abh. Math. Sem. Hamburg 3, 31–56.
Thomson, W., Tait, P.G., 1878/1883. A Treatise on Natural Philosophy, second ed. Cambridge University Press. The second edition was published in two parts. See especially Sections 639, 642, and 720.
Wilhelm, J., Frey, E., 2003. Phys. Rev. Lett. 91, 108103.

Willmore, T.J., 1982. Total Curvature in Riemannian Geometry. Ellis Horwood, Chichester. (Section 5.2).
Willmore, T.J., 1993. Riemannian Geometry. Oxford University Press. (Chapter 7).
Zeman, K., Engelhardt, H., Sackmann, E., 1990. Eur. Biophys. J. 18, 203.
Zidovska, A., Sackmann, E., 2006. Phys. Rev. Lett. 96, 048103.
Zilker, A., Engelhardt, H., Sackmann, E., 1987. J. Phys. (Paris) 48, 2139.
Zilker, A., Ziegler, M., Sackmann, E., 1992. Phys. Rev. A. 46, 7998.